Large-scale atmospheric circulation driving extreme climate events in the Mediterranean and related impacts (chapitre 6)

Elena Xoplaki, Ricardo M Trigo, Ricardo García-Herrera, David Barriopedro, Fabio D'andrea, Erich M Fischer, Luis Gimeno, Celia Gouveia, Emiliano Hernández, Franz G Kuglitsch, et al.

CHAPTER 6

LARGE-SCALE ATMOSPHERIC CIRCULATION DRIVING EXTREME CLIMATE EVENTS IN THE MEDITERRANEAN AND RELATED IMPACTS

E. Xoplaki[1,2], R.M. Trigo[3], R. García-Herrera[4], D. Barriopedro[5], F. D'Andrea[6], E.M. Fischer[7], L. Gimeno[8], C. Gouveia[3], E. Hernandez[9], F.G. Kuglitsch[1], A. Mariotti[10], R. Nieto[8], J.G. Pinto[11], D. Pozo-Vázquez[12], H. Saaroni[13], A. Toreti[1], I.F. Trigo[14], S.M. Vicente-Serrano[15], P. Yiou[16], B. Ziv[17]

[1] *Department of Geography, Justus-Liebig University of Giessen, Giessen, Germany*
Email: elena.xoplaki@geogr.uni-giessen.de; andrea.toreti@geogr.uni-giessen.de

[2] *Institute of Geography, Climatology and Meteorology, University of Bern, Bern, Switzerland*

[3]*IDL at University of Lisbon and Universidade Lusófona, Lisbon, Portugal*
Email: rmtrigo@fc.ul.pt; cmgouveia@fc.ul.pt

[4]*Dto Física de la Tierra II, Universidad Complutense, Madrid, Spain*
Email: rgarcia@fis.ucm.es

[5]*IDL at University of Lisbon, Lisbon, Portugal*
Email: dbcepero@fc.ul.pt

[6]*LMD, Paris, France*
Email: Fabio.Dandrea@lmd.ens.fr

[7]*Institute for Atmospheric and Climate Science, ETH Zürich, Switzerland*
Email: erich.fischer@env.ethz.ch

[8]*Facultad de Ciencias de Ourense, Universidad de Vigo, Ourense, Spain*
Email: l.gimeno@uvigo.es; rnieto@uvigo.es

[9]*Dto Física de la Tierra II, Universidad Complutense, Madrid, Spain*
Email: emiliano@fis.ucm.es

[10]*ENEA, Italy and ESSIC, University of Maryland, USA*
Email: amariott@casaccia.enea.it

[11]*Institute for Geophysics and Meteorology, University of Cologne, Cologne, Germany*
Email: jpinto@meteo.uni-koeln.de

[12]*Department of Physics, University of Jaén, Jaen, Spain*
Email: dpozo@ujaen.es

[13]*Department of Geography and the Human Environment, Tel Aviv University, Tel Aviv, Israel*
Email: saaroni@post.tau.ac.il

[14]*Instituto de Meteorologia and IDL at University of Lisbon, Portugal*
Email: isabel.trigo@meteo.pt

[15]*Instituto Pirenaico de Ecología, Consejo Superior de Investigaciones Científicas, Zaragoza, Spain*
Email: svicen@ipe.csic.es

[16]*LSCE/CEA/IPSL/UVSQ, Gif–sur–Yvette, France*
Email: pascal.yiou@lsce.ipsl.fr

[17]*Department of Natural Sciences, The Open University of Israel, Raanana Israel*
Email: baruchz@openu.ac.il

It is widely accepted that the Mediterranean basin represents one of the most prominent “hotspots” of climate change and particularly vulnerable regions in the world. Recent trends towards a hotter and drier climate appear to be related to changes in atmospheric circulation patterns, particularly over western Mediterranean. The combined effects of precipitation decrease and surface temperature increase in the Mediterranean will most probably lead to important changes in the region’s water cycle. In fact, the present tendency towards a drier climate with higher frequency of drought events agrees with climate change scenarios that point to increasing probabilities of drought episodes and severe heat waves. Here, is provided a multi-disciplinary review on the state–of–the–knowledge science of these two natural hazards in the Mediterranean. The chapter covers a wide range of atmospheric circulation phenomena with direct impact on climate and socio-economic activities in the twentieth century and with relatively high probabilities of changing significantly throughout the present 21st century (e.g., water resources, renewable energy, agriculture, vegetation dynamics) but also natural hazards (e.g., droughts, heat waves, sea surges and flooding in Venice).

Keywords
Mediterranean, heat waves, drought, water cycle, vegetation, energy, atmospheric circulation, teleconnections, tropical plumes, ex-hurricanes, Venice sea surges

6.1. Introduction

During the last decade a number of studies have been published on the evolution of precipitation, drought conditions and moisture availability in the Mediterranean during the twentieth century and early 21st century (e.g., Xoplaki *et al.*, 2004; Trigo *et al.*, 2006; García-Herrera *et al.*, 2007; Mariotti *et al.*, 2008; Lopez-Moreno *et al.*, 2009; Sousa *et al.*, 2011, among others). Overall, these works confirm a decrease in rainfall and moisture availability during the twentieth century, albeit with the exception of eastern Mediterranean, namely Turkey. In parallel to that, severe drought episodes have become more frequent and persistent late in the century, in both eastern (Xoplaki *et al.*, 2004) and western (García-Herrera *et al.*, 2007) sectors of the Mediterranean basin. Recent changes in atmospheric circulation patterns are partially responsible for declining precipitation trend and major drought episodes (García-Herrera *et al.*, 2007), particularly over the western Mediterranean (Paredes *et al.*, 2006; Trigo *et al.*, 2006). Furthermore, the tendency towards a drier climate with higher frequency of droughts is in agreement with climate change scenarios (Giorgi, 2006). For a detailed overview the reader is referred to Chapters 7 and 8 of this book. Recent studies have shown that the occurrence of major droughts in southern Europe during the preceding winter and spring seasons can enhance the amplitude of heat waves on the following summer (Seneviratne *et al.*, 2006; Fischer *et al.*, 2007ab). Thus, both phenomena, droughts and heat waves, should be linked.

The Fourth IPCC Assessment Report (AR4; IPCC, 2007) identifies the Mediterranean Basin as a climate change and biodiversity "hot spot" (Giorgi, 2006; Christensen *et al.*, 2007; Diffenbaugh *et al.*, 2007; Schneider *et al.*, 2007) with high probability of more frequent drought episodes and severe heat waves. The vast majority of studies based on global and regional climate model results suggest that the Mediterranean area will experience a general trend towards less precipitation during the 21st century (Gibelin and Deque, 2003; Giorgi and Lionello, 2008; Mariotti *et al.*, 2008). The combined effects of precipitation decrease and surface temperature increase in the Mediterranean will most probably lead to important changes in the region's water cycle. According to Mariotti *et al.* (2008), the CMIP3 ensemble of multi-model simulations projects towards the end of the 21st century a 20% decrease in land surface water availability and a 24% increase in the loss of fresh water over the Mediterranean Sea due to precipitation reduction and warming–enhanced evaporation. Twentieth century simulations and observations indicate that the rising tendency of recent decades towards drier conditions in the Mediterranean basin will continue in the 21st century (Mariotti *et al.*, 2008; see also section 8.3.2, this book).

Changes of precipitation regimes in the Mediterranean are known to be associated with storm tracks changes that are controlled by large scale circulation modes, such as the North Atlantic Oscillation (NAO), the East Atlantic/Western Russia Pattern (EA/WR) or the Scandinavian Pattern (SCAND) (Quadrelli *et al.*, 2001; Trigo *et al.*, 2002; Duenkeloh and Jacobeit, 2003; Xoplaki *et al.*, 2004). Changes of the precipitation regime, (annual average as well as seasonal cycle) are associated with major impacts in the availability of water resources for agriculture (Iglesias and Quiroga, 2007), vegetation dynamics (Gouveia *et al.*, 2008) and energy production (Trigo *et al.*, 2004). In this regard, the pronounced decline of precipitation throughout the western Mediterranean (particularly over Iberia) since the 1960s in late winter and early spring and observed impacts (Paredes *et al.*, 2006; Trigo *et al.*, 2008; González-Hidalgo *et al.*, 2009) could be used as an early indication of the future climate impacts in the

region, namely in water resources and drought frequency. Therefore it is of paramount importance to understand the links between the large scale patterns and the regional climate at surface and its evolution under climate change.

Summer heat waves are controlled by intense anticyclonic circulation, often associated with upper tropospheric blocking high. Heat waves have been shown to be responsible for excessive mortality, particularly during prolonged events such as the 2003 heat wave in Europe and part of western Mediterranean that was associated with 40,000 fatalities (García-Herrera *et al.*, 2010) and the devastating 2010 eastern European/western Russian heat wave with 55,000 fatalities and 25% annual crop failure in Russia only (preliminary estimates, Barriopedro *et al.*, 2011). Equally, heat wave events can be the main drivers of large wildfires occurrence, such as those that occurred in Portugal in 2003 with more than 430,000 ha burnt area (García-Herrera *et al.*, 2010), or more recently, in Greece in 2007 with more than 310,000 ha of burnt area and 80 fatalities (European Commission, 2008).

Extreme events, like droughts, heat waves and their changes in frequency and intensity as well as changes in Mediterranean water cycle lead to some of the major socioeconomic impacts in the area. The reader is also referred to Navarra and Tubianna (2011) for a comprehensive review of impacts associated to climate change in the Mediterranean derived from the CIRCE project (www.circeproject.eu).

This chapter provides information on the above phenomena and the associated atmospheric circulation and patterns which were not addressed in the first MedCLIVAR book (Lionello *et al.*, 2006). Section 6.2 reports on heat wave events. Related impacts in different parts of the Mediterranean are presented in the form of case studies. Mediterranean droughts and the influence of teleconnections are given in section 6.3. A review on the Mediterranean water cycle based on observations and modeling results is analyzed in section 6.4. The socioeconomic impacts of climate change and variability are caused by the changes in local conditions. As stated previously, in the Mediterranean, the local climates are driven by a diversity of large circulation patterns, one of which is the NAO. Section 6.5 provides an overarching view of the most relevant NAO socioeconomic impacts. The chapter ends analyzing how some precipitation extremes are associated to circulation anomalies in the region.

6.2. Heat wave mechanisms and impacts

Heat waves have discernible impacts including rise in mortality and morbidity (Knowlton *et al.*, 2009), an increased strain on infrastructure (power generation, water supply, transportation) (Smoyer-Tomic *et al.*, 2003) and consequent impacts on society. Further impacts may include effects on agricultural resources, the retail industry, ecosystem services and tourism (Ferris *et al.*, 1998; Ciais *et al.*, 2005). Large financial losses due to crop shortfall, forest fires or increased mortality highlight the strong impact potential of heat waves on the environment, society and economy (Kovats and Koppe, 2005; Poumadère *et al.*, 2005; IPCC, 2007).

With regards to human mortality, morbidity and comfort the importance of high night-time temperatures, high relative air humidity and low wind speed have been highlighted by a number of works (e.g., Steadman, 1979; Karl and Knight, 1997; Conti *et al.*, 2005; Grize *et al.*, 2005, among others). Fischer and Schär (2010) state that the most severe impacts arise from multi-day heat waves, associated with warm night-time temperatures and high relative air humidity. Warm nights hamper recovery from the day-time heat and stress additionally the human body through

the reduced rejuvenating effect of sleep and thus strongly amplify health effects (Fischer and Schär, 2010). Fischer and Schär (2010) point to the particularly relevant stress factor of high relative air humidity for human thermoregulation. In cases of high relative air humidity, the effectiveness of the human body temperature control mechanism (evaporative cooling through sweating) is reduced, due to the lower evaporation rate.

Especially coastal, urban and lowland areas are affected by such conditions during severe summer heat waves. (Karl and Knight, 1997; Kuglitsch *et al.*, 2010; Kuglitsch, 2010) and are likely affected in the future in southern Europe and the Mediterranean (Fischer and Schär, 2010).

However, a universal definition of heat waves does not exist, and it has been shown that the number, length and intensity of summer heat waves are most crucial for impact research (Changnon *et al.*, 1996; Trigo *et al.*, 2009; Kuglitsch *et al.*, 2010). Kuglitsch *et al.* (2009; 2010) applied a heat wave definition aiming to be applicable to the assessment of climate impacts for the eastern Mediterranean taking into account both day- and night-time temperatures, thus daily maximum and minimum temperatures — presented in section 6.2.2.

Throughout the 21st century the Mediterranean area is expected to be one of the most prominent and vulnerable climate change "hot spots" (Giorgi, 2006). According to Diffenbaugh *et al.* (2007) the Mediterranean will experience a larger number of extremely hot temperature events, a further increase of the already observed summer heat wave frequency and duration (Türkeş *et al.*, 2002; Founda *et al.*, 2004; Kostopoulou and Jones, 2005; Della-Marta *et al.*, 2007; Kuglitsch *et al.*, 2010) and increasing summer temperature variability. A recent study has analysed in detail the likely changes on geographical patterns of heat waves based on six high resolution regional climate models of the ENSEMBLES multimodel scenario experiment (Fischer and Schär, 2010). It shows that for Iberia and the Mediterranean region, the frequency of heat wave days (defined as those days when the 90th percentile of the local maximum temperature distribution is surpassed on at least six consecutive days) is projected to increase from an average of about two days per summer during 1961–1990 to 40 days for 2071–2100. Along with the increasing frequency, heat waves are projected to become longer lasting and more intense (Schär *et al.*, 2004; Meehl and Tebaldi, 2004; Giorgi *et al.*, 2004; Beniston *et al.*, 2007; Tebaldi *et al.*, 2006; Fischer and Schär, 2009, 2010). The projected changes in heat wave characteristics relate to strong mean summer warming and enhanced temperature variability. Changes in the summer temperature variability are expected both on interannual and subseasonal time scales (Fischer and Schär, 2009). The key mechanisms vary between time scales and generally relate to a combined effect of changes in atmospheric circulation and the transition from a relatively wet to dry soil moisture regime (Vidale *et al.*, 2006; Lenderink *et al.*, 2006; Seneviratne *et al.*, 2006; Fischer and Schär, 2009).

The next section of the chapter analyses some of the most relevant mechanisms leading to heat waves and then focuses on most severe recent heat waves and associated circulation for the eastern and western parts of the Mediterranean basin based on two different approaches.

6.2.1. Atmospheric circulation and heat waves

Persistent circulation anomalies

Surface climate variables are primarily the result of the weather conditions at the synoptic scale. Although in localized areas the importance of mesoscale perturbations is prevalent (see e.g.

Jansá *et al.*, 2001), extreme meteorological events — in particular high temperature — are strongly influenced by persistent large scale circulation patterns. Historically, the first such pattern to be identified by synoptic meteorologists was the so called atmospheric blocking (Rex, 1950), consisting of a persistent high pressure anomaly that displaces northward the mid-latitude jet, hence blocking it from hitting a particular region. Atmospheric blocking tends to appear with a certain frequency in well-defined regions of the world (D'Andrea *et al.*, 1998; Barriopedro *et al.*, 2010b), namely over northeastern Atlantic Ocean and Europe, and over the northern Pacific Ocean. Successive objective analysis led to the identification of other persistent anomalies that have a recurrent character in a given region, and that influence local climate. These are often referred to as "weather regimes". Extensive investigations have been carried out on wintertime regimes, and comparatively less during the other seasons. The patterns, however, appear to be quite stable across seasons (compare e.g., Mukougawa and Sato, 1999 and Michelangeli *et al.*, 1994). Summertime weather regimes of geopotential height at 500 hPa (Z500) for the Euro-Atlantic region in summer are shown in Figure 6.1, reproduced and elaborated from Cassou *et al.* (2005). Other than blocking, that can be seen in panel a, the regimes consist of: a low pressure system located in the centre of the north Atlantic (panel b), an enhanced Greenland ridge (panel c), and a high pressure in the centre of the North Atlantic, accompanied by a low to the north (panel d). Despite the two figures refer to different seasons and timescales, and are obtained with different techniques, the partial correspondence of these patterns with those of Figure 5.1 (Chapter 5 this book), can be seen especially in the NAO– and the Atlantic low, called EA pattern by Barnston and Livezey (1987). Identifying the persistent large scale anomalies that lead to large amplitude excursions of surface variable is a relevant issue for seasonal prediction as well as for future local climate projections and impacts. In fact, small scale climate projections are often based on statistical downscaling approaches (Zorita *et al.*, 1995) based on large scale predictors such as atmospheric flow, even though additional predictors generally provide better downscaling estimations (Charles *et al.*, 1999; Xoplaki *et al.*, 2004).

Cassou *et al.* (2005) have identified, among the four regimes presented in Figure 6.1, those two that are linked to hot summer temperatures in France. These are the blocking (Figure 6.1a) and Atlantic low (Figure 6.1b) regimes. Figure 6.1 shows next to each regime of the left column the corresponding relative frequency change of high temperature episodes in France (see the caption of Figure 6.1 and Cassou *et al.*, 2005 for details). The two regimes have dynamical characteristics that are quite different and seem to cause heat and drought in France and western Europe for at least partially different reasons. The Atlantic low puts western Europe, from the Iberia to the British Isles, under southerly wind conditions that are likely connected with warm air advection over the area for purely dynamical reasons. Conversely, blocking isolates the northern part of western Europe (including northern France, connected to the enhanced frequency of extreme warm days shown in Figure 6.1e) from Atlantic influence, increased stability, decreasing moisture flux, favouring dry and clear sky conditions. Also the Atlantic low regime (Figure 6.1b) affects in a similar way the main continental part of Europe, as can be seen by the corresponding temperature conditions over France (Figure 6.1f).

Periods of anomalously high temperatures over Europe and the Mediterranean have been connected with anticyclonic conditions over the area in several works (e.g., Xoplaki *et al.*, 2003b; Black *et al.*, 2004; Yiou and Nogaj, 2004; Cassou *et al.*, 2005; Yiou *et al.*, 2008). Cassou *et al.* (2005) described the 2003 European heat wave in terms of weather regimes, verifying like this the hypothesis formulated in the work of Reinhold and Pierrehumbert (1982) that large excursions from climatological values of surface variables in a season could be

explained by the anomalous frequency of a given weather regime occurrence. Cassou *et al.* (2005) related the occurrence of high temperature episodes in France to a large anomaly in regime frequency during a season. They showed that the frequency of occurrence of the Atlantic low regime was largely above its climatological mean during summer 2003. The synoptic situation during summer 2003 was strongly projecting on the Atlantic low regime, especially in June, but partially also in August (e.g., Beniston and Diaz, 2004; Ogi *et al.*, 2005; Trigo *et al.*, 2005; Vautard *et al.*, 2007; García-Herrera *et al.*, 2010 and references therein).

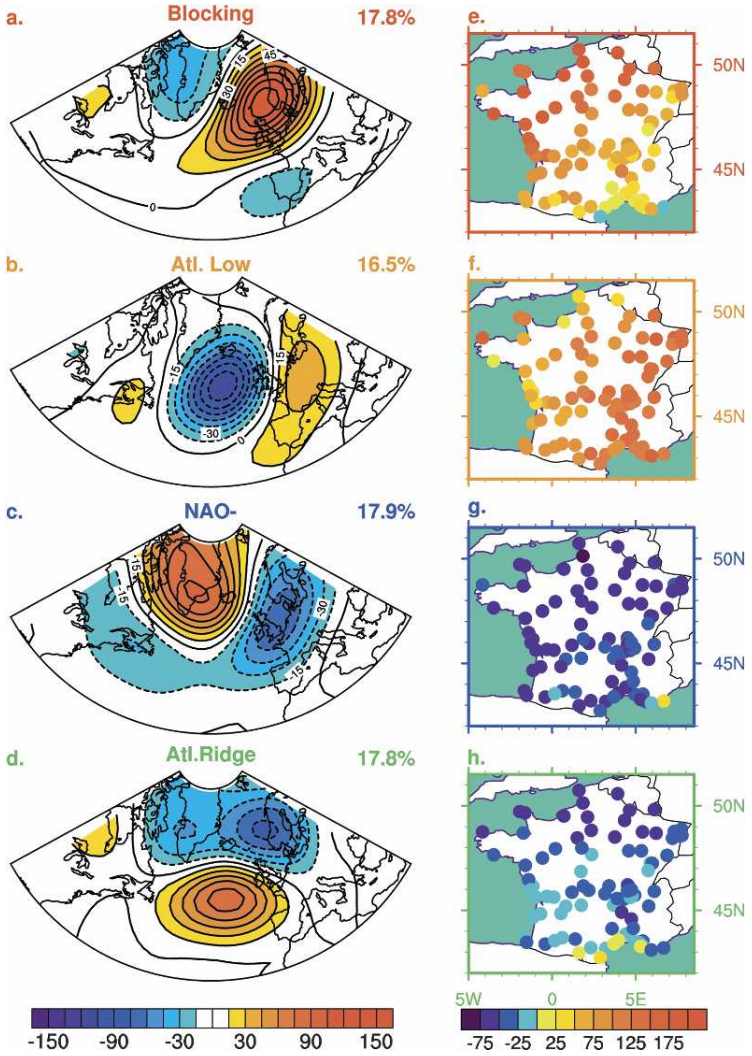

Figure 6.1. (a)–(d): Summer Z500 weather regimes computed over the North Atlantic–European sector from 1950–2003. Contour interval is 15 m, dashed lines denote negative values. To eliminate transient and ambiguous episodes, only sequences of five-days or more occupied by the same cluster are retained. As a result of such a five-day cut-off, the sum of the four regimes 54-yr-averaged occurrence, shown for each weather regime map, is not equal to 100% but around 70%; (e)–(h): Relative changes (%) in the frequency of extreme warm days for each individual regime. Interval of 25% from –100% to 200%, and red above that (max equal to 233%). As an example, 100% corresponds here to the likelihood for extreme warm days to occur multiplied by two. Figure and caption from Cassou *et al.* (2005) © Copyright 2005 American Meteorological Society (AMS).

The onset and decay of persistent circulation anomalies are due to the nonlinear dynamics of the synoptic scale flow, which involves large scale Rossby waves, their interaction with baroclinic perturbations, as well as topographic effects. Nevertheless, the probability of

occurrence of one or the other of the regimes has been shown to be influenced — in a measurable if small amount of its total variance — by a number of external forcing mechanisms, ranging from local or remote sea surface temperatures (SST) to stratospheric circulation anomalies. The study of these forcing mechanisms is particularly interesting because it influences the predictability of regimes occurrence, and hence of the seasonal climate in a region. Some of those forcings are discussed in the following section.

Large scale forcing mechanisms

In the context of temperature extremes in Europe and the Mediterranean, different driving mechanisms have been analysed, and the case of the 2003 heat wave has been the most studied (e.g., Schär *et al.*, 2004; Stott *et al.*, 2004; García-Herrera *et al.*, 2010 and references therein).

Mediterranean SSTs (averaged over the entire Mediterranean basin) during the 2003 heat wave (May to August) were constantly above the corresponding mean averaged for the previous 45 years (Grazzini and Viterbo, 2003). Although the geopotential height anomalies over Europe and persistent SST anomalies are likely to be closely linked, the exact role of high SSTs in the Mediterranean for the 2003 heat wave is not clear (Beniston and Diaz, 2004). The global-scale SST anomalies effect on the large pressure pattern found in summer 2003 was studied by Feudale and Shukla (2007) who obtained a pressure anomaly similar to the Atlantic low regime (Figure 6.1b) when forced a GCM simulation with observed global SSTs. Forcing with the SST anomalies in the Mediterranean only produced a similar pressure anomaly though of a lower amplitude. Black and Sutton (2007) suggested a combined effect of SST anomalies in the Indian Ocean and the Mediterranean. Their findings suggest that the Mediterranean contributed most strongly to the early part of the 2003 heat wave and that the Indian Ocean enabled the positive temperature anomalies to persist well into August. Using a different model, Ferranti and Viterbo (2006) and Jung *et al.* (2006), found somewhat conflicting results, suggesting that the enhanced SSTs in the Mediterranean had only a marginal influence on the mid-tropospheric dynamical circulation and temperature in Europe.

Cassou *et al.* (2005) analyzed in a GCM integration the effect of an increase of tropical Atlantic convective activity on the regime frequency by prescribing anomalous diabatic forcing due to water condensation in the cumulus clouds. They found that the frequency of the two regimes presenting anticyclonic/blocking conditions over the Euro-Atlantic area (Figures 6.1a and 6.1b) is largely increased in this case. Cassou *et al.* (2005) suggest the existence of a mechanism linking SST anomalies - via its influence on convective activity - to circulation regimes in the extra-tropics.

Several studies suggest an important contribution of land surface-atmosphere feedback mechanisms to the amplification of recent heat waves (Black et al. 2004, Ferranti and Viterbo 2006, Fischer et al. 2007a,b). In 2003, large sectors of Europe suffered from persistent dry conditions in late winter and spring, before even reaching the summer heat wave event. Over large parts of Central Europe, average precipitation was reduced by more than 50% in the four months between February and May 2003 (Fischer et al. 2007b). The persistent surface net radiation excess and the early vegetation onset (Zaitchik et al. 2006) during the same period, resulted in enhanced evapotranspiration and thereby further contributed to rapid soil drying (Fischer et al. 2007a). The drying of the land surface act on surface temperatures through the change of turbulent heat fluxes partitioning (e.g. Vautard *et al.*, 2007; García-Herrera *et al.*, 2010) — or Bowen ratio. The reduction in latent heat flux induced by a lack of moisture availability in the surface results in enhanced sensible heat flux. Fischer *et al.* (2007b) suggested

that given essentially identical continental-scale circulation, however without anomalous soil drying, the 2003 JJA maximum temperature anomalies would have been regionally reduced by around 1-3°C (40-50% of 2003 summer anomalies). A good representation of these anomalous land surface conditions has been found to substantially improve the predictability of the 2003 heat wave retrospective forecasts performed at European Centre for Medium Range Weather Forecast (Weisheimer *et al.*, 2011).

While the land surface feedbacks mainly act through local effects on the surface energy budget, it has been suggested that during the 2003 heat wave dry land surface conditions likely amplified and elongated the (pre-existing) anticyclonic circulation anomalies, which in turn positively fed back on surface temperatures (Fischer *et al.*, 2007a). Zampieri *et al.* (2009) recently underlined this finding by showing the non-local effect of soil moisture anomaly in the Mediterranean on temperature in the centre of continental Europe, through both changes of air cloudiness and humidity, but also through the creation of a large scale pressure anomaly pattern, closely resembling blocking.

Dry land surfaces can further affect other variables such as precipitation through direct effects, i.e. regulation of absolute moisture input resulting from modified evapotranspiration, and indirect effects, i.e., the impacts on the boundary-layer stability and precipitation formation (Seneviratne *et al.*, 2010 and references therein). The local changes in convective stability on the other hand are also capable of creating a larger scale atmospheric response that projects on the weather regimes and in turn affecting temperature and other surface climate variables (Shukla and Mintz, 1982; Rowntree and Bolton, 1983).

Trends in temperature/atmospheric circulation relationship

Over the North Atlantic region, the increased frequency of the positive NAO phase during the 1990s induced more anticyclonic weather over southern and central Europe and enhanced southwesterlies associated with mild winter weather in Northern Europe (Hurrell *et al.*, 2004). Over European land areas, trends in the statistics of surface temperatures and their extremes have been detected (e.g., Klein Tank and Können, 2003; Moberg and Jones, 2005, among others), with a high warming rate of 0.5° C/decade over the past 30 years (Xoplaki *et al.*, 2005; van Oldenborgh *et al.*, 2009).

Extreme warm anomalies can also occur during the cold seasons of the year (fall and winter), which have important effects on ecosystems (e.g., Piao *et al.*, 2008). The long-lasting temperature anomaly of fall–winter 2006–2007 in Europe was also unprecedented (Luterbacher *et al.*, 2007; van Oldenborgh, 2007; Yiou *et al.*, 2007), and was comparable in amplitude to the 2003 summer heat wave. The work of Yiou *et al.* (2007) has shown that the probability of surface temperature variations during the cold seasons can be explained by atmospheric flow alone was actually high until the mid-1990s, but that this relationship starts to diverge after 1995, until a maximum in 2006/2007.

Based on analysis of atmospheric circulation analogues, Vautard and Yiou (2009) showed that the control of surface weather changes by Euro-Atlantic large scale circulation changes is large in the winter season, but not in summer. Wintertime temperature is only partially reproduced by flow-analogue time series. The eastern Atlantic SST trend also has a significant contribution (Cattiaux *et al.*, 2009), as well as other processes like aerosols and snow cover. In summer, atmospheric flow changes do not seem to drive temperature trends, where temperature strongly interacts with the water cycle (Vautard and Yiou, 2009).

Another conclusion is that an acceleration of the observed trends has taken place in the latest half of the record, i.e. during the past three decades (Vautard and Yiou, 2009). For most variables observed and constructed trends from analogues have a larger difference than when considered over the whole record, indicating an evolution to less atmospheric flow control, this is illustrated in Figure 6.2, taken from Vautard and Yiou (2009). If this late behavior is extrapolated, it is not clear whether the atmospheric flow control will still apply in the next decades, and it is expected that its influence will weaken.

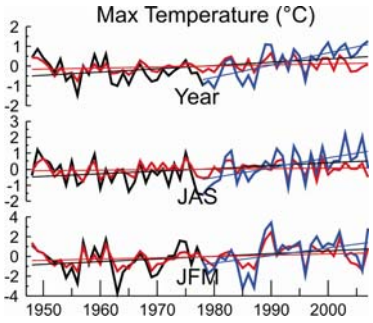

Figure 6.2. Time evolution of the annual and seasonal average, over an ensemble of European stations, of observed (black curves for the earliest 30 years and blue curves for the latest 30 years) or constructed (red curve) anomalies, together with linear regression lines of maximum temperature (°C) for (top) annual average, (middle) summer (JAS) average, and (bottom) winter average. Figure and caption adapted from Vautard and Yiou (2009) published at Geophysical Research Letters

6.2.2. Heat waves and their impacts in the eastern and western Mediterranean

Heat waves in the eastern Mediterranean

Heat wave events, changes and connected atmospheric circulation in the eastern Mediterranean, an area characterized by strong environmental gradients, climate extremes and diverse economic, social and cultural identities, have been analyzed for the period 1960–2006 by Kuglitsch *et al.* (2009; 2010) and Kuglitsch (2010). They used high quality and homogenized daily maximum (TX) and minimum (TN) air temperature data and percentile (95th) based temperature thresholds (Karl and Knight, 1997; Gosling *et al.*, 2009; Kuglitsch *et al.*, 2009). The importance of considering TN was highlighted by Karl and Knight (1997) who concluded that three or more consecutive nights with no relief from very warm night-time (minimum) temperatures may be most important for human health impacts. It has to be noted that an extension of this analysis to cover the whole Mediterranean has for the moment not been done due to station daily time series availability, quality control and correction issues over other parts of the basin.

For their analysis, Kuglitsch *et al.* (2009; 2010) and Kuglitsch (2010) define a hot day (night) as a day (night) when the daily TX (TN) exceeds the long-term (1969–1998) daily 95th percentile within the extended summer June–September season (122 days). For each June–September day, the 95th percentile is calculated from a sample of 15 days (seven days on either sides of the respective day) using data over the 1969–1998 period. Following the works by Meehl and Tebaldi (2004), Díaz *et al.* (2006) and Della-Marta *et al.* (2007), Kuglitsch *et al.* (2009; 2010) and Kuglitsch (2010) defined a heat wave (HW) as a period of *three* or more

consecutive hot days and nights not interrupted by more than one non-hot day or night. Figure 6.3 provides a schematic overview of heat waves detected for the station of Ankara (Turkey) for the summer of 2006.

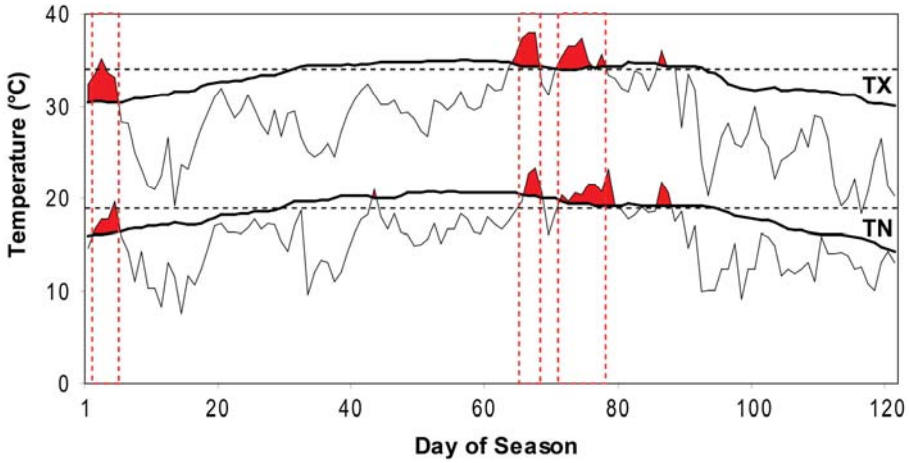

Figure 6.3. Schematic overview of heat wave detection. The thick black lines indicate the daily 95th percentile and daily values of 2006 (thin black lines) for TX and TN for the station of Ankara, Turkey. Red areas characterize hot days and nights. Red dotted frames indicate the three 2006 heat waves in Ankara. Adapted from Kuglitsch *et al.* (2010) published at Journal of Geophysical Research-Atmospheres.

TX and TN series of 246 stations across the eastern Mediterranean region have been homogenized (Kuglitsch *et al.*, 2010) for the period 1960–2006. The inhomogeneity affected temperature time series underwent a negative adjustment in the 1960s that revealed the earlier underestimation of daily temperature tendency in the area and consequently an enhancement of heat waves number, intensity and duration.

Linear trends of *HWN95* (number of summer heat waves per year), *HWL95* (in days) and *HWI95* (summation of the local TX and TN exceedances, i.e. degree days in ° C) and their significance are estimated using the ordinary least square technique (OLS) and the Mann-Kendall rank correlation test for the period 1960 to 2006.

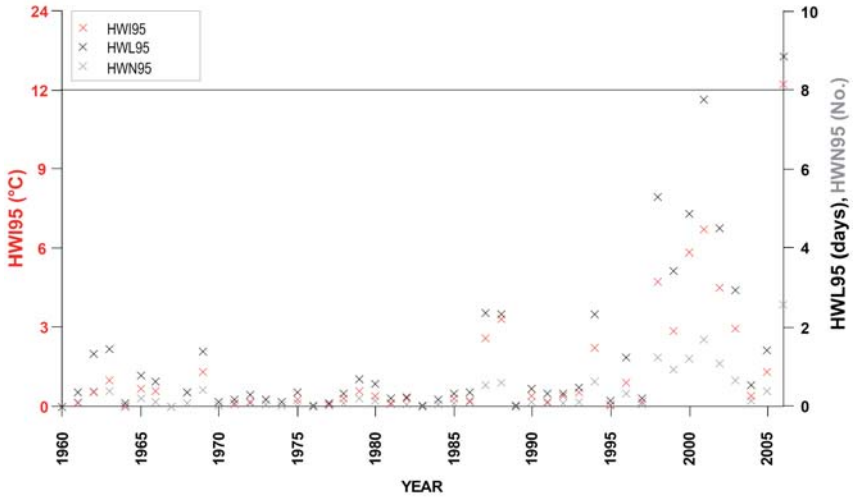

Figure 6.4. Eastern Mediterranean summer *HWN95* (grey crosses), *HWL95* (black crosses) and *HWI95* (red crosses), 1960–2006. From Kuglitsch *et al.* (2010) published at Geophysical Research Letters.

Spatially averaged hot summer daytime (TX 95th percentile) and night-time temperatures (TN 95th percentile) have increased by +0.38 ± 0.04° C/decade and +0.30 ± 0.02° C/decade, respectively since the 1960s. During the same period, the mean heat wave intensity (*HWI95*), heat wave length (*HWL95*) and heat wave number (*HWN95*) increased by a factor 7.6 ± 1.3, 7.5 ± 1.3 and 6.2 ± 1.1, respectively (Figure 6.4; see Kuglitsch *et al.*, 2010 for details).

"Hot spots" of heat wave changes are identified along the eastern parts of the Turkish Black Sea coastline, in western, southwestern and central Turkey, and across the western Balkans (Figure 6.5). Kuglitsch *et al.* (2009; 2010) and Kuglitsch (2010) have further shown that the increase in *HWI95* and *HWL95* is much more pronounced than changes in the intensity and length of the longest heat wave per season. This implies that the eastern Mediterranean is more affected by an accumulation of short (< 6 days) but more intense heat wave events compared to earlier decades. At many stations, the longest heat wave event per year has not lengthened and intensified, yet, however, longer lasting and more intense events have been detected since 2000.

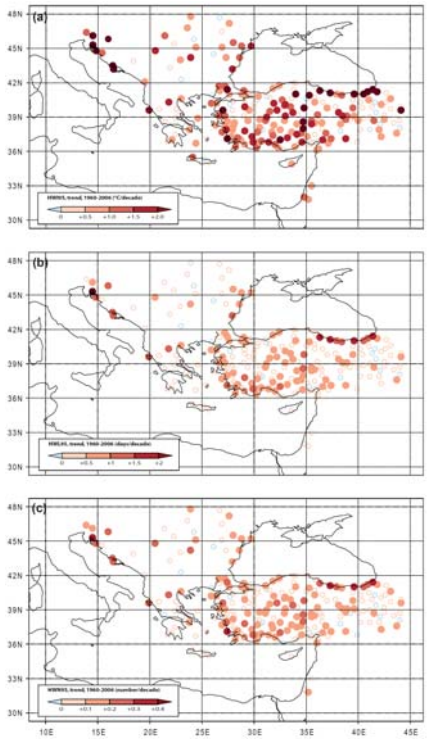

Figure 6.5. Linear trends of (a) *HWI95* (° C/decade), (b) *HWL95* (days/decade) and (c) *HWN95* (number/decade), 1960–2006 using Ordinary Least Squares. Red (blue) dots indicate significant positive (negative) linear trends at the 95% significance level (Mann–Kendall test). Open circles characterize non-significant trends. From Kuglitsch *et al.* (2010) published at Geophysical Research Letters.

Deadly heat waves in the eastern Mediterranean

Between 1960 and 2006, the ten most severe heat wave summers, in terms of heat wave length and intensity, affecting large areas of the eastern Mediterranean are identified in 1987, 1988, 1994, 1998, 1999, 2000, 2001, 2002, 2003 and 2006 (c.f., Fig. 1 in Kuglitsch *et al.*, 2010) and agree with the most deadly heat waves reported by EM–DAT (The International Disaster Database, www.emdat.be) and WHOSIS (World Health Organization Statistical Information System; www.who.int/whosis/en/index.html). Table 6.1 summarizes the number of people killed during the most severe heat wave summers in the eastern Mediterranean countries. In these summers, at least one large scale — areas between several 10,000 and several 100,000

km^2 — heat wave is found. Summers when only single (usually urban) stations were affected by heat waves indicate the importance of local climate effects. In the following section, the large scale atmospheric circulation and relative air humidity related to heat waves affecting larger areas in the Eastern Mediterranean have been analyzed.

The large scale atmospheric circulation at 500 hPa geopotential height level (Z500) and SLP and relative humidity (RH) anomaly composites (with respect to 1968–1999) of the ten most severe summer heat waves in the eastern Mediterranean are shown in Figure 6.6. The data stem from the NCEP-NCAR reanalysis dataset (Kalnay *et al.*, 1996; Kistler *et al.*, 2001).

Table 6.1. Number of fatalities during summer heat waves in eastern Mediterranean countries. NA characterizes the years when no heat wave related mortality data has been reported. (Data source: EM-DAT [The International Disaster Database, www.emdat.be] and WHOSIS [World Health Organization Statistical Information System; www.who.int/whosis/en/index.html])

COUNTRY	1987	1988	1998	1999	2000	2001	2002	2003	2005	2006	ALL YEARS
Albania	NA	NA	8	6	0	0	NA	NA	NA	NA	**14**
Bulgaria	NA	NA	54	35	56	27	90	NA	NA	NA	**262**
Croatia	NA	NA	15	0	40	0	0	788	22	69	**934**
Cyprus	NA	NA	52	NA	5	NA	NA	NA	NA	0	**57**
FYROM	NA	NA	0	0	0	NA	NA	NA	NA	NA	**0**
Greece	> 2,000	56	1,976	378	27	0	NA	NA	NA	NA	> 4,437
Israel	NA	NA	160	33	0	0	0	37	0	NA	**230**
Romania	NA	38	20	280	123	84	129	220	368	611	**1,873**
Serbia	NA	NA	50	0	3	0	0	55	0	116	**224**
Slovenia	NA	NA	0	0	0	0	0	289	0	12	**301**
Turkey	NA	NA	NA	NA	11	NA	NA	NA	NA	NA	**11**
ALL COUNTRIES	> 2,000	**94**	**2,335**	**732**	**265**	**111**	**219**	**1,389**	**390**	**808**	> 8,343

The 500 hPa composites indicate positive large scale anomalies as a long belt extended from the southeastern to the northwestern edges of the spatial window covering the whole Mediterranean area. Negative anomalies are centered over the British Isles. At sea level the negative anomalies are extended south- and southeastward restricting the above normal pressure over the Caspian Sea. These patterns have a strong resemblance to those found by several authors (e.g., Xoplaki *et al.*, 2003ab) for extreme warm summers in Greece and the eastern Mediterranean. They have investigated the large scale atmospheric circulation at different geopotential height and thickness levels and found that the dominating warm air over the eastern Mediterranean is connected with an anomalous northeasterly-to-easterly continental flow and subsidence at upper levels (Figs 5 and 6 in Xoplaki *et al.*, 2003b) in addition to the warm and dry air advection from the Persian Gulf towards the eastern Mediterranean (Figure 6.6, this study). Such atmospheric conditions lead to increased stability and inhibition of convection resulting in clear skies and maximum insolation and reduced relative air humidity with greater reduction in most continental regions (eastern Balkans, eastern Turkey). High air temperatures over land in combination with high SSTs lead to increased latent and sensible heat fluxes (Xoplaki *et al.*, 2003ab). Due to the stability of the atmosphere, the vertical heat flux is restricted to the lower boundary layer, the mixing is reduced and the warm air masses are trapped within the boundary layer.

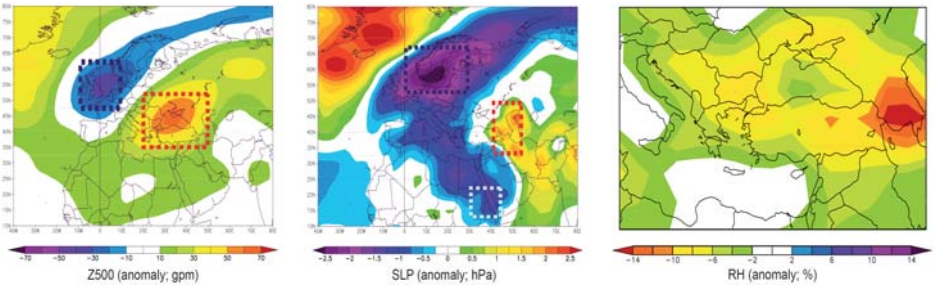

Figure 6.6. Composite anomalies of Z500 (gpm; left), SLP (hPa; centre) and RH (%; right) (with respect to 1968–1999) during heat wave days in the 10 most extreme summer heat waves in the eastern Mediterranean. In rectangles are the centers of positive (red) and negative anomalies (blue). Data stem from NCEP-NCAR reanalysis dataset (Kalnay *et al.*, 1996; Kistler *et al.*, 2001).

The western Mediterranean: the 2003 heat wave case study

The case-study of the summer 2003 heat wave (EHW03) in the western Mediterranean is analyzed due to the unprecedented impacts of the heat wave in the area and also because EHW03 can be considered as representative of a future scenario (Beniston, 2004; Schär *et al.*, 2004; Stott *et al.*, 2004).

During the summer 2003, areas of western Mediterranean countries, such as France, Spain and Portugal experienced record-breaking temperatures (García-Herrera *et al.*, 2010 and references therein). Daily TX during this EHW03 period exceeded 40° C across most of interior Spain and central Portugal, 36–38° C across southern and central France. In general, these temperatures were 7.5–12.5° C above average (García-Herrera *et al.*, 2010). In Portugal, the historical record of absolute extreme temperatures was surpassed on the 1st of August, with the TX (TN) reaching a new all-time record of 47.3º C (30.6º C) near the border with Spain (Trigo *et al.*, 2006). However, the most relevant feature of the EHW03 was possibly not the record-breaking temperatures but the absence of cooler night-temperatures and the large number of very warm days (Rebetez, 2004), also in countries as Spain where no historical records were exceeded. At European scale, it has been estimated that the summer of 2003 is extremely likely the hottest for at least the last half of the millennium (Luterbacher *et al.*, 2004).

Figure 6.7 shows the bi-daily temperature anomalies at the 850 hPa geopotential height level (T850) of the period 3–13 August 2003 with respect to the 1958–2002 mean (see also Fig. 4 in García-Herrera *et al.*, 2010 for the whole period 1-14 August 2003). The data stem from the NCEP-NCAP reanalysis (Kalnay *et al.*, 1996; Kistler *et al.*, 2001). The temperature anomalies have been computed following the procedure suggested by Trigo *et al.* (2005, 2006) that calculates and presents as well the area where previous absolute maximum temperature values were exceeded in the European sector. When the value for a region exceeds the daily mean maximum temperature, the difference to the 45-year (1958–2002) absolute maximum is plotted (solid lines). The previous absolute maximum is exceeded for the first time over southern Portugal on the 1st of August, when the anomalies achieved values higher than 9º C (not shown, from Fig. 4 in García-Herrera *et al.*, 2010). Again, on the second of August the central sector of Portugal and western Spain recorded new extreme values, with anomalies of up to 11º C (not shown). As shown in Figure 6.7, the anomaly migrated northeast on third August, presenting a core sector (>11º C) that stretches from northwestern Spain to western France. Interestingly, this anomaly does not exceed previous maxima of the period 1958–2002. The daily patterns between 5 and 13 August showed record breaking anomalies over northern France and southern England (daily anomalies higher than 13º C). The first day with no historical record surpassed was the 14th of August (not shown).

This persistent anomaly throughout a long period was due to a number of forcings, some of which are still under discussion. Among those forcings, the most widely cited are (i) an extremely persistent blocking; (ii) the northward displacement of the Azores anticyclone and the African ITCZ; (iii) a strong positive phase of the East Atlantic teleconnection pattern; (iv) the southward shift of the extratropical storm tracks; (v) the strong amplitude of the summer

Northern Annular Mode; (vi) tropical Atlantic anomalies in the form of wetter than average conditions in the Caribbean basin and the Sahel; (vii) the anomalously clear skies and the downward net radiative fluxes; (viii) the prolonged high SSTs in the northern North Atlantic and the Mediterranean; and (ix) the intense negative soil moisture anomaly in central Europe and the resulting feedback mechanism (see García-Herrera *et al.*, 2010 and references therein for details). Despite the long list of candidate mechanisms, it seems clear that the blocking circulation over most of western Europe and the extremely dry soils during the previous seasons were the main drivers (e.g., Beniston and Diaz, 2004; Black *et al.*, 2004; Fink *et al.*, 2004; Cassou *et al.*, 2005; Ogi *et al.*, 2005; Trigo *et al.*, 2005; Della-Marta *et al.*, 2006; Ferranti and Viterbo, 2006; Zaitchik *et al.*, 2006; Fischer *et al.*, 2007ab; Vautard *et al.*, 2007; García-Herrera *et al.*, 2010; Alexander, 2011). These factors do not act independently and are also related with the monthly climatic anomalies observed for the previous winter and spring months, which were characterized by large positive temperature anomalies in the lower troposphere and at the surface extending between the British Isles and Scandinavia. Simultaneously, large and persistent negative precipitation anomalies between Scandinavia and the central Mediterranean. On the contrary, the western (Iberia) and eastern sections (Turkey) of the Mediterranean basin experienced higher than average precipitation. It seems undoubtedly that this previous dry season lead to a severe soil moisture deficit which amplified the effect of the blocking-type anomaly (Fink *et al.*, 2004; Lakshmi *et al.*, 2004; Della-Marta *et al.*, 2006; Ferranti and Viterbo, 2006; Vautard *et al.*, 2007; Zaitchik *et al.*, 2006; Seneviratne *et al.*, 2006; Fischer *et al.*, 2007ab; García-Herrera *et al.*, 2010).

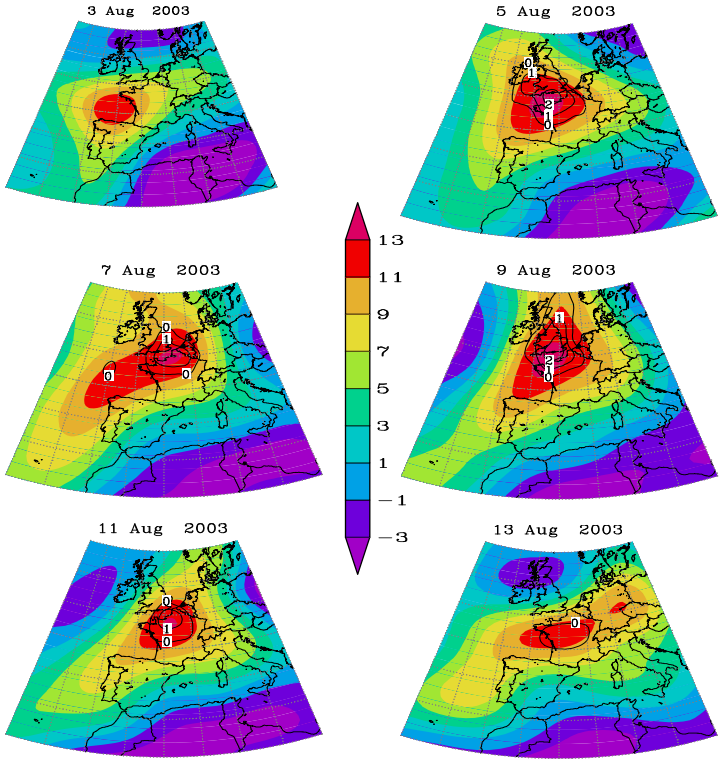

Figure 6.7. Sequence of bi-daily 850 hPa air temperature anomalies (º C) from 3–13 August 2003. Days are identified on the top of each panel. Regions with temperature above the historical maximum are delimited by solid contours (º C). All data stem from NCEP-NCAR reanalysis dataset (Kalnay *et al.*, 1996; Kistler *et al.*, 2001). Adapted from García-Herrera *et al.* (2010) published at Critical Reviews in Environmental Science and Technology

The extreme weather conditions recorded during the summer 2003 heat wave were responsible for more than 40,000 deaths in affected countries in the central and western Europe and western Mediterranean. Women older than 75 years were the most heavily impacted group in all the countries (García-Herrera *et al.*, 2010). In Portugal, the forest fires broke all previous records and almost 5% of the total territory was burnt (Trigo *et al.*, 2006). Europe-wide, as a consequence of the extreme warm and dry conditions primary productivity was reduced in around 30% (Ciais *et al.*, 2005) and the losses in the agricultural sector have been estimated in around 10 billions USD (Munich Re, 2004). Tropospheric ozone information thresholds were surpassed in 23 countries according to the European Environmental Agency. The exceedance episodes were concentrated in southwestern France, southeastern Germany, Switzerland and northern Italy. The reader is referred to the work by García-Herrera *et al.* (2010) and references therein for a detailed discussion on the EHW03 impacts.

According to Stott *et al.* (2004), anthropogenic warming likely contributed to EHW03 by doubling its probability of occurrence. Different studies (e.g., Beniston, 2004; Beniston and Diaz, 2004; Meehl and Tebaldi, 2004; Schär *et al.*, 2004; Stott *et al.*, 2004) suggest that episodes similar to EHW03 may occur more frequently in the future due to global warming. The analysis of EHW03 has helped to mitigate the impact of similar future episodes (e.g., Paris). This has been achieved through the implementation of better forecasting and an improvement of the prevention services. In fact, this episode has been a landmark across Europe since currently all European countries have implemented early warning systems for high temperatures during the summer. For example, Portugal developed one of the first heat wave alert systems in Europe, labeled ÍCARO and implemented in 1999 for the capital city of Lisbon (Trigo *et al.*, 2009). The long-term maintenance of these systems should contribute to a reduction of the health impacts of heat waves.

6.3. Mediterranean droughts and the El Niño–Southern Oscillation

Drought is a natural, recurring, process that occurs when water availability is below normal levels over a long period that cannot supply the existing demand (Havens, 1954; Redmond, 2002). Climate droughts are usually characterized by below-normal precipitation over a period of months to years (Dai, 2011), although other climate variables (e.g., evapotranspiration, relative humidity, wind speed, etc.) also play a high role to define drought severity (Burton *et al.*, 1978). Unlike aridity, drought is a temporary anomaly, clearly distinguished from the well-defined dry season or the climatological aridity. It should be noted that drought events can exceed in length the dry season and persist for much longer time periods. According to WMO (2006), drought by itself is not a disaster. However, the vulnerability of societies, economies and the environment, and their resilience (the ability of systems to cope and recover from drought) ultimately determine the severity of drought and its impacts.

Compared to other natural hazards, drought differs in several ways (Wilhite, 2000): The onset, the end and the surface extent of a drought are difficult to determine unambiguously and this is usually done by using an arbitrary threshold level based on drought indices. Drought impacts linger for a considerable period of time following the return to normal precipitation and water availability levels (Changnon and Easterling, 1989; WMO, 2006). There is no single universally accepted definition of drought (Wilhite and Glantz, 1985), while due to its long-term development and duration, progressive character of its impacts and diffuse spatial limits, drought is the most complex natural hazard to be identified, analyzed, monitored and managed (Burton *et al.*, 1978; Wilhite, 1993). In addition, drought impacts are usually non-structural and

spread over large geographical areas in comparison to damages that may result from other natural hazards. Finally and unlike other natural hazards, human activities can directly trigger a drought mainly by altering the societies' and the environment vulnerability to drought. For example activities such as over-farming, excessive irrigation, deforestation, and erosion can degrade ecosystems, well adapted to the natural climate variability, and adversely impact the ability of soil to capture and hold water. In addition, over-demand of water resources may also increase the societal vulnerability to cope with drought periods. Nevertheless, human activities mainly aim at reducing the societies and economic systems vulnerability to drought, but also to improve the management of drought periods (e.g., adapting crops, drilling wells, building dams, etc).

Droughts are usually classified as a) meteorological, b) hydrological, c) agricultural and d) socioeconomic (Wilhite and Glantz, 1985; AMS, 1997; WMO, 2006; Mishra and Singh, 2010; Dai, 2011). The definitions of the different types of drought are determined, apart from the influence of precipitation deficit, by the climate regime of the region (meteorological drought), the recharge of surface and subsurface water supplies for established water uses of a given water resources management system (hydrological drought), the infiltration rates of precipitation into the soil and thus the soil water / soil moisture availability to support the crop and forage growth over a specified period of time (agricultural drought) and the relationship between the supply and demand for some commodity or economic good (socio-economic drought). Finally, the different drought types are connected since the response of the hydrological, agricultural, environmental and socioeconomic systems to the water shortages varies markedly and have different response times. This introduces the interesting concept of drought time-scale.

McKee *et al.* (1993) illustrated relevant drought characteristics by considering usable water resources including soil moisture, ground water, snowpack, river discharges, and reservoir storages. Since the time period from the arrival of water inputs to the availability of a given usable resource differs considerably, the time scale over which water deficits accumulate becomes extremely important, and functionally separates between hydrological, environmental, agricultural and other types of drought (Wilhite and Glantz, 1985).

In the Mediterranean region, droughts are a climatic risk that have severe consequences for agriculture and natural vegetation (Austin *et al.*, 1998; Lázaro *et al.*, 2001; Reichstein *et al.*, 2002; Iglesias *et al.*, 2003), increasing the frequency of fires (Colombaroli *et al.*, 2003; Pausas, 2004) and significantly reducing water availability for urban and tourist consumption (Morales *et al.*, 2000). Droughts are frequent, but not spatially uniform in the Mediterranean region (Briffa *et al.*, 1994; Lloyd-Hughes and Saunders, 2002a; van der Schrier *et al.*, 2006; López-Moreno and Vicente-Serrano, 2008), with a high spatial and temporal complexity (Vicente-Serrano *et al.*, 2004; Vicente-Serrano, 2006ab).

Drought indices associated with a specific timescale are useful tools for monitoring and management of drought. The study of the atmospheric mechanisms related to droughts further requires the consideration of different drought time-scales, but at present there are very few studies that analyse the role of the NAO on droughts at different time scales across the entire Mediterranean region (see López-Moreno and Vicente-Serrano (2008) and Vicente-Serrano *et al.* (2011) for the case of the North Atlantic Oscillation).

For the determination of drought conditions, Vicente-Serrano *et al.* (2010b) have developed a new dataset of a drought index – the "Standardized Precipitation Evapotranspiration Index (SPEI)" based on precipitation and potential evapotranspiration (PET) (Vicente-Serrano *et al.*, 2010a). The SPEI combines the sensitivity of the "Palmer Drought Severity Index" (PDSI) to changes in evaporative demand (related to temperature fluctuations and trends) with the multi-

temporal nature of the "Standardised Precipitation Index" (SPI). The SPEI gridded dataset covers time scales from 1-48 months, at a spatial resolution of 0.5°, and provides temporal coverage for the period 1901-2006. This dataset represents an improvement in the spatial resolution and operative capability of previous gridded drought datasets based on the PDSI, and enables identification of various drought types based on the time scales of their onset. Details of the dataset can be found in Vicente-Serrano *et al.* (2010b).

Figure 6.8 shows the evolution of the SPEI at the time scales of 3-, 8- and 18-months in the closest grid point to Istanbul (Turkey) (41.5º N / 29.0º E) for short to long time scales of drought events. The periods of negative SPEI values indicate drought conditions, whose intensity is proportional to the SPEI absolute value. The different time scales provided by SPEI can be related to different drought types in a region. Short time scales show a high relationship with variations of soil moisture, which determine water availability for vegetation and agriculture, while water resources in reservoirs are related to longer time scales.

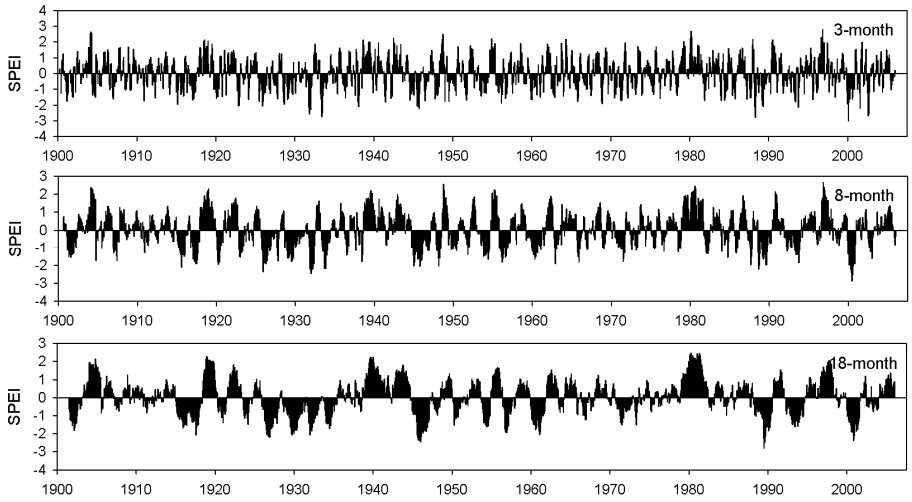

Figure 6.8. Evolution of the 3-month, 8-month and 18-month SPEI between 1901 and 2006 at 41.5º N / 29.0º E.

The Southern Oscillation (SO) is one of the main atmospheric drivers of climatic variability in the global climate system, with extreme episodes of this atmosphere-ocean coupled mode being known as El Niño and La Niña. Although the climatic influence of the SO is mainly detected in the inner-tropical areas, this atmosphere-ocean coupled mode affects the climate of other regions (Ropelewski and Halpert, 1987).

The influence of the SO on the atmospheric circulation over the North Atlantic has been widely recognized (see for a review Brönnimann, 2007 and references therein). At present, the mechanism of propagation of the SO effects to the North Atlantic region is not well understood; however, the influence of the SO on European climate, and in most cases on parts of Europe, has been described in a number of studies (van Oldenborgh *et al.*, 2000; Mariotti *et al.*, 2002b; Pozo-Vázquez *et al.*, 2005; Brönnimann, 2007; Brönnimann *et al.*, 2007, among others). Most of the studies show that the ENSO influence undergoes a seasonal modulation or is nonlinear. Thus, the signal can be modified by other factors and be non-stationary, contributing to a large interdecadal variability (Brönnimann, 2007). With respect to the Mediterranean region, extreme phases of the ENSO (El Niño and La Niña) have been found to influence humid and drought conditions in the Mediterranean region. This influence is not homogeneous throughout the region and also large seasonal differences can be identified (Fraedrich and Müller, 1992; Rodó

et al., 1997; Stockdale *et al.*, 1998; van Oldenborgh *et al.*, 2000; Lloyd-Hughes and Saunders, 2002; Mariotti *et al.*, 2002b). Further, authors point to the high variability of the ENSO influence on the Mediterranean, e.g., Brönnimann *et al.* (2007).

Positive surface pressure anomalies are found in the North Atlantic area during La Niña years (Pozo-Vázquez *et al.*, 2001) and drier conditions in parts of Mediterranean region (Vicente-Serrano, 2005; Karabörk *et al.*, 2007; Karabörk and Kahya, 2009). However, seasonal and spatial differences in the precipitation anomalies related to strong La Niña events are shown in several studies for Europe (e.g., Pozo-Vázquez *et al.*, 2005; Vicente-Serrano, 2005; Brönnimann *et al.*, 2007). In this frame, western Mediterranean negative precipitation anomalies are mainly recorded in autumn (Rodó *et al.*, 1997; Vicente-Serrano, 2005), whereas winter precipitation shortages are observed in Eastern Europe and Turkey, although the significant areas are small (Brönnimann *et al.*, 2007; Karabörk and Kahya, 2009).

In the following subsection, Mediterranean multi-scalar droughts and their connection to extreme ENSO phases during the period 1901 - 2006 are elaborated.

6.3.1. Influence of ENSO extremes on drought conditions in the Mediterranean basin

An empirical methodology was used to determine the impact of El Niño and La Niña years on drought conditions in the Mediterranean region. Average SPEI anomalies at different time scales were calculated for El Niño and La Niña events, identified when El Niño 3.4 index was > 1 and < -1 respectively. Here, in order to determine whether the SPEI at different time scales represents significant humid or dry conditions during El Niño or La Niña phases, the Wilcoxon Mann-Whitney test was used. The sample of multi-scale SPEI values in each of the months of the El Niño and La Niña years was compared with the values of SPEI for the months of the normal years and with each other. The significance level was established at $\alpha < 0.05$.

The average values of the 3-, 6- and 12-month SPEI during La Niña years are shown in Figure 6.9. The El Niño years were also analyzed although these periods are generally dominated by positive values (not shown). In general, the negative SPEI values, associated to dry conditions, are only recorded during La Niña events whereas commonly observed in previous studies, humid conditions are generally recorded during El Niño events (Brönnimann, 2007). The maps show only the period from the winter of La Niña event to the summer of the following year (January to June), in which the strongest La Niña signal is found. A large spatial diversity in the influence of La Niña events on Mediterranean droughts can be seen in agreement with earlier studies. At the time scale of 3 months, dry conditions (average values of the SPEI) are recorded in the north of the basin, mainly over the Iberian Peninsula, the Balkans and Turkey. At the time scale of 6 months the negative values of the SPEI are dominant in most of the northern parts of the Mediterranean basin, and the drought conditions persist several months. The pattern is reinforced in some areas (e.g., the Iberian Peninsula) at longer time-scales (12-month).

Figure 6.10 shows the average values of the SPEI in the three regions where the most important influence of La Niña events is recorded: Eastern Spain, the Balkans and Turkey. In those three areas La Niña events are mainly related to negative SPEI anomalies, but there are noticeable differences in the months and the time-scales associated to the strongest anomalies recorded. In eastern Spain the main anomalies at the time scale of 3 months are recorded simultaneously to the occurrence of strong autumn and winter La Niña episodes. These anomalies are propagated throughout longer time-scales, with negative anomalies of the SPEI being recorded during 16 consecutive months at the time scale of 12 months. At the beginning

of La Niña events the Balkans are generally dominated by humid conditions (positive values of the SPEI), however, these are replaced by very strong negative anomalies during the late winter and early spring at the time scale of three months, with a clear propagation to the following months throughout longer time scales. Finally, Turkey shows a large spatial diversity of La Niña events and no important negative SPEI anomalies are recorded when the spatial average is obtained, although the negative averages are the dominant pattern during these events.

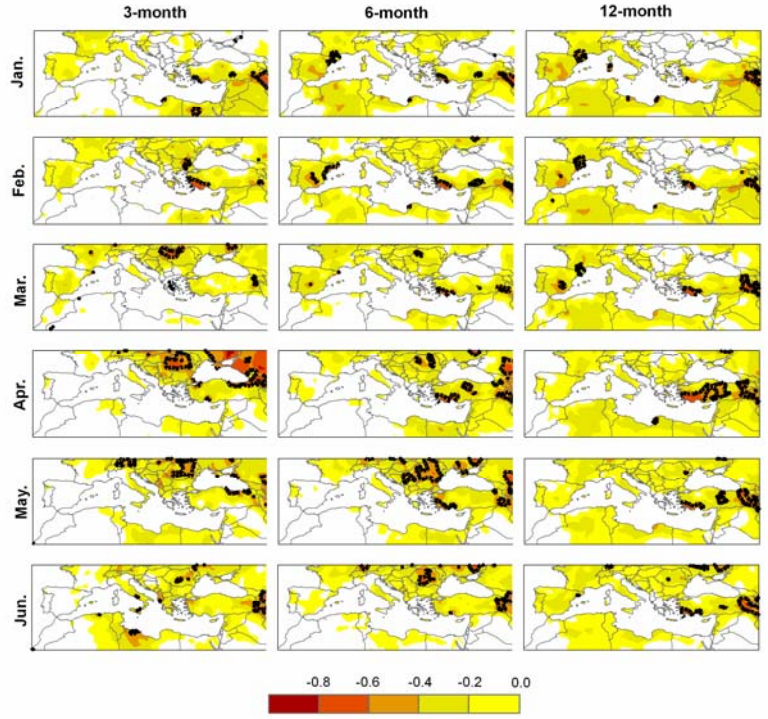

Figure 6.9. Spatial distribution of the composite anomalies of 3-, 6- and 12-month SPEI for the months following winters with La Niña events (from January to June). Dotted lines frame areas with statistically significant differences in the SPEI values between La Niña years and the remaining ones within the study period.

Pozo-Vázquez *et al.* (2001) identified a relatively strong anomalous pressure pattern over the North Atlantic during La Niña winters, with an anomalous high pressure band over the central Atlantic that resembles the positive phase of the NAO, with an intensification of the Azores high and drier conditions in southern Europe. This could explain the influence of La Niña events on drought conditions in areas of the Mediterranean basin and also the regional differences found across the basin.

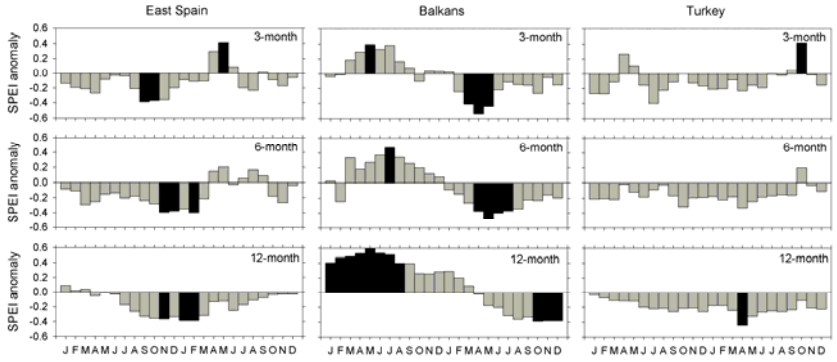

Figure 6.10. Average values of the 3-, 6- and 12-month SPEI in East Spain, the Balkans and Turkey during La Niña events. Black bars show significant differences in the SPEI anomalies between the years in which La Niña events are

recorded and the rest of the years. The figure shows the SPEI anomalies from January of the year in which La Niña event is developing and the following year. The winter months in which the ENSO events are commonly stronger are boxed in the figure.

The SO effects are shown to have a lag, because the main negative and significant averages in SPEI values are recorded between the autumn and winter of the year of the ENSO event, which commonly initiates in the previous spring. This result also agrees with other works that reported the lag of several months of the SO influence on European climate (e.g., van Oldenborgh *et al.*, 2000). The prediction of ENSO events has increased with the refinement of numerical models (e.g., Chen *et al.*, 2004; Tippet and Barnston, 2008; Sordo *et al.*, 2008). Brönnimann (2007) pointed to the average-to-weak, although statistically significant, ENSO signal on Europe and the Mediterranean, which is however important for events with particularly strong effects. Further, Brönnimann (2007) raised the importance of better understanding ENSO effects on Europe and the Mediterranean for the aspect of the potential predictability on a seasonal scale and our understanding and assessment of future climate change.

6.4. Mediterranean water cycle

In view of the semi-enclosed nature of the Mediterranean/Black Sea system, connected to the Atlantic Ocean via the Strait of Gibraltar, and the semi-arid/arid conditions in land regions downstream of Mediterranean moisture fluxes, the impacts of changes in Mediterranean water cycle may be substantial. For example, increases in sea water evaporation (the biggest single component of Mediterranean water cycle) and fresh water loss affect the salt, water and energy budgets. These changes have potentially important implications for Mediterranean Sea salinity, circulation and sea level (Tsimplis *et al.*, 2008), as well as for the Atlantic circulation via changes in Gibraltar water fluxes (Lozier and Stewart, 2008). Additionally, an increase in evaporation (i.e. the amount of moisture the Mediterranean Sea injects into the overlying atmosphere) can enhance moisture fluxes to downstream regions, potentially affecting precipitation there, as it has been shown for the Sahel (Nieto *et al.*, 2006). Changes in Mediterranean precipitation, in large part associated to the variability of the NAO, can significantly impact surface fresh water fluxes and river discharge especially in western parts of the Mediterranean basin (Mariotti *et al.*, 2002a; Struglia *et al.*, 2004).

A better depiction and understanding of recent past long-term water cycle changes in the Mediterranean region is urgently needed since, as mentioned in the introduction, projections of future global climate change indicate major changes for this region in particular as a “hot spot” in hydrological change. A number of investigations indicate significant impacts on both mean precipitation and variability (Giorgi and Lionello, 2008). However, the combined effects of future precipitation decrease and increasing surface temperature on Mediterranean water cycle, and in particular the impact on Mediterranean Sea water budget, are less well known.

Here two complementary approaches are presented for the analysis of moisture sources in the area based from a Lagrangian perspective and an Eulerian analysis based on dynamical regional model projections and observations for the last fifty years and an analysis of the long-term water cycle changes in the twentieth century based on observations. More specifically, the Eulerian method can quantify flows of moisture to and from a defined region but cannot identify the real sources. With the Lagrangian approach instead, the trajectories of selected particles can be followed in the space and through time.

6.4.1. Characterising major external and internal moisture sources affecting the Mediterranean basin

The Mediterranean hydrological cycle is especially sensitive to the timing and the location of the winter storms as they move into the region (Trigo *et al.*, 2002) strongly influenced by the NAO and, to a lesser, extent ENSO. In boreal summer, when the advection of moisture from the Atlantic is weaker and the Hadley cell moves northwards, there is evidence of connection with the Asian and African monsoon. The Mediterranean Sea itself is also an important source of atmospheric moisture and the characteristics of the local water budget influence the amount of moisture that flows into northeastern Africa and the Middle East (Peixoto *et al.*, 1982). Past and future global climate change as well as changes in regional land-surface conditions may be linked to significant changes of the hydrological cycle in the Mediterranean. An improved knowledge of the Mediterranean hydrological cycle and its variability would support a better management of water resources over the area in the e.g., agricultural or energy production sectors.

Several studies have identified geographical sources or sinks of moisture over the Mediterranean Sea based on different methodologies (most attaining information in an Eulerian framework) and input data with results varying significantly among authors. As an example, Mariotti *et al.* (2002a) performed a budget analysis to study contributions to the freshwater flux into the Mediterranean Sea, including atmospheric as well as river discharge inputs, during the last 50 years using recent atmospheric reanalyses and observational datasets. Their analysis shows an annual moisture flux from west to east, with a southward component during summer, from the eastern Mediterranean into northeastern Africa and the Middle East. A different approach was employed by Fernández *et al.* (2003) who integrated the atmospheric moisture fluxes across the region boundaries. These works have clearly shown that the precipitation variability within the Mediterranean basin is closely related to the structure of the vertically integrated moisture transport fluxes, inside the domain and at the borders.

This type of analysis with Eulerian methods or moisture divergence flux applications is not able to compute moisture sources with high precision, both in terms of magnitude and location, in part because they do not imply real trajectories of atmospheric particles. An alternative approach is the use of Lagrangian methods to obtain more precise information concerning the trajectories of air masses and their moisture variability in comparison to the traditional Eulerian techniques. In order to determine the moisture sources over the Mediterranean basin Nieto *et al.* (2010), based on Stohl *et al.* (1998), used the Lagrangian particle dispersion model FLEXPART. This method has been widely applied over distinct climatic regions of the world, including the Sahel (Nieto *et al.*, 2006), the Iberian Peninsula (Gimeno *et al.*, 2010ab), the Antarctic (Nieto *et al.*, 2010), the South American Monsoon System (Drumond *et al.*, 2008) and Central America (Durán-Quesada *et al.*, 2010). For additional information on the FLEXPART model and details on the methodology readers are referred to the corresponding papers. Nieto *et al.* (2010) used the European Centre for Medium-Range Weather Forecasts data to track different meteorological parameters for the entire atmosphere along backward and forward trajectories.

Figure 6.11 shows the annual, summer and winter vertically integrated moisture flux divergence fields. For the backward trajectories, the origin of air-masses residing within the atmosphere over eight different continental regions surrounding the Mediterranean Basin was tracked (red letters in Figure 6.11a): Iberia, France, Italy, the Balkans, the Eastern Mediterranean, and three regions over North Africa: western, central and eastern Northern

Africa. With respect to forward trajectories, three areas provide maximum water supply to the atmosphere: the Balearic Sea (the western Mediterranean), the southern Ionian Sea (central Mediterranean Sea, between Italy and the African coast), eastern Mediterranean into northeast Africa and the Middle East (Figure 6.11a, numbered 1, 2 and 3, respectively). This structure was found to be stable.

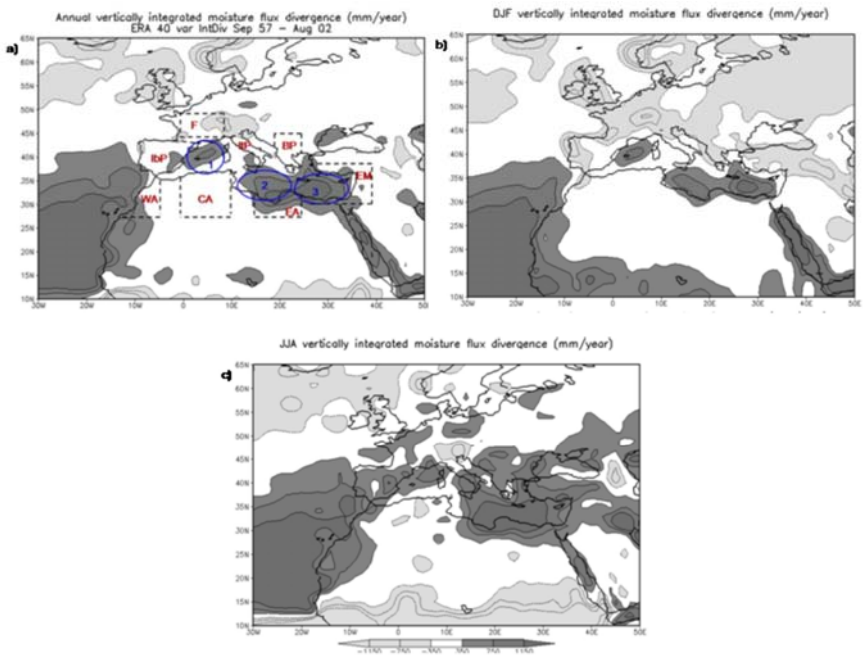

Figure 6.11. a) Climatological annual vertically integrated moisture flux divergence (shaded and contour lines, in mm/year). The boxes indicate the moisture regions studied through the integrations (red are backward trajectories; blue are forward trajectories); b) the same as in a), but for winter; c) the same as in a), but for summer.

Main moisture sources

The high spatial discretisation of the Mediterranean region allows for a detailed view on the moisture sources and sinks for the different regions of the extended Mediterranean area. Figure 6.12 shows the annual $(E–P)_{1,10}$ values for the three Mediterranean Sea areas (left), and the annual $(E–P)_{1,10}$ values for the eight land Mediterranean regions (right).

Figure 6.12a-c suggests that moisture transport processes to different target regions undergo significant changes with the meridional position of each region. In general, the moisture budget of each region is mostly influenced by the surrounding areas and the local dominant flows of air masses over the land areas. The western Mediterranean Sea (Figure 6.12a) contributes directly to precipitation (bluish colors) over the Alps, the Balearics and the Strait of Gibraltar and plays a significant role for the humidity transport over Algeria and Libya. The central Mediterranean Sea area affects mostly the Greek Peninsula and the islands and the central part of North Africa. On the other hand, the eastern Mediterranean Sea influences the regions of Middle East and Egypt.

Figure 6.12d-k reveals that the moisture sources for each continental area differ due the location of the target regions around the Mediterranean and, in general, the importance of those surrounding areas in providing the moisture. Although nearest areas are the most important moisture sources, it should be noted that for the western Mediterranean lands (Iberia, France, and western North Africa) the contribution of the Tropical–Subtropical North Atlantic Ocean (TSNA), including the Gulf of Mexico, is of relevance. For Iberia (Figure 6.12d) and France

(Figure 6.12e), the western Mediterranean Sea area appears as one of the main moisture sources but those target regions are as well the most affected by the TSNA moisture contribution. For the Italian and Balkan Peninsulas (Figure 6.12f,g) the western and central Mediterranean act as the main moisture sources, accompanied by weaker contributions from southern Europe and Northern Africa. The contribution of the TSNA is also identified for Italy. The eastern Mediterranean surrounding sea area (Figure 6.12h) is the major source of moisture, followed by the contributions from Eastern Europe, Middle East, eastern North Africa as well as the TSNA. The contribution from Europe is limited over the western Mediterranean land areas, especially the Iberia. In addition, the North Atlantic oceanic area close to Europe becomes an important moisture source together with northern Africa and the TSNA.

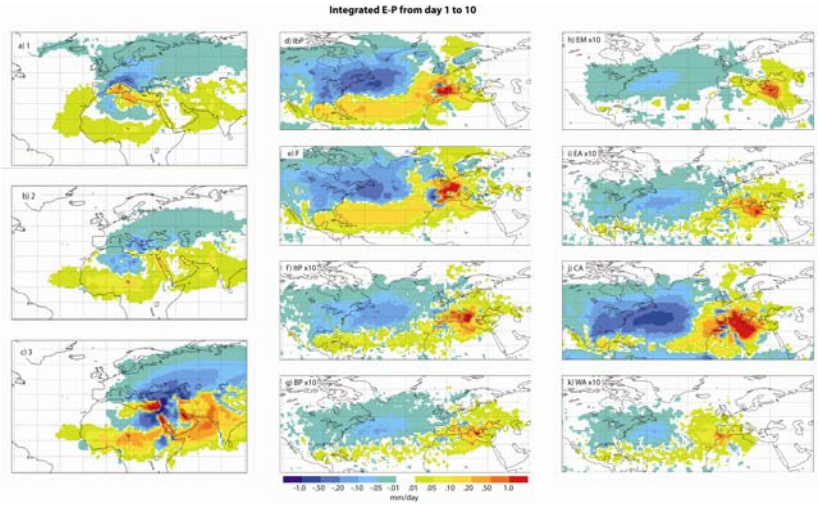

Figure 6.12. Annual average values of $(E–P)_{1,10}$ for the period 2000–2004 determined from: (left) forward tracking for the a) Western Mediterranean Sea, b) Central Mediterranean Sea and c) Eastern Mediterranean Sea regions; and (right) backward tracking for the d) Iberia, e) France, f) Italy, g) Balkans, h) eastern Mediterranean, i) eastern North Africa, j) central North Africa and k) western North Africa regions. Scale in mm/day (scale multiplied by a factor of 10 in b, f–i and k). Blue colors (E–P <0) reveal regions where precipitation dominates over evaporation, being the moisture sink. Red colors (E–P >0) indicate the opposite behavior, corresponding with moisture source regions.

In general, the forward air-masses tracking revealed that for the three selected areas the main moisture sources are the surrounding areas and that the air masses are transported throughout the local dominant flows.

The backward trajectories show that the North Atlantic basin and the western Mediterranean Sea are the main moisture source regions affecting the western Mediterranean lands. The eastern Mediterranean regions are generally affected by the corresponding surrounding sea areas.

6.4.2. Long-term Mediterranean water cycle changes in observations

An analysis of observed twentieth century long-term changes in the water cycle of Mediterranean land areas is presented by Mariotti *et al.* (2008) and summarized here (unless otherwise stated, results below are from this study). Considering linear trends, a weak albeit significant long-term negative precipitation trend is found using both Global Historical Climatology Network data (GHCN; Vose *et al.*, 1992) and the Dai *et al.* (1997; DAI hereafter) land data over the Mediterranean region (for GHCN this trend is –0.005 +/– 0.003 mm/d per decade). In these datasets, winter season precipitation shows a major downward deviation over the period 1960–2004 (–0.09 +/– 0.02 mm/d per decade). The winter precipitation decrease

during the mid-1960s to early-1990s is largely related to the behavior of the North Atlantic Oscillation (NAO) during this period (Hurrell, 1995; Hurrell *et al.*, 2003). Dry season negative trends over the period 1950–2000 have also been reported in relation to a blocking-like pattern deflecting storms away from much of western and southern Europe (Pal *et al.*, 2004). The Palmer Drought Severity Index (PDSI; Dai *et al.*, 2004), which reflects the combined effects of precipitation and surface temperature changes, shows a progressive and substantial drying of Mediterranean land surface since 1900 (–0.2 PDSI units/decade) consistent with a decrease in precipitation and an increase in surface temperature. The inter-decadal fluctuations are similar to those of precipitation, with wetter 1960s compared to the drier 1940s. Consistently with PDSI behavior, a number of Mediterranean rivers for which long-time series are available also show long-term decreases in discharge during the twentieth century. Such river discharge decreases are likely in part due to intensified water use (Mariotti *et al.*, 2008).

An analysis of observed long-term Mediterranean Sea water cycle changes since 1958 is presented in Figure 6.13 (see Mariotti, 2010 for more details). Only indirect estimates of Mediterranean Sea precipitation are available before 1979, based on precipitation reconstruction (REOFS, Smith *et al.*, 2008) and land-gauge precipitation from regions surrounding the sea. The analysis presented here considers together Mediterranean Sea estimates (Global Precipitation Climatology Project data (GPCP), Adler *et al.*, 2003; Remote Sensing Systems (REMSS) data, Wentz *et al.*, 2007; and REOFS) and those from the land-gauges (PRECL data from Chen *et al.*, 2002; the East Anglia University Climatic Research Unit (CRU) data, Mitchell and Jones, 2005; and GHCN). During 1979–2006, decadal variations characterize the low-frequency variability of Mediterranean precipitation. These are quite similarly represented in the various datasets: a substantial decrease of 0.2–0.3 mm/d (about 15%–25% of climatology) during the 1980s followed by a rapid increase in precipitation (about 0.2 mm/d) until the mid-1990s; after that, precipitation is seen to decrease slightly up until the turn of the twentieth century, with a recent tendency to increase. Despite the general similarity, differences exist among the various estimates, owing in part to the different areas considered in the spatial averages (land-only versus sea-averages) and differing spatial resolutions of the datasets. Overall, for the period 1958–2006 both REOFS and the land-gauge estimates suggest that these decadal variations were superimposed on a long-term negative trend (–0.03 to –0.04 mm/d per decade or –4 % of climatology per decade; various estimates are statistically consistent). In contrast, for the shorter 1979–2006 period there is no significant precipitation trend.

A variety of sea-surface evaporation data sources are available for the period 1996–2005. All datasets unanimously show an increase in Mediterranean Sea evaporation leading up to the current period. However, the increase rates vary significantly among datasets. Only the OAFlux (Objectively Analyzed Air–sea Fluxes Project, Yu *et al.*, 2008) and NOCS (National Oceanography Centre Southampton NOCS Flux Dataset v2.0, Berry and Kent, 2008) datasets are available going back to the 1970s. According to OAFlux, the recent evaporation increase is part of a long-term progressive evaporation increase which started in the mid-1970s, when E was about 0.1 mm/d below the 1988–2000 mean. Similarly to OAFlux, NOCS also shows mid-1970s evaporation rates lower than the 1988–2000 mean and progressively increasing.

However during the 1980s, before the common evaporation increase of the 1990s, the two datasets are inconsistent. These datasets give an overall trend for the period 1979–2006 of 0.1–0.2 mm/d per decade (4%–8% of climatology per decade; these trends are significant and statistically consistent). Only OAFlux is available since the 1960s. According to this dataset, evaporation rates in the 1960s were comparable to those of the late-1990s, and subsequently decreased up until the mid-1970s before the increase leading up to the current period.

Considering the whole 1958–2006 period, these interdecadal variations have amounted to an equivalent linear mean evaporation increase of 2% per decade (0.06 mm/d per decade or 22 mm/y per decade).

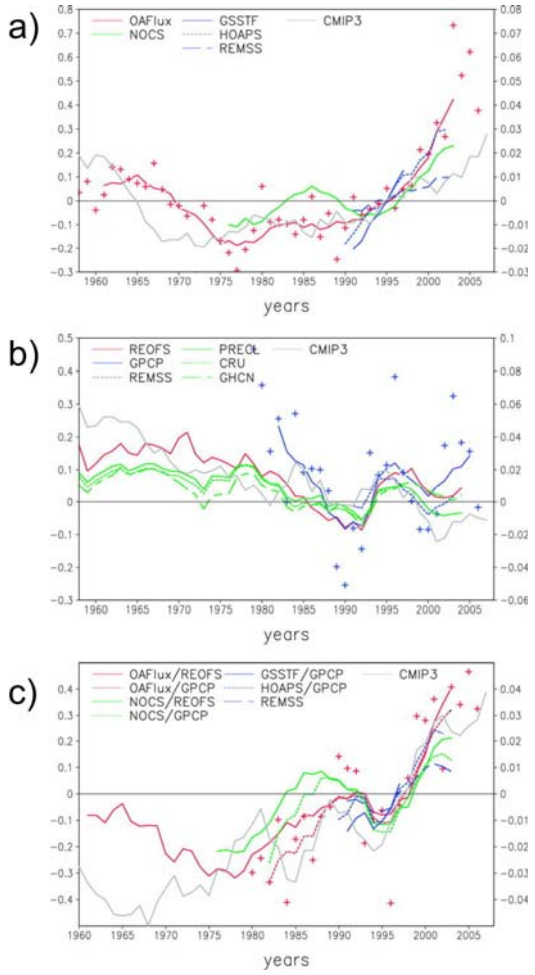

Figure 6.13: Observed decadal variations in Mediterranean Sea water cycle over the period 1958-2007. Shown are 6-yrs running means of a) evaporation, E, b) area-averaged precipitation, P and c) E–P area-averaged anomalies relative to the period 1988-2000 (lines). Various observational sources are used (see legends; left hand scale). For precipitation, PRECL, CRU and GHCN are land-only averages for the region surrounding the Mediterranean Sea; REOFS, GPCP and REMSS are Mediterranean Sea-only averages. Annual mean values are also displayed (symbols) based on GPCP precipitation and OAFlux evaporation.CMIP3 models' ensemble running mean averages are also displayed (grey line; note different scale at right). Units are mm/d. Adapted from Mariotti (2010) © Copyright 2010 American Meteorological Society (AMS)

The combination of the evaporation and precipitation changes described above resulted in significant long-term changes in Mediterranean Sea surface fresh water fluxes during the period 1958–2006. Estimates based on OAFlux/REOFS suggest a substantial increase in E–P over this period (~0.5 mm/d or 182 mm/y in total). Considering the 1979–2006 sub-period, E–P rate of increase is estimated 0.1–0.3 mm/d per decade (estimates are mostly statistically consistent). The E–P increase during the 1980s was primarily driven by the decrease in precipitation during this period. Similarly, the "dip" in E–P during the mid-1990s was also precipitation-driven, and is depicted quite consistently across data sources. In contrast, the most recent E–P increase was dominated by evaporation increase.

6.5. The North Atlantic Oscillation impact on renewable energy and vegetation dynamics

The NAO corresponds to one of the most important large scale modes of atmospheric circulation in the Northern Hemisphere (Barnston and Livezey, 1987; Hurrell *et al.*, 2003). Most works for Europe and/or the Mediterranean basin that have been focused explicitly on the NAO consider the winter season (December to March) when the impact is greatest and is particularly associated with precipitation variability (Quadrelli *et al.*, 2001; Trigo *et al.*, 2002; Goodess and Jones, 2002; Haylock *et al.*, 2004; Xoplaki *et al.*, 2004). Using high and low NAO index (NAOI) composites Trigo *et al.* (2002; 2004) have computed anomaly fields of climate variables (including total precipitation, precipitable water, precipitation rate, maximum and minimum temperatures, cloud cover, wind speed and direction, vorticity, storm-track density) and their associated physical mechanisms for the entire Europe, including the Mediterranean basin. However, in recent years it has been shown that the NAO exerts an important influence on Europe's precipitation throughout most of the year, strongest during winter, and that the spatial signature is relatively similar for winter, spring and autumn, while being significantly smaller and mostly restricted to France in summer (Figure 6.14). Apart from the summer months, the impact exerted by NAO on the precipitation regime is associated to corresponding changes in the storm tracks location over the North Atlantic and Europe (Trigo, 2006) including the Eastern Mediterranean (Turkey; Türkeş and Erlat, 2005). While the impact of the NAO on precipitation shows a decreasing influence in the eastern and southern sectors of the basin, it has been shown that it can significantly impact the precipitation variability over Turkey (Cullen and deMenocal, 2000; Struglia *et al.*, 2004; Türkeş and Erlat, 2005). The most important season for recharge and water resources is the extended winter December to March. This period receives the largest fraction of the annual precipitation total, both in the western and most importantly in the eastern basin (Xoplaki, 2002).

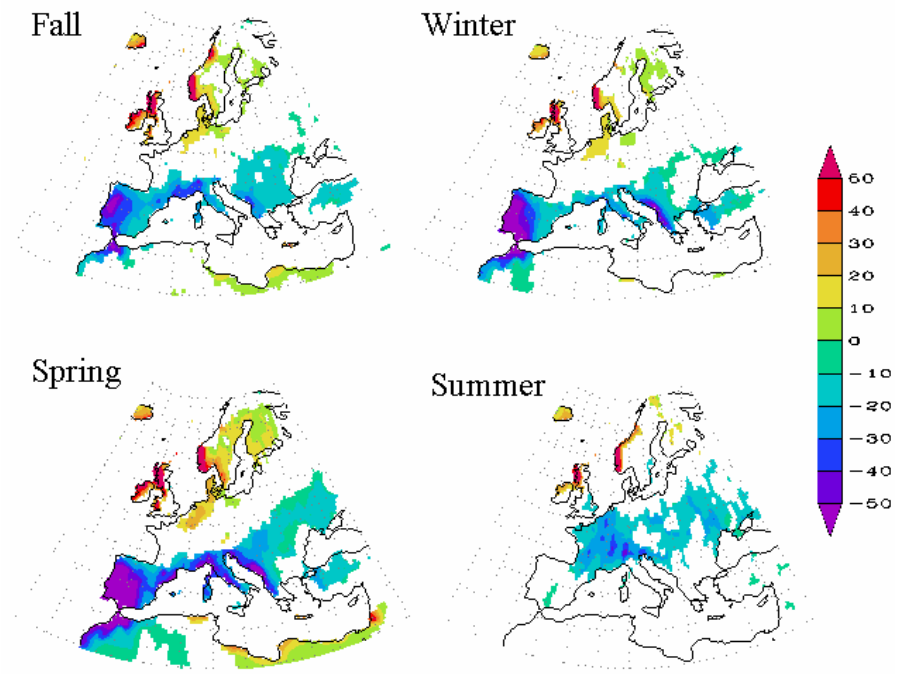

Figure 6.14. Seasonal precipitation differences (mm) between seasons with NAOI > 1 and NAOI < –1 (period 1958–1997). The monthly gridded precipitation data stem from the CRU 2.1 0.5° resolution dataset. Only significant values at the 95% level are shown

6.5.1. The role of winter NAO in modulating cloud cover and available solar energy in the western Mediterranean

Along the next decades, solar energy is expected to play an important role for electricity generation in the Mediterranean (IEA, 2010). For example, nowadays in Spain the solar electricity technologies account for about 5% of the total electricity installed capacity (5 GW) and the aim is to reach 10% by 2020. Accurate resource evaluation is a key issue in the first stages of a renewable energy project. Particularly, as the life span of the solar plants is about 20 years, the economic feasibility study of the Spanish project should consider an adequate estimation of the solar radiation interannual variability (Lohmann *et al.*, 2006).

Although other phenomena, such as aerosols or the solar cycle, may play a significant role, interannual variability of the solar radiation is mainly related to changes in the cloud cover associated with changes in the large scale circulation patterns (Sanchez-Lorenzo *et al.*, 2008 and 2009; Chiacchio and Wild, 2010; Papadimas *et al.*, 2010). The NAO variability is associated with basin-wide changes in the intensity and location of the North Atlantic jet stream and storm tracks, and therefore with changes in the zonal and meridional heat and moisture transport patterns from the Atlantic Ocean to Europe. This impacts the cloud cover over Southern Europe and especially the Iberian Peninsula (hereafter IP), with the positive NAO phase being associated with clear sky conditions (Trigo *et al.*, 2002; Pozo-Vázquez *et al.*, 2004). Figure 6.15 shows the changes during the winter in the cloud cover in the IP associated with the two phases of the NAO. Data (period 1961-1995) stem from the CRU TS 1.0 dataset at a 0.5° resolution (New *et al.*, 2000). During the positive NAO phase, below normal cloud cover is found over the whole IP, with stronger deviations in the central and southwestern area. A similar pattern, of the opposite sign, is found for negative NAO conditions. When comparing anomalies during the two NAO phases, the differences reach 0.7 oktas in southwestern Iberia. Therefore, in this area, interannual – winter-to-winter – changes in the cloud cover of about 9% could be expected to be associated with the NAO variability. The relationships discussed here are consistent with precipitation findings (see also section 6.5).

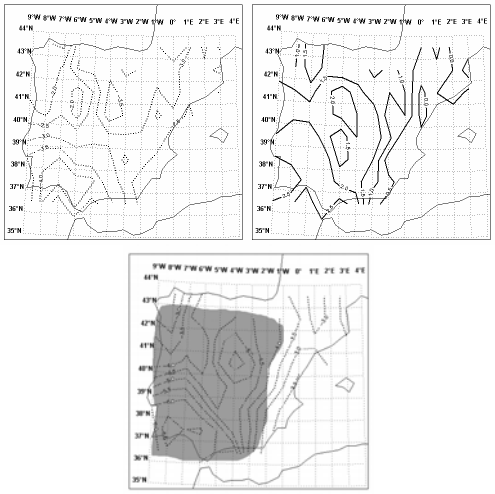

Figure 6.15. Composites of winter (DJF) cloud cover anomalies (in oktas by ten) for the period 1961–1995. Top left NAOI > 1; top right NAOI < –1; bottom difference NAOI > 1 minus NAOI < –1. Continuous lines indicate positive or zero anomalies and dotted lines indicate negative anomalies. Shaded areas indicate statistical significance of the difference at 95% level between NAOI > 1 and NAOI < –1

The cloud cover variability associated with the NAO phases presents an important influence on the solar radiation spatial and temporal variability over the IP (Pozo-Vázquez *et al.*, 2004; Sanchez-Lorenzo *et al.*, 2008; Sanchez-Lorenzo *et al.*, 2009; Chiacchio and Wild 2010). To illustrate this relationship, an analysis of the NAO-solar radiation relationship has been carried out. Solar radiation data from 700 stations for the 10-year period 1981–1990 is available from the European Solar Radiation Atlas (ESRA) (Greif and Scharmer, 2000; Page *et al.*, 2001). These data consist of monthly sums of sunshine duration (MSD). A winter mean MSD data set was obtained by averaging the December, January and February MSD data and anomalies were derived considering the complete study period. Although the database covers a relatively short period, it is the single database of measured solar radiation data covering the whole Europe. Furthermore, as observed in Figure 6.16 (right panel), during the decade 1981–1990 a wide range of phases and intensities of the NAO were observed. Therefore, results could be considered representative of the longer-term NAO-solar radiation relationship. The station winter MSD data were gridded to a 5° × 5° dataset by Pozo-Vázquez *et al.* (2004). The sample correlation coefficients between the NAOI and the gridded MSD over the European-North Atlantic area are presented in Figure 6.17. A dipolar pattern can be observed. Positive correlations are prevalent over southwestern Europe, while most of northern Europe areas are negatively correlated with NAOI. Maximum positive correlation values are found for the Iberian Peninsula and Morocco with correlations reaching 0.75. Maximum negative correlations are found for the northern British Isles (values between -0.6 and -0.8). Similar results were obtained by Pozo-Vázquez *et al.* (2004) using the NCEP-NCAR reanalysis solar radiation data.

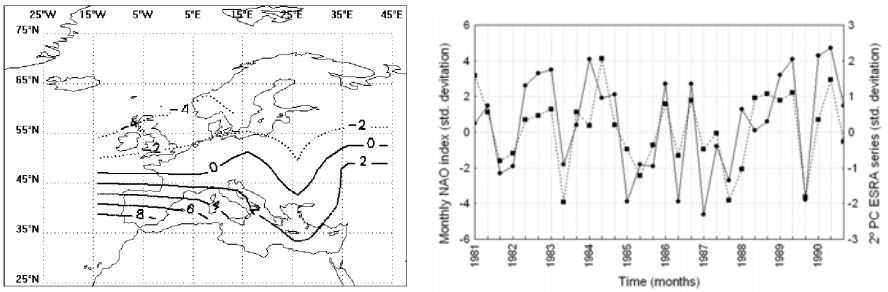

Figure 6.16. (left) Loading factors (x 10) of the second mode resulting from the PCA of the winter solar radiation anomalies data. (right) Winter NAOI series (solid line); PC series corresponding to the second mode resulting from PCA of the winter solar radiation anomalies (dashed line). Units are standard deviation. The year in the bottom axis refers to the month of December

For further investigations, Pozo-Vázquez and colleagues performed a Principal Component Analysis (PCA) for the gridded winter season MSD. Three significant modes, accounting for 67% of the total variance were identified, subject to a varimax rotation. The leading mode (not shown) explaining 33.1% of the total variance presents a coherent mode of variability for the whole study area. The pattern of the second mode that explains 22.4% of the total winter MSD variance is shown in Figure 6.16 (left panel) and the associated PC series and the NAOI series are represented in Figure 6.16 (right panel). This second mode of variability shows a clear gradient with positive winter MSD loadings over the western Mediterranean, reaching values of 0.8 over the southern Iberian Peninsula. Negative loadings of up to –0.4 can be found over the British Isles and Scandinavia. Therefore, the pattern is mainly representative of the solar resources variability over the western Mediterranean area. The correlation coefficient between the PC series and the NAOI is +0.69 (statistically significant at 99% level). Thus, this second spatio-temporal mode of variability can be associated with the NAO. Results are in agreement

with Papadimas *et al.* (2010), who presented the existence of a Mediterranean solar radiation spatial variability mode associated with the NAO during the winter and the patterns presented in Figure 6.15.

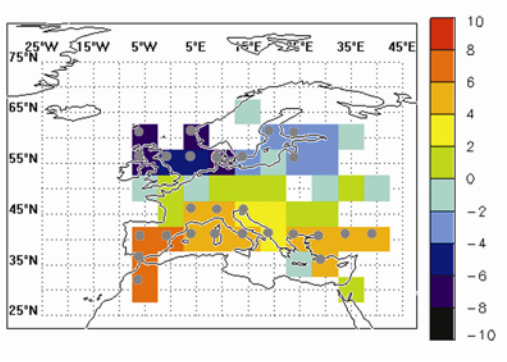

Figure 6.17. Winter correlation (x10) between the NAOI and solar radiation data. Analyzed period is 1981-1990. The dot in the upper-left corner indicates local statistical significance of the correlation value at the 95% level. From Pozo-Vázquez *et al.* (2004) published at Geophysical Research Letters

6.5.2. Assessing the role of NAO and climate variability in the vegetation dynamics over Iberia. Wheat production in Portugal: a case study

Among the wide range of socio-economic activities that are influenced by the climatic conditions, the status of vegetation and the crop monitoring and yield are at the top of the interest list. The influence of the NAO pattern on vegetation-related variables is therefore the focus of this subsection. During the last decades, the study of weather conditions and their connection to plant growth, carbon absorption by living plants and crop yield became a crucial research question. On the other hand, the widespread changes of land use may alter the role of land areas from carbon dioxide sinks to carbon dioxide sources and vice-versa. This observation requires quantification in the current climate change frame. In this context, remote sensing technology provides a large amount of applications for the evaluation and monitoring of vegetation greenness, vegetation annual cycle, as well as agriculture related parameters, such as crop identification, crop growth monitoring and yield prediction.

Changes in the vegetation annual cycle can be detected, using satellite information, namely with the Normalised Difference Vegetation Index (NDVI), an index that has been widely used to assess vegetation dynamics (Stöckli and Vidale, 2004; Vicente-Serrano and Heredia-Laclaustra, 2004). Special attention has been devoted to the investigation of relationships between vegetation dynamics and the NAO. Cook *et al.* (2004) modelled the dependence of phenological variability in Europe on NAO, as a result of NAO influence on synoptic scale winter temperature variability, and reproduced the growing degree-days patterns observed over Europe. Stöckli and Vidale (2004) found that spring phenology over Europe correlates well with anomalies in winter temperature and winter NAOI (see also section 6.2.1). They established the existence of trends to a longer duration of the spring vegetation growing period, as well as the earlier onset over Central Europe. Maignan *et al.* (2008) showed that the vegetation onset is strongly driven by the NAO over a large fraction of Northern Europe, where the vegetation is highly controlled by temperature. The pattern of the NAO impact on vegetation dynamics is clearly apparent with a north-south gradient (Gouveia *et al.*, 2008). It must be recognized that most of the studies mentioned above are related to northern and central sectors of Europe, i.e. considerably outside the geographical area under investigation in this chapter. However,

considering the smaller amount of research focusing on southern Europe, their inclusion is well justified and helpful and provides the appropriate context to the addressed problem.

Taking into account the strong NAO impact on the western Mediterranean precipitation (Trigo *et al.*, 2004) and water resources (López-Moreno *et al.*, 2007) (see also section 6.15) and consequently its impact on vegetation and vegetation dynamics, a similar analysis for the Iberian Peninsula is presented here. Vicente-Serrano and Heredia-Laclaustra (2004) analyzed the relationship between the NAOI and vegetation productivity trends over the Iberian Peninsula. The NAO influence was stronger in southern Iberia corresponding to areas of stable or decreasing vegetation productivity. On the other hand the NAO influence, on vegetation dynamics is weaker at the north of the peninsula where significant positive productivity trends occur. It is shown that the NAO controls the inter-annual variability of the vegetation dynamics and that this is mostly associated with the impact exerted by the NAO on the precipitation regime over large areas of Iberia.

Figure 6.18 displays the spatial patterns, over a selected window, of point correlation values of winter NAO_{JFM} versus spring $NDVI_{MAM}$ and winter NAO_{JFM} versus summer $NDVI_{JJA}$ for the period between 1982 and 2002. All NDVI values were obtained from the Global Inventory Modelling and Mapping Studies – GIMMS group, with 8 km spatial resolution (Gouveia *et al.*, 2008). Results show a negative correlation over the Iberian Peninsula in spring and summer, some values reaching as low as –0.8. Positive correlations are found at eastern Iberia, particularly for the Murcia region during spring.

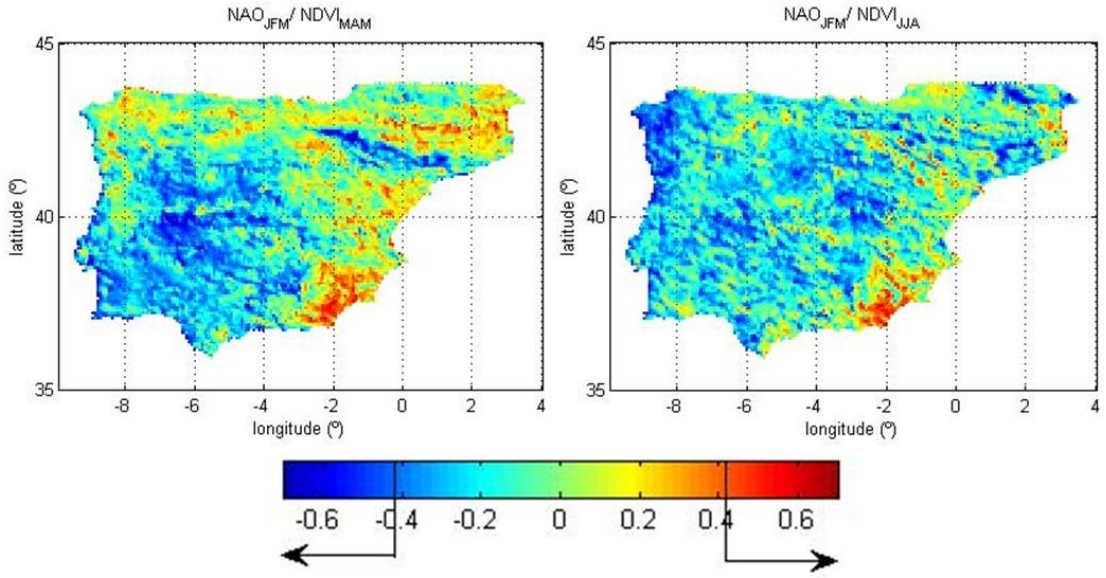

Figure 6.18. Point correlation fields of $NAOI_{JFM}$ vs. $NDVI_{MAM}$ (left panel) and $NAOI_{JFM}$ vs. $NDVI_{JJA}$ (right panel) over the period 1982–2002. The colours identify values of correlation and the two arrows indicate the ranges that are significant at the 95% level.

While it is known that the impact of NAO on temperature and precipitation is especially outstanding in winter (Trigo *et al.*, 2002, 2004; Vicente-Serrano and Heredia-Laclaustra, 2004, Cook *et al.*, 2004, Lopéz-Moreno *et al.*, 2007, among others; see also sections 6.2.1 and 6.5), the impact of NAO on vegetation activity is clearly noticeable both in spring and in summer (i.e., $NAOI_{JFM}$ versus $NDVI_{MAM}$ and $NAOI_{JFM}$ versus $NDVI_{JJA}$). It should be noted that although the number of pixels with significant correlations is relatively small, these pixels represent disproportionately those land-cover types that are most relevant for the study of the NAO

impact of vegetation (i.e., non-irrigated crops, scrublands and forests). The vast majority of the remaining pixels corresponds to less relevant land-cover types (bare soil, mixed mosaic pixels) or highly managed by humans (urban areas, irrigated crops).

The link between winter NAO and spring and summer vegetation health requires a more in depth analysis of the role played by winter temperature and precipitation in the following seasons. In fact, the results may be viewed in terms of the distinct responses of the various vegetation types to moisture and heat conditions prevailing during the previous winter. These conditions, in turn, are determined by the nature of the relationships between the surface annual variability of atmospheric parameters, winter precipitation (P_{JFM}) and temperature (T_{JFM}), and the different phases (NAO+ and NAO–) of the NAO_{JFM} atmospheric mode. It should be stressed that the correlation coefficient between winter NAOI and precipitation presents strong (and significant) negative values over the central and SW Iberia; while in the northern fringe of Iberia the correlation is not statistically significant (see also section 6.15). Figure 6.19 shows scatter plots of spring and summer anomalies of vegetation greenness against winter anomalies of temperature and precipitation. Each star corresponds to a pair of median values of a set of 500 selected pixels with the highest (lowest) values of positive (negative) correlations of NDVI with NAOI (NNCP; NAOI-NDVI Correlated Pixels), for a given year of the considered period (1982–2002), of winter anomalies of P_{JFM} (left panels) and T_{JFM} (right panels) versus anomalies of $NDVI_{MAM}$ (upper panels) and $NDVI_{JJA}$ (lower panels). Years belonging to the subset of NAO+ (NAO–) are marked in light (dark) grey and the variability of the NNCP is characterized by means of vertical and horizontal bars indicating the correspondent interquartile ranges across 500 pixels. According to the land cover type associated to each pixel, as provided by the Global Land Cover 2000 (GLC2000) database, 64% of the NNCP corresponds to areas of spring crops and 17% to forests and shrublands. The relative proportion of the two types experiences a significant change in summer (47% to cultivated areas and 29% to forest and shrubland). However it is acknowledged that further investigations on the sensitivity of all land cover types is required.

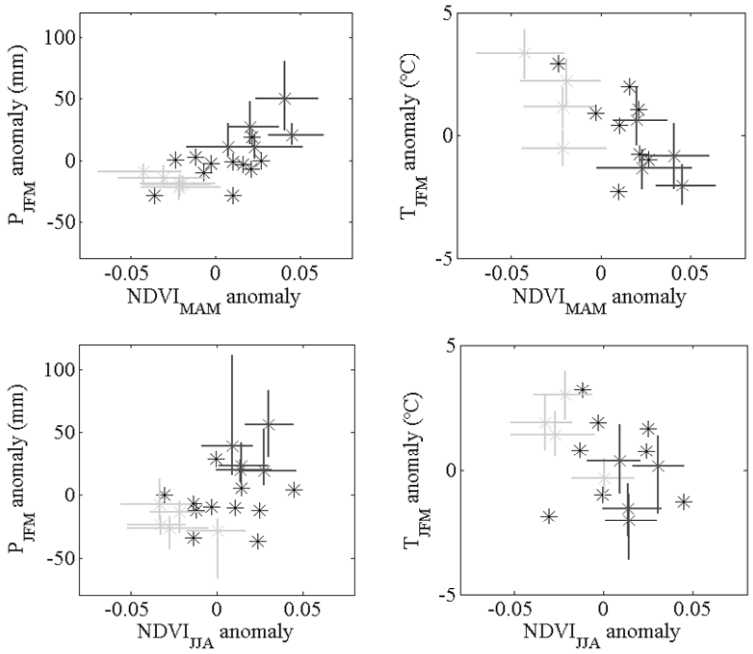

Figure 6.19. Dispersion diagrams of $NDVI_{\_MAM}$ (upper panels) and $NDVI_{JJA}$ (lower panels) versus P_{JFM} (left panels) and T_{JFM} (right panels) for selected pixels over the Iberia. 64% of the 500 selected pixels are spring, not irrigated

crops and 17% are forest and shrubland. Each asterisk represents a pair of median values of a given set of the selected pixels, for a given year of the considered period (1982–2002). Years that belong to the subset of NAO+ (NAO–) are marked in light (dark) grey and the respective variability is characterized by means of vertical and horizontal bars indicating the interquartile ranges.

As shown in Figure 6.19, Iberia presents an increase (decrease) of spring and summer vegetation greenness with precipitation for NAO– (NAO+) years. In both seasons there is more variability of precipitation in the set of NAO– NNCP than in that of NAO+, especially in spring. In the case of spring, there is a slight dependence of vegetation greenness on temperature, with $NVDI_{MAM}$ median values showing a tendency to increase from NAO+ to NAO–. The results highlight the stronger dependence of spring/summer vegetation greenness on winter precipitation anomalies compared to temperature. It should be stressed again that the selected pixels correspond to not irrigated crops and in their majority are spring varieties. This dependence is coincident with the stronger influence of NAO on the Iberian precipitation regime, whereas the impact of NAO on temperature is less clear. The most interesting feature for both spring and summer is that the highest impact of NAO occurs during the periods of the year characterized by more intense vegetation activity, i.e. around April (June) in the case of the NNCP for spring (summer). As mentioned above, in spring, two thirds of the NNCP correspond to cultivated areas that consist mainly of crops adapted to the relatively dry Iberian conditions. For NAO– years the vegetation growth cycle, that starts when water is available, is usually shorter due to the observed high temperatures. During summer the response to precipitation tends to extend late in the year, as the vegetation that is most affected by NAO initiates its growing period later. (Menzel, 2003; Julien *et al.*, 2006; Gouveia *et al.*, 2008).

Case study: Portuguese Wheat Production

Winter atmospheric circulation affects the regional distributions of temperature and precipitation in Europe and relations have been found between these variables and wheat yield for the European countries (Cantelaube *et al.*, 2004). Other studies have shown that a high NAOI in winter is associated with better quality of the UK wheat crop (Atkinson *et al.*, 2005) and with better wheat, rye, oat and citrus yields in the Iberian Peninsula (Gimeno *et al.*, 2002). Estimations of the effects of climate variability on the final crop yields has also been evaluated at five sites in Spain (Iglesias and Quiroga, 2007) and wheat and barley yields were predicted in February, four months before harvest, in the Ebro valley using drought indices and remote sensing data (Vicente-Serrano *et al.*, 2006). Rodríguez-Puebla *et al.* (2007) derived a statistical model able to integrate effects of climate variables (including minimum temperature, precipitation and zonal wind at 200 hPa) as well as the NAO on winter cereals productivity in Spain. The model integrates the effects of abundant precipitation together with dynamic aspects of the air masses, during the maturation. The positive effects of warm winters at the beginning of the cereal growing season were also considered. Several authors have tried to integrate crop simulation models with remote sensing data through data assimilation methods (De Melo *et al.*, 2008; Fang *et al.*, 2008).

For this case study by Gouveia and Trigo (2008), the analysis is focused on the quantification of the climate impact on the wheat yield in Portugal. The majority of wheat in Portugal is sown in October / November and harvested in June / July of the following year. However, it should be kept in mind that Portuguese wheat yields —similar to those of other Mediterranean countries— are considerably smaller than those in northwestern European

countries, with cold (but not very wet; ≤ 50mm/month) winters and relatively wet summers (Gouveia and Trigo, 2008). The aim is to integrate remote sensing information about vegetation (in terms of NDVI) in order to construct a simple seasonal crop model that takes into account the spring NDVI for simulating wheat yield. For this purpose the grid point correlations between spring $NDVI_{MAM}$ composites and wheat yield considering the 18 year period 1982–1999 were obtained (Figure 6.20, left panel). It is worth noticing that the highest positive and significant correlations (at the 99% significance level) are found over the southern region of Alentejo, a region that contributes with more than 80% of the national total wheat production, and concentrates more than 95% of the total of hard wheat production in Portugal.

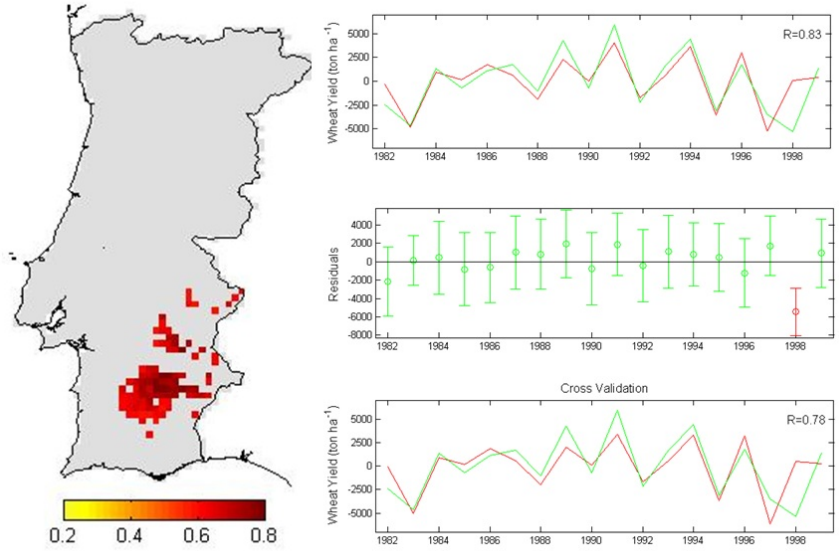

Figure 6.20. (Left) Patterns of Pearson correlation coefficient values between spring $NDVI_{MAM}$ composites and wheat yield in Portugal, for the period of 1982–1999, for pixels coded as arable non irrigated land and significant at the 99% level. (Right) Upper panel: Time series (1982–1999) of observed (grey curve) wheat yield in Portugal and corresponding modeled values (black curve) from a linear regression model based on spring NDVI and NAO in June. Middle panel: Time series (1982–1999) of residuals and respective 95% significance level range; the single outlier (in 1998) is highlighted. Lower panel: Time series (1982–1999) of observed (grey curve) wheat yield in Portugal and corresponding modeled values (black curve) from the leave-one-out cross-validation procedure.

The impact of meteorological factors on wheat yield was further assessed by computing monthly correlations between the anomalies of wheat yield and monthly values of net shortwave radiation, temperature and precipitation as well as with NAO (averaged over the above mentioned homogenous region). All time series were detrended to remove spurious influence from trends. In particular the yield trend is due essentially to improvements in farm management practices. Thus, to study the effect of climate related variability on crop yield, the technological driven trend was removed from the raw time series, in order to work on yield anomalies only. Obtained results are summarized in Table 6.2 and it is worth pointing out that they are in good agreement with the empirical findings about the role (and temporal influence) of the different meteorological variables along the different stages of the wheat vegetative cycle (Sampaio, 1990; Feio, 1991; Gouveia and Trigo, 2008). For instance, the positive impact of cold temperature during winter and early spring on wheat yield is well illustrated by the persistent negative values of correlation, those obtained for February and March being statistically significant at the 95% level, for both months. The positive impact of precipitation in February and March is evident by the respective positive values of correlation (statistically significant at

the 95% level) for March. The crucial role of solar radiation in March to the photosynthetic process is reflected by the high negative correlation (significant at the 99% level). It is worth noting that obtained results are in good agreement with the findings by Rodríguez-Puebla *et al.* (2007) for Spain.

The values of correlation between NAO and wheat yield also reflect the changing role of NAO along the vegetative cycle of wheat. In fact, the difference between late winter/early spring and late spring/early summer is clear, with negative correlations between NAO and yield in February and March and positive correlations in April and June, both statically significant at the 95% level. This behaviour may be viewed as reflecting the integrated impact on radiation, temperature and precipitation fields of the large scale atmospheric circulation patterns associated to the different phases of NAO. In this context the impact of extreme events like droughts, namely during the spring time, have a strong impact in wheat production. This was the case of the outstanding drought episode of 2004-2005 (García-Herrera *et al.*, 2007), with more than one third of Portugal affected by high levels of vegetation stress during nine months or longer, leading to a low wheat production in this year (Gouveia *et al.*, 2009). In this context, droughts may cause significant economic losses (Iglesias *et al.*, 2003), due to the fact that there is a strong dependence of the economy and society on agriculture yields (Vicente-Serrano, 2006a).

Table 6.2. Correlation coefficient values between annual wheat yield in Portugal and monthly net long wave radiation, air surface temperature and precipitation (from January to June) for the pixels coded as arable land not irrigated. Bold values are representing correlations values that are significant at 95% level and underlined value is significant at 99% level

	JAN	FEB	MAR	APR	MAY	JUN
Radiation	0.13	-0.09	**-0.73**	-0.12	0.31	0.12
Temperature	-0.37	**-0.50**	**-0.49**	-0.25	-0.07	0.16
Precipitation	0.06	0.35	**0.54**	-0.17	-0.06	-0.27
NAO	0.09	-0.28	-0.21	**0.48**	0.07	**0.53**

The above results suggest that combined spring NDVI and meteorological variables are suitable to build a simple model of wheat yield in Portugal for the period 1982–1999. A good model was obtained using as predictors $NDVI_{MAM}$ together with the NAO for June. Figure 6.20 (right-upper panel) presents the time series of observed and modeled wheat yield. There is an overall agreement with the two time-series presenting a correlation of 0.83. Figure 6.20 (right-central panel) shows the time series of residuals, defined as departures of observed values from modeled ones. The 95% significance level range relative to these residuals are plotted as error bars and it may be noted that 1998 represents the single outlier since its error bar does not cross the zero reference line. Figure 6.20 (right-lower panel) presents the results obtained from the leave-one-out cross validation. The good agreement between the modeled time series by the regression model (upper panel) and the one obtained by the cross validation indicate that the developed model seems to be robust. This fact is further supported by the slight decrease (from 0.83 to 0.78) of the correlation between original and modeled time series.

The usefulness of this simple model derives from the high impact of both predictor variables. Spring NDVI is an indicator of the healthiness/greenness of wheat during the growing stage. On the other hand, NAO in June is an indicator of the large-scale circulation affecting Portugal related to regional conditions in terms of radiation, temperature and precipitation. Despite the relatively low variance explained by this predictor, it corresponds to an important index of a variable that has a significant role during the process of wheat maturation. Despite the use of a

monthly predictor that is closer to the end of the wheat vegetative cycle, this analysis allows developing and implementing a tool that contributes to improve yield forecasts through the use of seasonal climate forecasts. Results attained by this relatively simple model can be considered satisfactory and are expected to be useful to perform agricultural monitoring.

6.6. Extreme weather associated with exceptional large scale circulation

Large scale circulation does not only impact on climatic conditions, but also modulates weather extremes such as thunderstorms and floods, landslides, strong winds, storm surges and high waves. These weather extremes are usually associated with the formation and passage of cyclones. However, the relationship between the cyclone and the associated impacts is not straightforward. Therefore, the specific characteristics of the cyclone can be influenced by its origin and evolution (e.g., transitioned tropical cyclones) which, in turn, are largely determined by the large scale atmospheric circulation. On the other hand, the influence of the large scale can arise at different temporal scales, ranging from weekly (e.g., mid- and upper-tropospheric air mass intrusions) to seasonal (e.g., fluctuations of the main modes of atmospheric circulation). In this section, interesting examples of weather extremes related to cyclones are analyzed which, because of their sensitivity to climate change are of scientific interest and general public concern. The associated physical mechanisms are described, stressing the influence of the large scale forcing. For a more general description of weather extremes associated with cyclones across the Mediterranean, the reader is referred to Lionello *et al.* (2006) and to Chapter 5 in this book.

6.6.1. Tropical–extra-tropical interactions

Due to the intrinsically different dynamics, tropical and extra-tropical atmospheric circulations are often regarded separately. However, there are important links between the lower and mid-latitudes, typically named as tropical–extra-tropical interactions, which are very relevant for both the tropics and the extra-tropics. Among these tropical–extra-tropical interactions, two are related to heavy rain-storms over the Mediterranean region: (i) tropical plumes, and (ii) tropical systems in tropical–extra-tropical transition.

Tropical Plumes

The tropical plume (TP) is an interesting dynamic phenomenon, which reflects tropical–extra-tropical interaction. Tropical plumes have an annual average of 30-40 occurrences over Northern Africa and the subtropical Northern Atlantic, especially in the cold season (Zohdy 1991). However, most of them are in the form of Cirrus clouds (Ziv, 2001), and only small portion of them produce considerable rain. Rubin *et al.* (2007) found only 10 such cases within 18 years in the eastern Mediterranean. In spite of the relatively low occurrence compared to other systems in the area, TP may develop heavy rainstorms which have far reaching impacts on the weather and water regimes in the arid parts of the Mediterranean, as well as in other subtropical regions in the world. A fatal flooding, associated with TP event, occurred in February 1975 in southern Israel and the Sinai Peninsula (analyzed by Dayan and Abramski, 1983), caused casualties and severe damage. In January 2010 an extreme TP-related rainstorm

filled all of the water reservoirs over the Negev Desert, Israel, within one night, but the floods caused two fatalities and caused severe damage to the infrastructure.

Tropical plumes (TPs; Figure 6.21) are continuous bands of (non-precipitating) upper- and mid-tropospheric clouds that extend from the tropics into the mid-latitudes (crossing 15° N), usually with a length of at least 2,000 kilometers (McGuirk *et al.*, 1987). Commonly, TPs are narrow at the lower latitudes (15º–20º N), but at times they broaden near 30º N to form rainstorms (e.g., Rubin *et al.*, 2007).

Tropical plumes often originate from upper level outflow associated with tropical systems or large scale deep tropical convection and are associated with synoptic scale mid-latitude troughs extending to lower latitudes. Tropical plumes have been shown to contribute to heavy precipitation events along the southern Mediterranean, from Morocco to Israel (Krichak and Alpert, 1998; Ziv, 2001; Knippertz *et al.*, 2003). Rainstorms associated with TPs are typified by stratiform cloudiness, but may produce large amounts of rain, exceeding 10 mm and even 50 mm over arid regions, resulting in destructive floods (Dayan and Abramski, 1983; Ziv, 2001; Kahana *et al.*, 2002; Rubin *et al.*, 2007).

The TPs develop ahead of a positively aligned (southwest–northeast) upper-level extra-tropical trough, which penetrates into the lower subtropics (Figure 6.21). The trough is accompanied by an intense southwesterly subtropical jet (STJ) ahead, where the cloud band is found (e.g., McGuirk *et al.*, 1988; Ziv, 2001; Knippertz, 2005; Knippertz and Martin, 2005). The typical TP lifetime varies between two and nine days (Thepenier and Cruette, 1981; McGuirk *et al.*, 1987; Rubin *et al.*, 2007) and constitutes a visible signature of tropical–extra-tropical interaction. That is why McGuirk and Ulsh (1990) regarded TPs and their associated transports as "a large component of the Pacific general circulation".

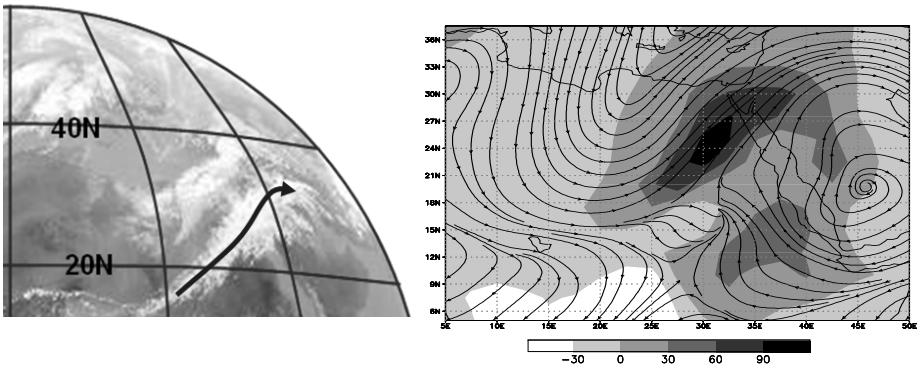

Figure 6.21. (left) Satellite Infra Red imagery (METEOSAT) for 12 UTC 21 March 1991, showing a TP that extends from central Africa toward the eastern Mediterranean; (right) Meridional specific humidity transport (in 30 g kg-1 m s-1 increments) and streamlines on 315 K isentropic surface at 18 UTC 21 March 1991, based on NCEP-NCAR reanalysis. From Rubin *et al.* (2007) © Copyright 2007 American Meteorological Society (AMS).

TPs occur in the Northern Hemisphere mainly during the winter and transition seasons (McGuirk *et al.*, 1987; Kuhnel, 1989; Iskenderian, 1995). Detailed studies of TPs for the Pacific were done by McGuirk *et al.* (1987, 1988), McGuirk and Ulsh (1990), McGuirk (1993), Blackwell (2000) and others. Studies dealing with TPs over North Africa were done by Zohdy (1989, 1991), Ziv (2001), Knippertz *et al.* (2003), Knippertz (2005) and Knippertz and Martin (2005).

McGuirk *et al.* (1988) attributed the development of TPs to coincidence of deep upper-troughs with tropical easterly waves and showed that they result from a combination of poleward advection of Cirrus clouds formed from the tops of tropical convection and dynamical

processes associated with the STJ. These results are supported also by Mecikalski and Tripoli (1998), Ziv (2001) and Knippertz (2005). Kiladis and Weickmann (1992a, b), Iskenderian (1995) and Kiladis (1998) confirmed this view by demonstrating statistical relationship between enhanced tropical convection, TP formation, and wave trains in the extratropics.

A major effort in the TP studies was devoted to point at the detailed moisture transport of TPs. Zangvil and Isakson (1995) showed that the moisture over Israel was transported in the mid-levels, above the 750 hPa, from tropical Africa. Ziv (2001), Knippertz *et al.* (2003) and Rubin *et al.* (2007) showed that the tropical moist air contained in TPs tend to be detached from the underlying dry Saharan PBL. Therefore the moist air is prevented from mixing with the underlying dry air mass so the moisture is preserved to produce considerable rain over the target regions. Rubin *et al.* (2007), who analyzed ten TP events that produced considerable rain over Israel, found that the Gulf of Guinea and its adjacent land are the preferred origin (in agreement with Kuhnel, 1989). They showed that the plume itself is the major moisture source rather than local lower-level moisture sources (as is the case of Mediterranean Cyclones).

Several ageostrophic effects enhance the TP-induced rain (Ziv, 2001). One is the divergence taking place in the right hand side of the STJ entrance, which enhances tropical convection in the TP origin. Second is the deviation of the southwesterly wind to the left, which enhances the meridional moisture transport from the convective clouds. The third is the upper-air divergence in the inflection point ahead of the trough, which induces high vertical velocity, which is further enhanced due to the high wind velocity and the low Coriolis parameter typifying TPs. Based on the above mentioned ten cases over the EM, Rubin *et al.* (2007) pointed at four processes that contribute to the effectiveness of these TPs in producing rain:

(i) The TP develops within several consecutive days ahead of a stationary subtropical trough, in which the TP is "charged" with moisture. Similar results were found by Knippertz and Martin (2005) for western North Africa;
(ii) The absence of upward motion along the central part of the plume prevents loss of moisture via condensation and/or precipitation;
(iii) The detachment of the plume from the underlying arid air mass (Figure 6.21) prevents moisture loss by mixing;
(iv) The coherence of the flow within the plume diminishes turbulence and so minimizes turbulent diffusion of moisture, at least in its core.

Ex-Hurricanes

The influence of ex-tropical systems on extreme precipitation events is less frequent than for tropical plumes. Such systems are recurring tropical cyclones tracking northeastward typically along the North American east coast into the mid-latitudes that undergo extra-tropical transition along the way. As suggested by Pinto *et al.* (2001), such systems may induce strong precipitation events in the Mediterranean in a number of ways: (i) northward moving tropical storms could dynamically force a downstream development/intensification of a persistent trough (Riemer *et al.*, 2008); when the persistent trough is located near the British Isles, it induces optimal large scale forcing for large scale upward movements over the western Mediterranean; (ii) tropical storms typically bring large moisture amounts from the tropics (usually within preferential paths, cf. Knippertz and Wernli, 2010). This enhanced moisture may be then advected towards the Mediterranean in the following days by other mid-latitude systems or by the large scale flow itself (Krichak and Alpert, 1998; Reale *et al.*, 2001; Turato *et al.*, 2004) and (iii) tropical storms (or their remnants) may move directly close to or even into the

Mediterranean (e.g., hurricane *Vince* in October 2005, of subtropical origin that reached the hurricane strength close to Madeira).

Such developments have been associated with flood events over the Mediterranean, particularly on the northern side of the western basin (Krichak and Alpert, 1998; Turato *et al.*, 2004). A striking feature is that typically no intense cyclone is present in the Mediterranean — one that could potentially be responsible for the extremeness of the event by itself. This fact points to remote large scale forcing mechanisms and also to a collection of moisture that could occur on time scales much longer than the lifetime of the weather systems involved (Turato *et al.*, 2004; Pinto *et al.*, 2011).

An illustrative case is presented below for the extreme precipitation and following flooding event that affected Piedmont, Italy, between 13 and 16 October 2000 and led to landslides, destroyed roads and houses, electricity cuts and traffic disruption in the whole Po Valley area. Heavy precipitation in this area is typically forced by the large scale circulation over the western Mediterranean, with continuous south–southwesterly flow against the southern Alpine flanks (Rudari *et al.*, 2005). The very complex orography of this area leads to highly heterogeneous precipitation distributions both in space and time (Frei and Schär, 1998), due to the influence of orographic precipitation mechanisms like downwind sheltering (Smith and Barstad, 2004). During the 13–16 October 2000 event extraordinary rainfall amounts were observed over the whole southern Alpine flanks, with a maximum accumulated precipitation over four days (13-16.10) exceeding 700 mm (in the upper Po Valley). The extreme precipitation amount led to an extended flood in the Po Valley following the event. The extreme event was locally triggered by a shallow cyclone that appeared on the 12 October 2000 over the western Mediterranean and was only the final trigger in a chain of developments that induced it: one week earlier, hurricane *Leslie* moved northward along the North American east coast bringing a huge amount of moisture into the extra-tropics (Figure 6.22), and underwent extra-tropical transition on 8–9 October. The remnants of *Leslie* propagated eastward towards the British Isles in the form of an extra-tropical cyclone transporting a large amount of moisture eastward over Europe. Backward trajectories (from 12 October) confirm that a significant part of the moisture traces back to an area near Newfoundland where *Ex-Leslie* was located on 9–10 October (cf. with Turato *et al.*, 2004 and Pinto *et al.*, 2011). This contribution is relevant in a time scale of about 5–15 days preceding the event.

For shorter timescales, local evaporation from the Mediterranean, water vapor recycling, and orographically induced low-level convergence enhanced and concentrated the moisture over the area where heavy precipitation occurred. Additionally, water vapor intrusions from the African intertropical convergence zone and evaporation from the eastern Atlantic also played a role. Large scale moist dynamics were therefore important in enabling the moderate Mediterranean cyclone (appeared on 12 October 2000 in the basin) to produce heavy precipitation. In total, more than half of the moisture amounts associated with this event originated from the North Atlantic (Figure 6.22).

These results are in line with works (e.g., Martius *et al.*, 2006) that have stressed the link between the presence of an upper level trough (analyzed as potential vorticity structures) over western Europe and high precipitation events in the Alpine area. Similar structures have also been identified by Massacand *et al.* (1998). Further, higher percentiles of heavy precipitation events over northwest Italy are associated with enhanced moisture advection from the North Atlantic into the western Mediterranean (Rudari *et al.*, 2005; Pinto *et al.*, 2011) and in some cases ex-hurricanes (Pinto *et al.*, 2011). The cyclones are however not as intense to justify the event by themselves. Influences from the North Atlantic have been documented also for the

eastern Mediterranean (Krichak *et al.*, 2004; 2007). Locally, the events are typically triggered by lee cyclogenesis over the western Mediterranean (Buzzi and Tibaldi, 1978). See section 6.4.1 for a comprehensive analysis of moisture origins in the Mediterranean basin.

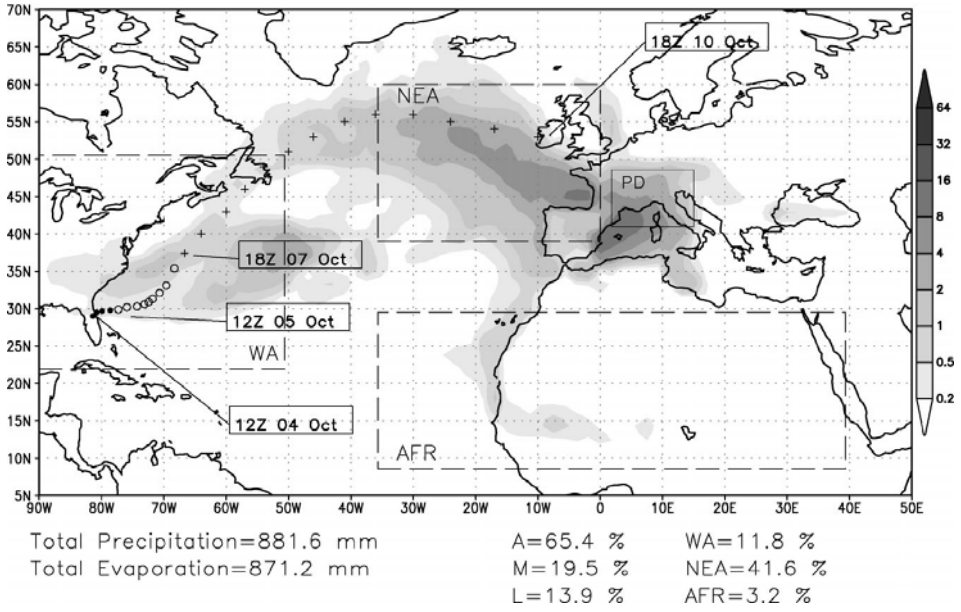

Figure 6.22. Accumulated evaporative sources (kg m^{-2}) collected over the entire domain and contributing to rainfall over Po Valley area (PD) during the period 10–14 Oct 2000 for days minus 5 to minus 15. Total precipitation fallen over PD and total evaporation collected over the entire domain are on the bottom left of the panel; fractional evaporative sources computed over sub domains WA, NEA, and AFR, as marked on the map, are 11.8%, 41.6% and 3.2%, respectively. Track of Tropical Storm *Leslie* (from the National Hurricane Centre, USA) from 4 to 10 October 2000, at various stages: subtropical depression (dots), tropical storm (circles), extra-tropical system (crosses). From Turato *et al.* (2004) © Copyright 2004 American Meteorological Society (AMS).

6.6.2. Sea surges and flooding: Venice as a case study

Acqua alta

From the perspective of climate change, coastal regions are among the most important "hot spots" to address in the Mediterranean, as they represent highly populated areas exposed to a large variety of extreme events and also to changes in sea level. In particular, Venice has captured the interest of many studies as a case of coastal vulnerability and a model to test adaptation and mitigation strategies.

Since Venice's foundation in 400 AD, the sinking of the city has always been of great concern, as evidenced by local efforts to provide a continuous sea level reference: from the early indirect estimates of Comune Marino (a 'C' mark engraved in canals and buildings) since 1440, to the most recent and accurate system of tide gauges since 1872. A mean relative sea level trend of ~2.4 mm/yr has been reported for the instrumental period (since the 1870s) (Camuffo and Sturaro, 2004; Frassetto, 2005; APAT, 2006). The accelerated change of the last century has been attributed to several factors (e.g., Camuffo and Sturaro, 2004, and references therein): (i) sea level rise caused by global warming (thermal expansion of oceans and increased melting of glaciers and ice caps), which has accounted for about 1–1.5 mm/yr, (ii) local land subsidence

due to geological processes and mainly anthropogenic activities, the most important one being the excessive ground-water extraction for industry, which caused subsidence rates of ~2.5 mm/yr in 1930–1970 and (iii) changes in the damping of waves and in water flux exchanges with the Adriatic Sea due to works in morphology of the lagoon. The two first processes seem to have contributed almost equally to the total ~25–30 cm submersion of the twentieth century (see also Lionello (2011) for a detailed discussion).

Within this context of loss elevation, Venice is frequently affected by floods of more than ~90 cm above the mean sea level (MSL), locally called *acqua alta*, which cause damages to the historical centre (e.g., Pirazzoli, 1991). The duration of the *aqcua alta* is usually less than four hours, and hence, the relative phase of the sea surge and the tide is critical (Tomasin, 2005). However, as the astronomical tide alone (lower than 74 cm above MSL) is unable to flood the city, most of the flooding events result from severe meteorological conditions (Tomasin, 2005) and they are referred to as storm surges. Storm surges are usually identified as independent surges (not necessarily floods) separated by at least 72 hours (e.g., Lionello, 2005), thus excluding secondary surge events that are typically caused by *seiches* (resonant modes of oscillation in the Adriatic).

Reconstructions of the frequency of past floods since the eighth century (Camuffo and Sturato, 2004) indicate periods with anomalous frequency of sea surges and an exponentially increasing trend during the twentieth century (Figure 6.23). The particularly pronounced increase of surge events after 1900 is found to be mainly due to the local submersion, since no trend is evident when the effects of sea level rise and subsidence are removed from the raw data (Lionello, 2005). In fact, for the second half of the twentieth century, the occurrence of secondary surges continued to increase, as a likely consequence of sea level rise. However, the frequency of independent flooding events does not show evidence of any significant trend during the same period, in general agreement with the decrease in intensity of Mediterranean cyclones (Trigo and Davies, 2002). In general the analysis of storm surge events in the period 1940-2008 shows only very weak and marginally negative trends in the intensity of storm surge events (Lionello *et al.*, 2010).

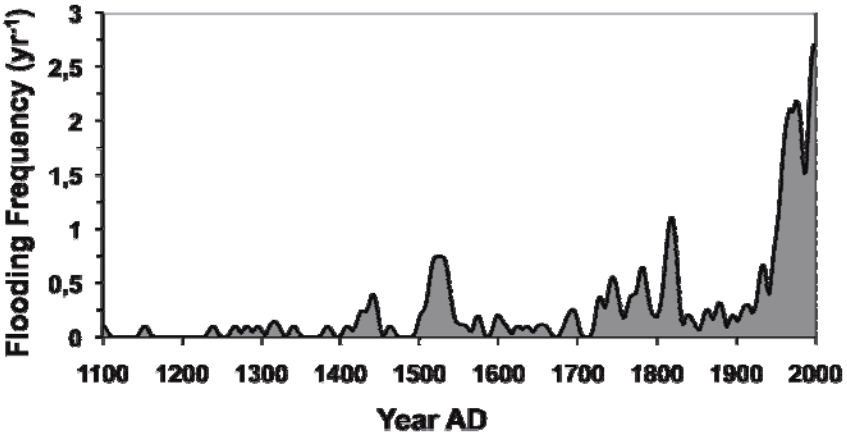

Figure 6.23. Frequency distribution of flooding surges in the documentary (1200–1871) and instrumental (1872–2000) periods. The data has been smoothed with the Hamming–Tuckey filter with 19-year window and 2-year step (courtesy of Dario Camuffo)

Synoptic patterns associated with surges in Venice

The preferred season for the occurrence of sea surges is October–January, which concentrates about ¾ of all occurrences in a year, and the annual cycle of events only displays small differences when different peak surge thresholds are considered (Lionello *et al.*, 2010). This asymmetry in the annual distribution of sea surges is mainly related to seasonal climatological regimes, namely a relative persistence of southeasterly (*Sirocco*) and northeasterly (*Bora*) winds whose synergistic effect is an accumulation of sea water around Venice (e.g., Trigo and Davies, 2002, and references therein).

Sea surges occur after the concurrence of a set of 'adverse' conditions with enhanced duration and intensity (Trigo and Davies, 2002). These meteorological conditions are generally triggered by large low pressure systems over the Atlantic travelling along a northwest–southeast axis towards central Europe (Figure 6.24), and whose interaction with the orography induces secondary pressure minima over the Mediterranean. Although this is the typical picture associated with cyclogenesis at the lee of the Alps, the persistence and stationarity of lows over northern Italy is particularly favourable for the occurrence of sea surges. More detailed synoptic analyses have shown that the preferred cyclogenetic region of cyclones inducing extreme surges is located at the western Mediterranean (Lionello *et al.*, 2010). The physical mechanisms involved at the time of the surge are well documented (e.g., Trigo and Davies, 2002): (i) the hydrostatic balance induced by the low air pressure over northern Italy and the pressure gradient towards the southern Adriatic, (ii) *Sirocco* winds along the Adriatic Sea, which favour the channelling of wind along the basin, high sea waves and the piling up of water at the northern end of the Adriatic Sea. These effects are reinforced by the bathymetry of the Adriatic Sea (deeper in the south and shallower in the north).

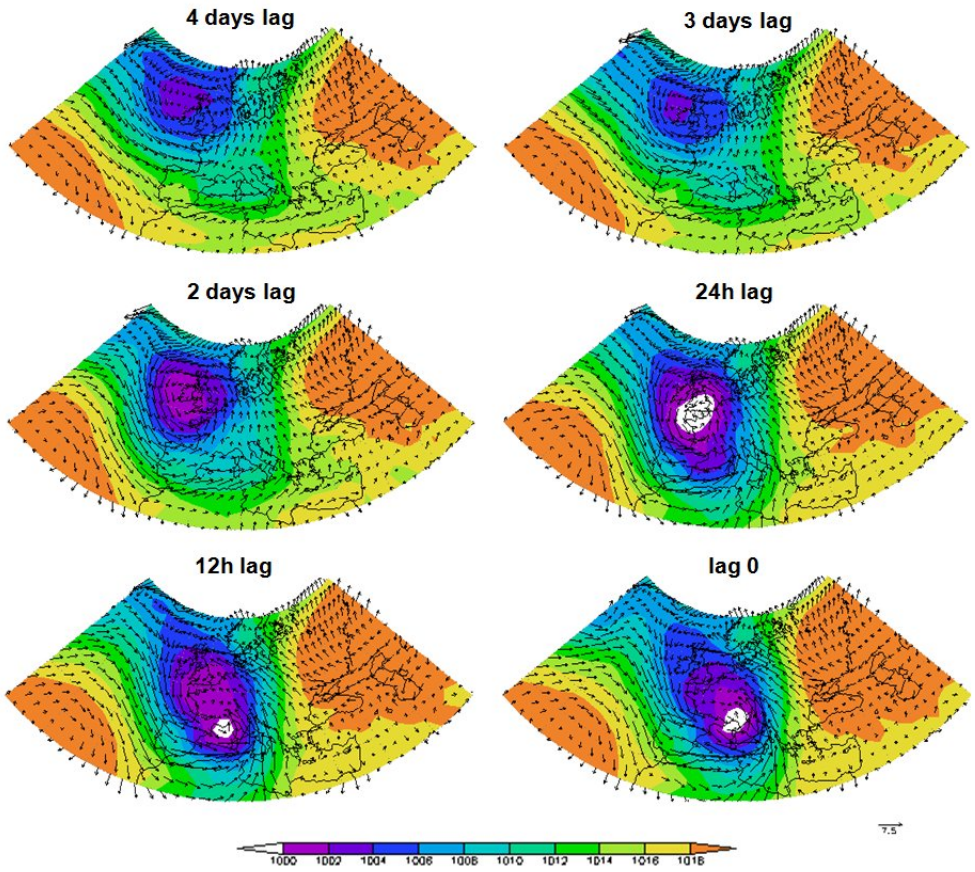

Figure 6.24. Composites of SLP (hPa) and 995 hPa wind (m/s), performed for the time lags indicated at the top of each panel, for independent sea surge events in Venice for the period 1948-1997 for 74 events. The detached arrows represent a unit speed of 7.5 m/s. SLP and wind data stem from NCEP-NCAR reanalysis dataset (Kalnay *et al.*, 1996; Kistler *et al.*, 2001); sea level data stem from Camuffo (1993).

Large scale patterns and inter-annual variability of surges

Superimposed to the long-term trend, the record of surges is dominated by large inter-annual–to–decadal variability, whose origin is not well understood. This variability has partially been attributed to the most prominent Euro-Atlantic teleconnections, whose fluctuations are mirrored in the MSL record of Venice for the period 1872–2004 (e.g., Zanchettin *et al.*, 2009). In particular, the NAO (see also Chapter 5, this book) has been reported to exert an influence on winter sea levels of the Adriatic (~50% of the MSL variance). In autumn, the SCAND and the EA/WR patterns (e.g., Fagherazzi *et al.*, 2005) are the main drivers of MSL fluctuations, accounting for about 25% of its variance. The key processes associated to fluctuations of these large-scale patterns involve the regional modulation of: (i) atmospheric pressure anomalies causing the hydrostatic barometric response of water masses, (ii) wind stress patterns and (iii) changes in air-sea fluxes, precipitation/evaporation patterns and freshwater input from the Po river, which exert a control in the temperature and salinity of near-surface layers and hence, in deep water formation and water exchange processes (e.g., Tsimplis *et al.*, 2008; Zanchettin *et al.*, 2009).

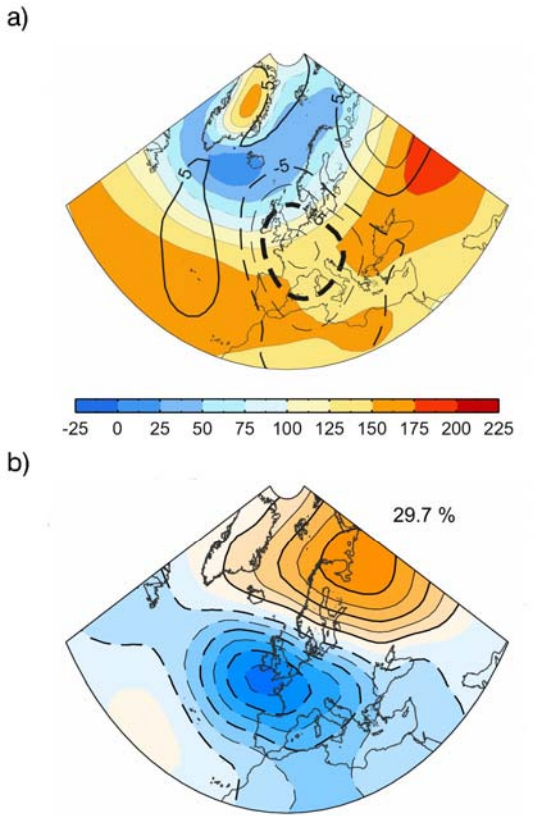

Figure 6.25. (a) October–November–December geopotential height at 1000 hPa (Z1000) averaged over the period 1948–2008 (shaded; gpm). Contours represent Z1000 composite differences between years with at least one surge event and years without any surge event for 1948–2008. Solid (dashed) lines indicate positive (negative) differences with 5 gpm contour interval, starting at 5 (–5) gpm. Thick lines denote significant differences at $p<0.05$; (b) EOF1 of

the October–November–December 1000 hPa geopotential height anomaly field for 1948–2008. Solid (dashed) lines indicate positive (negative) normalized loadings. The explained variance is indicated in the upper right corner. Data stem from NCEP-NCAR reanalysis (Kalnay *et al.*, 1996; Kistler *et al.*, 2001)

In accordance with the effects of teleconnection patterns in the Venetian MSL, the frequency and magnitude of high tides are also affected by oscillations of the main climatic patterns. The correlation is strongly negative with the NAO during winter months, whereas in the autumn, when most of the city floods occur, the NAO influence is negligible (e.g., Lionello, 2005), being rather the EA/WR the one that exerts a stronger influence on the tidal regime (Fagherazzi *et al.*, 2005). No evident teleconnection was found between ENSO and flooding events in Venice (Camuffo *et al.*, 2000).

The existence of seasonal mean configurations that enhance the occurrence of surge events in Venice demonstrates the importance of anomalous large scale conditions in driving the interannual variability of storm surges. The autumn geopotential height field during active years (those with at least one surge) is significantly different from that during quiet years (those with no surges at all). The corresponding difference field identifies the large scale pattern favorable for high surges and reveals an anomalous large scale signature suggestive of increased cyclone activity over Europe (Figure 6.25a). This seasonal configuration does not resemble the NAO, but rather a wave train, which is significantly related ($r = 0.86$, $p < 0.01$) to the main variability mode (EOF1) of the regional atmospheric circulation (Figure 6.25b).

Solar activity, and in particular, its 11-yr cycle, has also been proposed as a potential candidate to explain inter-decadal oscillations in the frequency of sea surges (Lionello, 2005). When the highest surge events are considered for the 1948–2008 period, solar maxima are significantly associated to a higher frequency of October–to–December surges (Barriopedro *et al.*, 2010a). It is clear that any physical mechanism connecting solar activity and surges should involve some large-scale feature with significant local effects in Venice (Tomasin, 2005). Recently, a hypothetical mechanism has been proposed through a solar modulation of the spatial patterns of the main mode of regional atmospheric variability (Figure 6.25b) and the favorable pattern for surge occurrence (Figure 6.25a). In this hypothesis, the interaction between the regional atmospheric variability and the favourable pattern for surge occurrence is enhanced during solar maxima and inhibited in solar minima (Barriopedro *et al.*, 2010a). However, at centennial time scales, the linkage between flooding and sunspots is not evident or masked by other factors (Camuffo and Sturaro, 2004; Figure 6.23), which may indicate a non-stationary or non-linear relationship (Zanchettin *et al.*, 2009; Barriopedro *et al.*, 2010a).

Conclusions

The Mediterranean is identified as one of the most prominent and vulnerable climate change “hot spot” areas of the world. Changes in the occurrence, frequency and intensity of extreme, high impact, events have already been observed in the last few decades. In this chapter an overview is given on the atmospheric circulation and atmospheric patterns associated with extreme events of most relevance to environmental and socio-economic impacts in the Mediterranean basin.

In the 21st century, summer heat waves are expected to further increase both in frequency, intensity and duration in parallel with an enhancement of the summer temperature variability. High temperature events are found to be strongly influenced by persistent large scale circulation patterns in the Euro-Atlantic region. Hot summer temperatures in the western Mediterranean

and France are linked to atmospheric blocking and the Atlantic low pattern. The two patterns, with different dynamical characteristics, are generally associated with hot and dry conditions.

The occurrence of those regimes is shown to be influenced by a number of external forcing mechanisms, ranging from local or remote SSTs to stratospheric circulation anomalies. Studies of the 2003 heatwave suggest the role of the Mediterranean, Indian and Atlantic Ocean SSTs, while land surface feedbacks mainly act through local effects on the surface energy budget.

Deadly heat waves in the eastern Mediterranean are connected with warm air advection from the Persian Gulf and atmospheric stability, in combination with high Mediterranean SSTs and enhanced heat fluxes.

Extreme phases of the ENSO are found to influence humid and drought conditions in the Mediterranean region. This influence is not homogeneous throughout the region and shows large seasonal differences. Dry conditions in the Mediterranean are connected with La Niña events whereas humid conditions are generally recorded during El Niño events. A large spatial diversity characterizes the influence of La Niña on the Mediterranean climate conditions, where the most important signal is found in eastern Spain, the Balkans and Turkey. This influence could be connected with a positive NAO-like pattern and the intensification of the Azores high during La Niña winters. However, relevant studies pointed to the average-to-weak, although statistically significant, ENSO signal on Europe and the Mediterranean. The ENSO signal being important for events with particularly strong effects further suggests the importance of better understanding the ENSO impact on the area.

The semi-enclosed Mediterranean/Black Sea system and the semi-arid/arid conditions in land regions downstream of Mediterranean moisture fluxes imply the significance of the Mediterranean water cycle changes and their impacts for the area. Analyses of the moisture budget show that Mediterranean regions are mostly influenced by the corresponding surrounding sea areas and the local dominant flows of air masses over land. However, the contribution of remote areas as the Tropical–Subtropical North Atlantic Ocean is found to be relevant for the western basin.

Mediterranean water cycle changes are identified in observational data. Winter precipitation decrease is related to the NAO behavior, while during the dry season the influence of a blocking-like pattern is associated with storms deflection from southern Europe. The substantial increase in E–P during the period 1958-2006 reflects the combined effects of precipitation and surface temperature changes. Subsequently, a number of Mediterranean rivers show long-term decreases in discharge during the twentieth century that is likely in part due to intensified water use.

Consistent with the relationship between the Mediterranean precipitation and the NAO, cloud cover variability over mainly the western basin is associated with the NAO phases and presents an important influence on the solar radiation spatial and temporal variability. Over the Iberian Peninsula, about 9% of the total interannual – winter-to-winter – cloud cover variability is associated with the NAO. Analyses of the mean winter sunshine duration sums reveal the existence of a Mediterranean solar radiation spatial variability mode associated with the NAO, mostly pronounced over the western basin.

It is also shown that the NAO controls the inter-annual variability of the vegetation dynamics and that this is mostly associated with the impact exerted by the NAO on the precipitation regime over large areas of Iberia.

Studies of the relation between the winter NAO and the spring and summer NDVI show negative correlations over the Iberian Peninsula. During spring, positive correlations are found at the eastern part of the peninsula. In both cases, significant correlations are found for non-

irrigated crops / land areas. The impact of NAO on vegetation activity is thus clearly noticeable also during other seasons apart from winter.

More specifically, the analysis of the climate impact on the wheat yield in Portugal revealed that combined spring NDVI and June NAO are suitable to build a simple model of wheat yield in Portugal for the period 1982-1999. In this case, spring NDVI is an indicator of healthiness/greenness of wheat during the growing stage, while the June NAO is an indicator of the large-scale circulation affecting Portugal related to regional conditions in terms of radiation, temperature and precipitation.

Tropical–extra-tropical interactions related to heavy rain-storms over the Mediterranean region are tropical plumes and tropical systems in tropical–extra-tropical transition.

Tropical plumes may develop heavy rainstorms with far reaching impacts on the weather and water regimes in the arid parts of the Mediterranean. They are continuous bands of (non-precipitating) upper- and mid-tropospheric clouds that extend from the tropics into the mid-latitudes. The tropical moist air contained in tropical plumes is preserved in the tropical plume due to the absence of upward motion along the central part of the plume, the detachment of the plume from the underlying arid air mass (e.g. Sahara) and the coherence of the flow within the plume. Major moisture source is the plume itself that is developed within several days ahead of a stationary subtropical trough.

Ex-tropical systems, ex-hurricanes, may induce strong precipitation events in the Mediterranean by (i) northward moving tropical storms that dynamically force a downstream development/intensification of a persistent trough, (ii) tropical storms typically bring large moisture amounts from the tropics that is advected towards the Mediterranean, (iii) tropical storms (or their remnants) may move directly close to or even into the Mediterranean. Such developments have been associated with flood events over the Mediterranean, particularly on the northern side of the western basin.

Acqua alta, the frequent Venice floods with consequent damages to the historical city, are taking place in the context of loss elevation of the area, due to mainly anthropogenic activities and result from severe meteorological conditions, the storm surges. Reconstructions of the frequency of past floods point to a pronounced increase of surge events after 1900 that is found to be mainly due to the local submersion, since no trend is evident when the effects of sea level rise and subsidence are removed. However, storm surge events show no trend in the second part of the twentieth century that is in agreement with the intensity decrease of the Mediterranean cyclones. *Acqua alta* occur in their majority during October – January and are mainly related to seasonal climatological regimes, namely a relative persistence of southeasterly (*Sirocco*) and northeasterly (*Bora*) winds whose synergistic effect is an accumulation of sea water around Venice. Large low pressure systems over the Atlantic travelling along a northwest–southeast axis towards central Europe interact with the orography and induce secondary pressure minima over the Mediterranean. The persistence and stationarity of lows over northern Italy is particularly favourable for the occurrence of sea surges, while preferred cyclogenetic region of cyclones inducing extreme surges is located at the western Mediterranean.

Acknowledgements

E. Xoplaki and A. Toreti acknowledge support by the EU FP6 IP CIRCE and EU FP7 IP ACQWA. R. Trigo and C. Gouveia were supported by the FCT (Portugal) through project ENAC (PTDC/AAC-CLI/103567/2008) and the EU FP6 IP CIRCE. D. Pozo-Vázquez was supported by the Spanish CICYT, Project ENE2007-67849-CO2-01 and Andalusia Regional

Government, P07-RNM 02872, financed this study. D. Camuffo and P. Lionello provided helpful comments for section 6.6.2 on sea surges and flooding in Venice. D. Camuffo kindly provided Figure 6.23.

References

Adler, R.F., Huffman, G.J., Chang, A., Ferraro, R., Xie, P.-P., Janowiak, J., Rudolf, B., Schneider, U., Curtis, S., Bolvin, D., Gruber, A., Susskind, J., Arkin, P., Nelkin, E., 2003. The version 2 Global Precipitation Climatology Project (GPCP) monthly precipitation analysis (1979-present). Journal of Hydrometeorology 4, 1147–1167.

Alexander, L., 2011. Climate science: Extreme heat rooted in dry soils. Nature Geoscience 4, 12-13.

AMS, 1997. Meteorological drought – policy statement. Bulletin of the American Meteorological Society 78, 847-849.

APAT, 2006. Aggiornamento sulle osservazioni dei livelli di marea nella laguna di Venezia, Rapporto no. 69/2006, Agency for Environmental Protection and Technical Services, Venice.

Atkinson, M.D., Kettlewell, P.S., Hollins, P.D., Stephenson, D.B., Hardwick, N.V., 2005. Summer climate mediates UK wheat quality response to winter North Atlantic Oscillation. Agricultural and Forest Meteorology 130, 27-37.

Austin, R.B., Cantero-Martínez, C., Arrúe, J.L., Playán, E., Cano-Marcellán, P., 1998. Yield-rainfall relationships in cereal cropping systems in the Ebro river valley of Spain. European Journal of Agronomy 8, 239-248.

Barnston, A.G., Livezey, R.E., 1987. Classification, seasonality and persistence of low-frequency atmospheric circulation patterns. Monthly Weather Review 115, 1083-1126.

Barriopedro, D., Fischer, E.M., Luterbacher, J., Trigo, R.M., García-Herrera, R., 2011. The hot summer of 2010: Redrawing the temperature record map of Europe. Science 332, 220-224.

Barriopedro, D., García-Herrera, R., Lionello, P., Pino, C., 2010a. A discussion of the links between solar variability and high-storm-surge events in Venice. Journal of Geophysical Research 115, D13101.

Barriopedro, D., García-Herrera. R., Trigo, R.M., 2010b. Application of blocking diagnosis methods to General Circulation Models. Part I: A novel detection scheme. Climate Dynamics 35, 1373-1391.

Beniston, M., 2004. The 2003 heat wave in Europe: A shape of things to come? An analysis based on Swiss climatological data and model simulations. Geophysical Research Letters 31, L02202.

Beniston, M., Diaz, H., 2004. The 2003 heat wave as an example of summers in a greenhouse climate? Observations and climate model simulations for Basel, Switzerland. Global Planetary Change 44, 73–81.

Beniston, M., Stephenson, D.B., Christensen, O.B., Ferro, C. A. T., Frei, C., Goyette, S., Halsnaes, K., Holt, T., Jylha, K., Koffi, B., Palutikof, J., Scholl, R., Semmler, T., Woth, K., 2007. Future extreme events in European climate: an exploration of regional climate model projections. Climatic Change 81, 71–95.

Berry, D.I., Kent, E.C., 2009. A new air-sea interaction gridded dataset from ICOADS with uncertainty estimates. Bulletin of the American Meteorological Society, 90, 645-656.

Black, E., Blackburn, M., Harrison, G., Hoskins, B., Methven, J., 2004. Factors contributing to the summer 2003 European heatwave. Weather 59, 217–221.

Black, E., Sutton, R., 2007. The influence of oceanic conditions on the hot European summer of 2003. Climate Dynamics 28, 53-66.

Blackwell, K.G., 2000. Tropical plumes in a barotropic model: A product of Rossby wave generation in the tropical upper troposphere. Monthly Weather Review 128, 2288-2302.

Briffa, K.R., Jones, P.D., Hulme, M., 1994. Summer moisture variability across Europe, 1892-1991: an analysis based on the Palmer drought severity index. International Journal of Climatology 14, 475-506.

Brönnimann, S., 2007. Impact of El Niño–Southern Oscillation on European climate. Reviews of Geophysics 45, RG3003.

Brönnimann, S., Xoplaki, E., Casty, C., Pauling, A., Luterbacher, J., 2007. ENSO influence on Europe during the last centuries. Climate Dynamics 28, 181-197.

Burton, I., Kates, R.W., White, G.F., 1978. The environment as hazard. Oxford University Press. New York, p. 240.

Buzzi, A., Tibaldi, S., 1978. Cyclogenesis in the lee of the Alps: A case Study. The Quarterly Journal of the Royal Meteorological Society 104, 271-287.

Camuffo, D., 1993. Analysis of the sea surges at Venice from A.D. 782 to 1990. Theoretical and Applied Climatology 47, 1-14.

Camuffo, D., Secco, C., Brimblecombe, P., Martin-Vide, J., 2000. Sea storms in the Adriatic Sea and the western Mediterranean during the last millennium. Climatic Change 46, 209-223.

Camuffo, D., Sturaro, G., 2004. Use of proxy-documentary and instrumental data to assess the risk factors leading to sea flooding in Venice. Global and Planetary Change 40, 93-103.

Cantelaube, P., Terres, J.-M., Doblas-Reyes, F.J., 2004. Climate variability influences on European agriculture. Analysis for winter wheat production. Climate Research 27, 135-144.

Carbognin, L., Teatini, P., Tomasin, A., Tosi, L., 2009. Global Change and relative sea level rise at Venice: What impact in term of flooding? Climate Dynamics 35, 1039-1047, doi: 10.1007/s00382-009-0617-5.

Cassou, C., Terray, L., Phillips, A.S., 2005. Tropical Atlantic influence on European heat waves. Journal of Climate 18, 2805–2811.

Cattiaux, J., Vautard, R., Yiou, P., 2009. Origins of the extremely warm European fall of 2006. Geophysical Research Letters 36, L06713.

Changnon, S.A., Easterling, W.E., 1989. Measuring drought impacts: the Illinois case. Water Resources Bulletin 25, 27-42.

Changnon, S.A., Kunkel, K.E., Reinke, B.C., 1996. Impacts and responses to the 1995 heat wave: A call to action. Bulletin American Meteorological Society 77, 1497-1506.

Charles, S.P., Bates, B.C., Whetton, P.H., Hughes, J.P., 1999. Validation of downscaling models for changed climate conditions: Case study of southwestern Australia. Climate Research 12, 1-14.

Chen, M.Y., Xie, P., Janowiak, J.E., Arkin, P.A., 2002. Global land precipitation: A 50-yr monthly analysis based on gauge observations. Journal of Hydrometeorology 3, 249-266.

Chen, D., Cane, M.A., Kaplan, A., Zebiak, S.E., Huang, D.J., 2004. Predictability of El Niño over the past 148 years. Nature 428, 733-736.

Chiacchio, M., Wild, M., 2010. Influence of NAO and clouds on long-term seasonal variations of surface solar radiation in Europe. Journal of Geophysical Research 115, D00D22, doi:10.1029/2009JD012182.

Christensen, J.H., Hewitson, B., Busuioc, A., Chen, A., Gao, X., Held, I., Jones, R., Kolli, R.K., Kwon, W.-T., Laprise, R., Magaña Rueda, V., Mearns, L., Menéndez, C.G., Räisänen, J., Rinke, A., Sarr, A., Whetton, P., 2007. Regional Climate Projections. In: Solomon, S., Qin, D., Manning, M., Chen, Z., Marquis, M., Averyt, K.B., Tignor, M., Miller, H.L. (Eds.), Climate Change 2007: The Physical Science Basis. Contribution of Working Group I to the Fourth Assessment Report of the Intergovernmental Panel on Climate Change. Cambridge University Press, Cambridge, United Kingdom and New York, NY, USA.

Ciais, P., Reichstein, M., Viovy, N., Granier, A., Ogée, J., Allard, V., Aubinet, M., Buchmann, N., Bernhofer, Chr., Carrara, A., Chevallier, F., De Noblet, N., Friend, A.D., Friedlingstein, P., Grünwald, T., Heinesch, B., Keronen, P., Knohl, A., Krinner, G., Loustau, D., Manca, G., Matteucci, G., Miglietta, F., Ourcival, J.M., Papale, D., Pilegaard, K., Rambal, S., Seufert, G., Soussana, J.F., Sanz, M.J., Schulze, E.D., Vesala, T., Valentini, R., 2005. Europe- wide reduction in primary productivity caused by the heat and drought in 2003. Nature 437, 529-533.

Colombaroli, D., Marchetto, A., Tinner, W., 2007. Long-term interactions between Mediterranean climate, vegetation and fire regime at Lago di Massaciuccoli (Tuscany, Italy). Journal of Ecology 95, 755-770.

Conti, S., Melia, P., Minellia, G., Soliminia, R., Toccacelia, V., Vichia, M., Beltranob, C., Perini, L., 2005. Epidemiologic study of mortality during the summer 2003 heatwave in Italy. Environmental Research 98, 390-399.

Cook, B.I., Mann, M.E., D'Odorico, P., Smith, T.M., 2004. Statistical simulation of the influence of the NAO on European winter surface temperatures: Applications to phenological modeling. Journal of Geophysical Research 109, D16106, doi:10.1029/2003JD004305.

Cullen, H.M., deMenocal, P.B., 2000. North Atlantic influence on Tigris–Euphrates streamflow. International Journal of Climatology 20, 853–863.

D'Andrea, F., Tibaldi, S., Blackburn, M., Boer, G., Deque, M., Dix, M.R., Dugas, B., Ferranti, L., Iwasaki, T., Kitoh, A., Pope, V., Randall, D., Roeckner, E., Straus, D., Stern, W., van den Dool, H., Williamson, D., 1998. Northern Hemisphere atmospheric blocking as simulated by 15 general circulation models in the period 1979-1988. Climate Dynamics 14, 385-407.

Dai, A., 2011. Drought under global warming: a review. Advanced Review, Wiley Interdisciplinary Reviews: Climate Change 2, 45-65, doi:10.1002/wcc.81.

Dai, A., Fung, I.Y., Del Genio, A.D., 1997. Surface observed global land precipitation variations during 1900-88. Journal of Climate 10, 2943-2962.

Dai, A.G., Trenberth, K.E., Qian, T.T., 2004. A global dataset of Palmer Drought Severity Index for 1870-2002: Relationship with soil moisture and effects of surface warming. Journal of Hydrometeorology 5, 1117-1130.

Dayan, U., Abramski, R., 1983. Heavy rain in the Middle East related to unusual jet stream properties. Bulletin of the American Meteorological Society 64, 1138-1140.

DeMelo, R.W., Fontana, D.C., Berlato, M.A., Ducati, J.R., 2008. An agrometeorological-spectral model to estimate soybean yield, applied to southern Brazil. International Journal of Remote Sensing 29, 4013-4028.

Della-Marta, P.M., Haylock, M.R., Luterbacher, J., Wanner, H., 2007. Doubled length of western European summer heatwaves since 1880. Journal of Geophysical Research 112, D15103.

Della-Marta, P.M., Luterbacher, J., von Weissenfluh, H., Xoplaki, E., Brunet, M., Wanner, H., 2006. Summer heat waves over western Europe 1880–2003, their relationship to large scale forcings and predictability. Climate Dynamics 29, 251–275.

Díaz, J., García-Herrera, R., Trigo, R.M., Linares, C., Valente, M.A., De Migule, J.M., Hernández, E., 2006. The impact of summer 2003 heat wave in Iberia: How should we measure it? International Journal of Biometeorology 50, 159-166.

Diffenbaugh, N.S., Pal, J.S., Giorgi, F., Xuejie, G., 2007. Heat stress intensification in the Mediterranean climate change hotspot. Geophysical Research Letters 34, L11706, doi:10.1029/2007GL030000.

Drumond, A., Nieto, R., Gimeno, L., Ambrizzi, T., 2008. A Lagrangian identification of major sources of moisture over Central Brazil and La Plata Basin. Geophysical Research 113, D14128, doi:10.1029/2007JD009547.

Dünkeloh, A., Jacobeit, J., 2003. Circulation dynamics of Mediterranean precipitation variability 1948-1998. International Journal of Climatology 23, 1843- 1866.

Durán-Quesada, A., Gimeno, L., Amador, J.A., Nieto, R., 2010. Moisture sources for Central America: Identification of moisture sources using a Lagrangian analysis technique. Journal of Geophysical Research 115, D05103, doi:10.1029/2009JD012455.

Esteban-Parra, M.J., Rodrigo, F.C., Castro-Díez, Y., 1998. Spatial and temporal patterns of precipitation in Spain for the period 1880-1992. International Journal of Climatology 18, 1557-1574.

European Commission, 2008. Forest Fires in Europe 2007. EUR 23492 EN, Office for Official Publications of the European Communities, Luxembourg. p. 77

Fagherazzi, S., Fosser, G., D'Alpaos, L., D'Odorico, P., 2005. Climatic oscillations influence the flooding of Venice. Geophysical Research Letters 32, L19710, doi:10.1029/2005GL023758.

Fang, H., Liang, S., Hoogenboom, G., Teasdale, J., Cavigelli, M., 2008. Corn-yield estimation through assimilation of remotely sensed data into the CSM-CERES-Maize model. International Journal of Remote Sensing 29, 3011-3032.

Feio, M., 1991. Clima e Agricultura. Ministério da Agricultura, Pescas e Alimentação- DGPA, p. 266.

Fernández, J., Sáenz, J., Zorita, E., 2003. Analysis of the wintertime atmosphere moisture transport and its variability over the Mediterranean Basin. Climate Research 23, 195-215.

Ferranti, L., Viterbo, P., 2006. The European summer of 2003: Sensitivity to soil water initial conditions. Journal of Climate 19, 3659–3680.

Ferris, R., Ellis, R.H., Wheeler, T.R., Hadley, P., 2003. Analysis of the wintertime atmosphere moisture transport and its variability over the Mediterranean Basin. Climate Research 23, 195-215.

Feudale, L., Shukla, J., 2007. Role of Mediterranean SST in enhancing the European heat wave of summer 2003. Geophysical Research Letters 34, L03811, doi:10.1029/2006GL027991.

Fink, A., Brücher, T., Krüger, A., Leckebusch, G., Pinto, J., Ulbrich, U., 2004. The 2003 European summer heat waves and drought–synoptic diagnosis and impacts. Weather 59, 209–216.

Fischer, E.M., Seneviratne, S.I., Lüthi, D., Schär, C., 2007a. Contribution of land-atmosphere coupling to recent European heatwaves. Geophysical Research Letters 34, L06707.

Fischer, E.M., Seneviratne, S.I., Vidale, P.L., Lüthi, D., Schär, C., 2007b. Soil moisture—atmosphere interactions during the 2003 European summer heatwave. Journal of Climate 20, 5081–5099.

Fischer, E.M., Schär, C., 2009. Future changes in daily summer temperature variability: driving processes and role for temperature extremes. Climate Dynamics, doi: 10.1007/s00382-008-0473-8.

Fischer, E.M., Schär, C., 2010. Consistent geographical patterns of changes in high-impact European heatwaves. Nature Geoscience 3, 398-403, doi: 10.1038/NGEO866.

Founda, D., Papadopoulos, K.H., Petrakis, M., Giannakopoulos, C., Good, P., 2004. Analysis of mean, maximum and minimum temperatures in Athens from 1897 to 2001 with emphasis to the last decade: trends, warm and cold events. Global and Planetary Change 44, 27-38.

Fraedrich, K., Müller, K., 1992. Climate anomalies in Europe associated with ENSO extremes. International Journal of Climatology 12, 25-31.

Frassetto, R., 2005. The facts of relative sea-level rise in Venice. In: Fletcher, C.A., Spencer, T. (Eds.), Flooding and Environmental Challenges for Venice and its Lagoon: State of Knowledge, Cambridge University Press, Cambridge, UK, pp. 29–40.

Frei, C., Schär, C., 1998. A precipitation climatology of the Alps from high-resolution rain-gauge observations. International Journal of Climatology 18, 873–900.

García-Herrera, R., Díaz, J., Trigo, R.M., Luterbacher, J., Fischer, E.M., 2010. A review of the European summer heat wave of 2003. Critical Reviews in Environmental Science and Technology 40**,** 267-306.

García-Herrera, R., Paredes, D., Trigo, R.M., Trigo, I.F., Hernández, H., Barriopedro, D., Mendes, M.T., 2007. The outstanding 2004/05 drought in the Iberian Peninsula: Associated atmospheric circulation. Journal of Hydrometeorology 8, 483-498.

Gibelin, A.L., Deque, M., 2003. Anthropogenic Climate Change over the Mediterranean region simulated by a global variable resolution model. Climate Dynamics 20, 327-339.

Gimeno, L., Ribera, P., Iglesias, R., Torre, L., Garcia, R., Hernández, E., 2002. Identification of empirical relationships between indices of ENSO and NAO and agricultural yields in Spain. Climate Research 21, 165-172.

Gimeno, L., Drumond, A., Nieto, R., Trigo, R.M., Stohl, A., 2010a. On the origin of continental precipitation. Geophysical Research Letters 37, doi: 10.1029/2010GL043712.

Gimeno, L., Nieto, R., Trigo, R.M., Vicente-Serrano, S.M., Lopez-Moreno, J.I., 2010b. Where does the Iberian Peninsula moisture come from? An answer based on a Largrangian approach. Journal of Hydrometeorology 11, 421-436, doi: 10.1175/2009JHM1182.1.

Giorgi, F., Bi, X.Q., Pal, J., 2004. Mean interannual variability and trends in a regional climate change experiment over Europe II: climate change scenarios (2071-2100). Climate Dynamics 23, 839-858.

Giorgi, F., 2006. Climate change hot-spots. Geophysical Research Letters 33, L08707.

Giorgi, F., Lionello, P., 2008. Climate change projections for the Mediterranean region. Global and Planetary Change 63, 90-104, doi:10.1016/j.gloplacha.2007.09.005.

González-Hidalgo, J.C., Lopez-Bustins, J.A., Stepanek P., Martin-Vide J., de Luis, M., 2009. Monthly precipitation trends on the Mediterranean façade of the Iberian Peninsula during the second half of the 20th century (1951-2000). International Journal of Climatology 29, 1415–1429

Goodess, C.M., Jones, P.D., 2002. Links between circulation and changes in the characteristics of Iberian rainfall. International Journal of Climatology 22, 1593–1615.

Gosling, S.N., Lowe, J.A., McGregor, G.R., Pelling, M., Malamud, B.D., 2009. Associations between elevated atmospheric temperature and human mortality: a critical review of the literature. Climatic Change 92, 299–341.

Gouveia, C., Trigo, R.M., 2008. Influence of climate variabiltiy on wheat production in Portugal. In: Soares, A., Pereira, C.M.J., Dimitrakopoulos, R. (Eds.), geoENV VI - Geostatistics for Environmental Applications, Springer, pp. 335-348.

Gouveia, C., Trigo, R.M., DaCamara, C.C., 2009. Drought and vegetation stress monitoring in Portugal using satellite data. Natural Hazards and Earth System Sciences 9, 185-195.

Gouveia, C., Trigo, R.M., DaCamara, C.C., Libonati, R., Pereira, J.M.C., 2008. The North Atlantic Oscillation and European vegetation dynamics. International Journal of Climatology 28, 1835–1847, doi:10.1002/joc.1682.

Grazzini, F., Viterbo, P., 2003. Record breaking warm sea surface temperature of the Mediterranean Sea. ECMWF Newsletter 98, 30–31.

ESRA - European Solar Radiation Atlas, 2000. Fourth edition. Edited by J. Greif, K. Scharmer. Scientific advisors: R. Dogniaux, J. K. Page. Authors : L. Wald, M. Albuisson, G. Czeplak, B. Bourges, R. Aguiar, H. Lund, A. Joukoff, U. Terzenbach, H. G. Beyer, E. P. Borisenko. Published for the Commission of the European Communities by Presses de l'Ecole, Ecole des Mines de Paris, France, France.

Grize, L., Huss, A., Thommen, O., Schindler, C., Braun-Fahrländer, C., 2005. Heatwave 2003 and mortality in Switzerland. Swiss Medical Weekly 135, 200-205.

Havens, A.V., 1954. Drought and agriculture. Weatherwise 7, 51-55.

Haylock, M.R., Goodess, C.M., 2004. Interannual variability of European extreme winter rainfall and links with mean large-scale circulation. International Journal of Climatology 24, 759-776.

Hurrell, J. W., 1995. Decadal trends in the North-Atlantic Oscillation - Regional temperatures and precipitation. Science 269, 676-679.

Hurrell, J., 2006. Influence of variations in extratropical wintertime teleconnections on Northern Hemisphere temperature. Geophysical Research Letters 23, 665-668.

Hurrell, J., Hoerling, M., Phillips, A., Xu, T., 2004. Twentieth Century North Atlantic climate change. Part I: Assessing determinism. Climate Dynamics 23, 371-390.

Hurrell, J.W., Kushnir, Y., Ottersen, G., Visbeck, M., 2003. The North Atlantic Oscillation: Climate Significance and Environmental Impact, p. 279.

IEA, 2010. Energy Technology Perspectives 2010 -- Scenarios & Strategies to 2050, ISBN 978-92-64-08597-8, (OECD Publication Service, Paris, p. 650.

Iglesias, A., Quiroga, S., 2007. Measuring the risk of climate variability to cereal production at five sites in Spain. Climate Research 34, 47–57.

Iglesias, E., Garrido, A., Gomez-Ramos, A., 2003. Evaluation of drought management in irrigated areas. Agriculture Economy 29, 211-229.

IPCC, 2007. Climate Change 2007: The Physical Science Basis. Contribution of Working Group I to the Fourth Assessment Report of the Intergovernmental Panel on Climate Change, Cambridge University Press, p. 996.

Iskenderian H., 1995. A 10-year climatology of Northern Hemisphere tropical cloud plumes and their composite flow patterns. Journal of Climate 8, 1630-1637.

Jansá, A., Genovés, A., Campins, J., Picornell, M.A., Riosalido, R., Carretero, O., 2001. Western Mediterranean ciclones and heavy rain. Part 2: Statistical approach. Meteorological Applications 8, 43-56.

Ji. L., Peters, A.J., 2003. Assessing vegetation response to drought in the northern Great Plains using vegetation and drought indices. Remote Sensing of Environment 87, 85-98.

Jones, G.S., Stott, P.A., Christidis, N., 2008. Human contribution to rapidly increasing frequency of very warm Northern Hemisphere summers. Journal of Geophysical Research 113, D02109, doi:10.1029/2007JD008914.

Julien, Y., Sobrino, J.A., Verhoef, W., 2006. Changes in land surface temperatures and NDVI values over Europe between 1982 and 1999. Remote Sensing of Environment 103, 43-55.

Jung, T., Ferranti, L., Tompkins, A.M., 2006. Response to the summer 2003 Mediterranean SST anomalies over Europe and Africa. Journal of Climate 19, 5439–5454.

Kahana, R., Ziv, B., Enzel, Y., Dayan, U, 2002. Synoptic climatology of major floods in the Negev desert, Israel. International Journal of Climatology 22, 867-882.

Kalnay, E., Kanamitsu, M., Kistler, R., Collins, W., Deaven, D., Gandin, L., Iredell, M., Saha, S., White, G., Woollen, J., Zhu, Y., Leetmaa, A., Reynolds, R., Chelliah, M., Ebisuzaki, W., Higgins, W., Janowiak, J., Mo, K.C., Ropelewski, C., Wang, J., Jenne, R., Joseph, D., 1996. The NCEP/NCAR 40-Year Reanalysis Project. Bulletin of the American Meteorological Society 77, 437-471.

Karabörk, M.C., Kahya, E., 2009. The links between the categorised Southern Oscillation indicators and climate and hydrologic variables in Turkey. Hydrological Processes 23, 1927-1936.

Karabörk, M.C., Kahya, E., Kömüşçü, A.Ü., 2007. Analysis of Turkish precipitation data: Homogeneity and the Southern Oscillation forcings on frequency distributions. Hydrological Processes 21, 3203-3210.

Kiladis, G.N., 1998.Observations of Rossby waves linked to convection over the eastern tropical Pacific. Journal of the Atmospheric Sciences 55, 321-339.

Kiladis, G.N., Weickmann, K.M., 1992a. Circulation anomalies associated with tropical convection during northern winter. Monthly Weather Review 120, 1900-1923.

Kiladis, G.N., Weickmann, K.M., 1992b. Extratropical forcing of tropical Pacific convection during northern winter. Monthly Weather Review 120, 1924-1938.

Karl, T., Knight, R., 1997. Secular trends of precipitation amount, frequency, and intensity in the United States. Bulletin of the American Meteorological Society 79, 1107-1119.

Kistler, R., Kalnay, E., Collins, W., Saha, S., White, G., Woolen, J., Chelliah, M., Ebisuzaki, W., Kanamitsu, M., Kousky, V., van den Dool, H., Jenne, R., Fiorino, M., 2001. The NCEP–NCAR 50-year reanalysis: monthly means CD-ROM and documentation. Bulletin of the American Meteorological Society 82, 247-267.

Klein-Tank, A., Können, G., 2003. Trends in indices of daily temperature and precipitation extremes in Europe, 1946–99. Journal of Climate 16, 3665–3680.

Knippertz, P., 2005. Tropical-extratropical interactions associated with an Atlantic tropical plume and subtropical jet streak. Monthly Weather Review 133, 1-18.

Knippertz, P., Fink, A.H., Reiner, A., Speth, P., 2003. Three late summer/early autumn cases of tropical–extratropical interactions causing precipitation in northwest Africa. Monthly Weather Review 131, 116-135.

Knippertz, P., Martin, J.E., 2005. Tropical plumes and extreme precipitation in subtropical and tropical West Africa. Quarterly Journal of the Royal Meteorological Society 131, 2337-2365.

Knowlton, K., Rotkin-Ellman, M., King, G., Margolis, H.G., Smith, D., Solomon, G., Trent, R., English, P., 2009. The 2006 California Heat Wave: Impacts on Hospitalizations and Emergency Department Visits. Environmental Health Perspectives 117, 61–67.

Kostopoulou, E., Jones, P.D., 2005. Assessment of climate extremes in the eastern Mediterranean. Meteorology and Atmospheric Physics 89, 69–85.

Kovats, R., Koppe, C., 2005. Heatwaves: Past and future impacts. In: Ebi, K., Smith, J., Burton, I. (Eds.), Integration of Public Health With Adaptation to Climate Change: Lessons Learned and New Directions. Taylor & Francis, Leiden, The Netherlands, pp. 136-160.

Krichak, S.O., Alpert, P., 1998. Role of large scale moist dynamics in November 1–5, 1994, hazardous Mediterranean weather. Journal of Geophysical Research 103, 19453-19468.

Krichak, S.O., Alpert, P., Dayan, M., 2004. Role of atmospheric processes associated with hurricane Olga in December 2001 floods in Israel. Journal of Hydrometeorology 5, 1259-1270.

Krichak, S.O., Alpert, P., Dayan, M., 2007. An evaluation of the role of hurricane Olga (2001) in an extreme rainy event in Israel using dynamic tropopause maps. Meteorology and Atmospheric Physics 98, 35-53, doi:10.1007/s00703-006-0230-7.

Kuglitsch, F.G., 2010, Extreme Temperature Events in the Mediterranean Region. Ph.D. thesis, Univ. of Bern, Bern, Switzerland, p. 117.

Kuglitsch, F.G., Toreti, A., Xoplaki, E., Della-Marta, P.M., Luterbacher, J., Wanner, H., 2009. Homogenization of daily maximum temperature series in the Mediterranean. Journal of Geophysical Research 114, D15108.

Kuglitsch, F.G., Toreti, A., Xoplaki, E., Della-Marta, P.M., Zerefos, C.S., Türkeş, M., Luterbacher, J., 2010. Heat wave changes in the eastern Mediterranean since 1960. Geophysical Research Letters 37, L04802, doi:10.1029/2009GL041841.

Kuhnel I., 1989. Tropical–extratropical cloudband climatology based on satellite data. International Journal of Climatology 9, 441-463.

Lakshmi, V., Piechota, T., Narayan, U., Tang, C., 2004. Soil moisture as an indicator of weather extremes. Geophysical Research Letters 31, L11401, doi:10.1029/2004GL019930.

Lázaro, R., Rodrigo, F.S., Gutiérrez, L., Domingo, F., Puigdefábregas, J., 2001. Analysis of a 30-year rainfall record (1967-1997) in semi-arid SE Spain for implications on vegetation. Journal of Arid Environments 48, 373-395.

Lenderink, G., van Ulden, A., van den Hurk, B., van Meijgaard, E., 2007. Summertime inter-annual temperature variability in an ensemble of regional model simulations: analysis of the surface energy budget. Climatic Change 81, 233-247.

Lionello, P., 2005. Extreme surges in the Gulf of Venice: present and future climate. In: Fletcher, C.A., Spencer, T. (Eds.), Flooding and Environmental Challenges for Venice and its Lagoon: State of Knowledge, Cambridge University Press, Cambridge, UK, pp. 59-70.

Lionello, P., 2011. The climate of the Venetian and North Adriatic region: variability, trends and future change. Physics and Chemistry of the Earth, accepted.

Lionello, P., Bhend, J., Buzzi, A., Della-Marta, P.M., Krichak, S.O., Jansá, A., Maheras, P., Sanna, A., Trigo, I.F., Trigo, R., 2006. Cyclones in the Mediterranean Region: Climatology and Effects on the

Environment. In: Lionello, P., Malanotte-Rizzoli, P., Boscolo, R. (Eds.), Mediterranean Climate Variability. Elsevier, The Netherlands, pp. 326-372.

Lionello, P., Cavaleri, L., Nissen, K.M., Pino, C., Raicich, F., Ulbrich, U., 2010. Severe marine storms in the Northern Adriatic: Characteristics and trends. Physics and Chemistry of the Earth, doi:10.1016/j.pce.2010.10.002.

Lloyd-Hughes, B., Saunders, M.A., 2002a. A drought climatology for Europe. International Journal of Climatology 22, 1571-1592.

Lloyd-Hughes, B., Saunders, M.A., 2002b. Seasonal prediction of European spring precipitation from El Niño–Southern Oscillation and local sea-surface temperatures. International Journal of Climatology 22, 1-14.

Lohmann, S., Schillings, C., Mayer, B., Meyer, R., 2006. Long-term variability of solar direct and global irradiance derived from ISCCP data and comparison with re-analysis data. Solar Energy 80, 1390-1401, doi: 10.1016/j.solener.2006.03.004

López-Moreno, J.I., Beguería, S., Vicente-Serrano, S.M., García-Ruiz, J.M. 2007. Influence of the North Atlantic Oscillation on water resources in central Iberia: Precipitation, streamflow anomalies, and reservoir management strategies. Water Resources Research 43, W09411, doi:10.1029/2007WR005864.

López-Moreno, J.I., Vicente-Serrano, S.M., 2008. Extreme phases of the wintertime North Atlantic Oscillation and drought occurrence over Europe: a multi-temporal-scale approach. Journal of Climate 21, 1220-1243.

López-Moreno, J., Vicente-Serrano, S., Gimeno, L., Nieto, R., 2009. Stability of the seasonal distribution of precipitation in the Mediterranean region: Observations since 1950 and projections for the 21st century. Geophysical Research Letters 36, L10703, doi:10.1029/2009GL037956.

Lorenzo-Lacruz, J., Vicente-Serrano, S.M., López-Moreno, J.I., Beguería, S., García-Ruiz, J.M., Cuadrat, J.M., 2010. The impact of droughts and water management on various hydrological systems in the headwaters of the Tagus River (central Spain). Journal of Hydrology 386, 13-26, doi:10.1016/j.jhydrol.2010.01.001.

Lozier, M.S., Stewart, N.M., 2008. On the temporally-varying northward penetration of Mediterranean overflow waters. Journal of Physical Oceanography 38, 2097-2103.

Luterbacher, J., Dietrich, D., Xoplaki, E., Grosjean, M., Wanner, H., 2004. European seasonal and annual temperature variability, trends and extremes since 1500. Science 303, 1499-1503.

Luterbacher, J., Liniger, M.A., Menzel, A., Estrella, N., Della-Marta, P.M., Pfister, C., Rutishauser, T., Xoplaki, E., 2007. The exceptional European warmth of Autumn 2006 and Winter 2007: Historical context, the underlying dynamics and its phenological impacts. Geophysical Research Letters 34, L12704, doi:10.1029/2007GL029951.

Maignan, F., Bréon, F.-M., Bacour, C., Demarty, J., Poirson, A., 2008. Interannual vegetation phenology estimates from global AVHRR measurements. Comparison with in situ data and applications. Remote Sensing of Environment, 112, 496-505.

Mariotti, A., 2010. Recent changes in Mediterranean water cycle: a pathway toward long-term regional hydroclimatic change? Journal of Climate 23, 1513–1525.

Mariotti, A., Struglia, M.V., Zeng, N., Lau, K.-M., 2002a. The hydrological cycle in the Mediterranean region and implications for the water budget of the Mediterranean Sea. Journal of Climate 15, 1674-1690.

Mariotti, A., Zeng, N., Lau, K.-M., 2002b. Euro-Mediterranean rainfall and ENSO—a seasonally varying relationship. Geophysical Research Letters 29, 1621, doi:10.1029/2001GL014248.

Mariotti, A., Zeng, N., Yoon, J., Artale, V., Navarra, A., Alpert, P., Li, L.Z.X., 2008. Mediterranean water cycle changes: transition to drier 21st century conditions in observations and CMIP3 simulations. Environmental Research Letters 3, 044001, doi:10.1088/1748-9326/3/4/044001.

Martius, O., Zenklusen, E., Schwierz, C., Davies, H.C., 2006. Episodes of Alpine heavy precipitation with an overlying elongated stratospheric intrusion: A climatology. International Journal of Climatology 26, 1149-1164. doi:10.1002/joc.1295.

Massacand, A.C., Wernli, H., Davies, H.C., 1998. Heavy precipitation on the Alpine southside: An upper-level precursor. Geophysical Research Letters 25, 1435-1438.

McGuirk, J.P., 1993. Impact of increased TOVS signal on the NMC global spectral model: A Tropical-Plume case study. Monthly Weather Review 121, 695-712.

McGuirk, J.P., Ulsh, D.J., 1990. Evolution of tropical plumes in VAS water vapor imagery. Monthly Weather Review 118, 1758–1766.

McGuirk, J.P., Thompson, A.H., Smith, N.R., 1987. Moisture bursts over the tropical Pacific Ocean. Monthly Weather Review 115, 787-798.

McGuirk, J.P., Thompson, A.H., Schaefer, J.R., 1988. An eastern Pacific tropical plume. Monthly Weather Review 116, 2505-2521.

McKee, T.B.N., Doesken, J., Kleist, J., 1993. The relationship of drought frecuency and duration to time scales. Eight Conf. on Applied Climatology. Anaheim, CA, American Meteorological Society, pp. 179-184.

Mecikalski, J.R., Tripoli, G.J., 1998. Inertial available kinetic energy and the dynamics of tropical plume formation. Monthly Weather Review 126, 2200-2216.

Meehl, G.A., Tebaldi, C., 2004. More intense, more frequent, and longer lasting heat waves in the 21st century. Science 305, 994–997.

Menzel, A., 2003. Plant phenological anomalies in Germany and their relation to air temperature and NAO. Climatic Change 57, 243-263.

Michelangeli, P.-A., Vautard, R., Legras, B., 2004. Weather regimes: Recurrence and quasi-stationarity. Journal of the Atmospheric Sciences 52, 1237-1256.

Mishra A. K., Singh, V.P., 2010. A review of drought concepts. Journal of Hydrology 391, 202–216.

Mitchell, T.D., Jones, P.D., 2005. An improved method of constructing a database of monthly climate observations and associated high-resolution grids. International Journal of Climatology 25, 693-712.

Moberg, A., Jones, P.D., 2005. Trends in indices for extremes in daily temperature and precipitation in central and western Europe 1901-1999. International Journal of Climatology 25, 1173-1188.

Morales, A., Olcina, J., Rico, A.M., 2000. Diferentes percepciones de la sequía en España: adaptación, catastrofismo e intentos de corrección. Investigaciones Geográficas 23, 5-46.

Mukougawa, H., Sato, H., 1999. Multiple Weather Regimes in the Summertime North Atlantic Circulation. Journal of the Meteorological Society of Japan 77, 483-494.

Munich Re, 2004. TOPICS geo 2003. Munich: Münchener Rückverischerungs-Gessellschaft.

Navarra, A., Tubiana, L., 2011. Regional Assessment of Climate Change in the Mediterranean, Springer, Dordrecht, The Netherlands, in press.

New, M., Hulme, M., Jones, P.D., 2000. Representing twentieth-century space-time climate variability. Part II: Development of 1901–96 monthly grids of terrestrial surface climate. Journal of Climate 13, 2217–2238.

Nieto, R., Gimeno, L., Drumond, A., Hernandez, E., 2010. A Lagrangian identification of the main moisture sources and sinks affecting the Mediterranean area. WSEAS Transactions on Environment and Development 5, 365-374.

Nieto, R., Gimeno, L., Trigo, R.M., 2006. A Lagrangian identification of major sources of Sahel moisture. Geophysical Research Letters 33, L18707, doi:10.1029/2006GL027232.

Nogaj, M., Yiou, P., Parey, S., Malek, F., Naveau, P., 2006. Amplitude and frequency of temperature extremes over the North Atlantic region. Geophysical Research Letters 33, L10801, doi:10.1029/2005GL024251.

Ogi, M., Yamazaki, K., Tachibana, Y., 2005. The summer northern annular mode and abnormal summer weather in 2003. Geophysical Research Letters 32, L04706, doi:10.1029/2004GL021528.

Page, J., Albuisson, M., Wald, L., 2001. The European Solar Radiation Atlas: a valuable digital tool. Solar Energy 71, 81-83.

Pal, J.S., Giorgi, F., Bi, X., 2004. Consistency of recent European summer precipitation trends and extremes with future regional climate projections. Geophysical Research Letters 31, L13202, doi:10.1029/2004GL019836.

Palmer, T., 1999. A nonlinear dynamical perspective on climate prediction. Journal of Climate 12, 575-591.

Papadimas, C.D., Fotiadi, A.K., Hatzianastassiou, N., Vardavas, I., Bartzokas, 2010. Regional co-variability and teleconnection patterns in surface solar radiation on a planetary scale. International Journal of Climatology 30, 2314-2329, doi:10.1002/joc.2031.

Paredes, D., Trigo, R.M., García-Herrera, R., Trigo, I.F., 2006. Understanding precipitation changes in Iberia in early spring: weather typing and storm-tracking approaches. Journal of Hydrometeorology 7, 101-113.

Pausas, J.G., 2004. Changes in fire and climate in the eastern Iberian Peninsula (Mediterranean basin). Climatic Change 63, 337-350.

Peixoto, J.P., De Almeida, M., Rosen, R.D., Salstein, D.A., 1982. Atmospheric moisture transport and the water balance of the Mediterranean Sea. Water Resources Research 18, 83–90, doi:10.1029/WR018i001p00083.

Philipp, A., Della-Marta, P.M., Fereday, D.T., Jones, P.D., Moberg, A., Wanner, H., 2007. Long-term variability of daily North Atlantic-European pressure patterns since 1850 classified by simulated annealing clustering. Journal of Climate 20, 4065-4095.

Piao, S., Ciais, P., Friedlingstein, P., Peylin, P., Reichstein, M., Luyssaert, S., Margolis, H., Fang, J., Barr, A., Chen, A., Grelle, A., Hollinger, D.Y., Laurila, T., Lindroth, A., Richardson, A.D., Vesala, T., 2008. Net carbon dioxide losses of northern ecosystems in response to autumn warming. Nature 451, 49-52, doi: 10.1038/nature06444.

Pinto, J.G., Klawa, M., Ulbrich, U., Rudari, R., Speth, P., 2003. Extreme precipitation events over northwest Italy and their relationship with tropical-extratropical interactions over the Atlantic. In: Deidda, R., Mugnai, A., Siccardi, F. (Eds.), Mediterranean storms. 3rd Plinius Conf., GNDCI Publication, Publ. No. 2560, pp. 321-332.

Pinto, J.G., Ulbrich, S., Boni, G., Parodi, A., Rudari, R., Ulbrich, U., 2011. Identification, ranking and meteorological characterization of extraordinary rainfall events over Northwest Italy. Journal of Geophysical Research – Atmospheres (submitted)

Pirazzoli, P.A., 1991. Possible defenses against the sea level rise in Venice area, Italy. Journal of Coastal Research 7, 231-248.

Poumadère, M., Mays, C., Le Mer, S., Blong, R., 2005. The 2003 Heatwave in France: dangerous climate change here and now. Risk Analysis 25, 1483-1494.

Pozo-Vázquez, D., Esteban-Parra, M.J., Rodrigo, F.S., Castro-Díez, Y., 2001. The association between ENSO and winter atmospheric circulation and temperature in the North Atlantic region. Journal of Climate 14, 3408–3420.

Pozo-Vázquez, D., Gámiz-Fortis, S.R., Tovar-Pescador, J., Esteban-Parra, M.J., Castro-Díez, Y., 2005. El Niño-Southern Oscillation events and associated European winter precipitation anomalies. International Journal of Climatology 25, 17-31, doi:10.1002/joc.1097.

Pozo-Vázquez, D., Tovar-Pescador, J., Gamiz-Fortes, S.R., Esteban-Parra, M.J., Castro-Díez, Y., 2004. NAO and solar radiation variability in the European North Atlantic region. Geophysical Research Letters 31, L05201, doi: 10.1029/2003GL018502.

Quadrelli, R., Pavan, V., Molteni, F., 2001. Wintertime Mediterranean precipitation patterns and their links with largescale circulation anomalies. Climate Dynamics 7, 457–466.

Reale, O., Feudale, L., Turato, B., 2001. Evaporative moisture sources during a sequence of floods in the Mediterranean region. Geophysical Research Letters 28, 2085–2088, doi:10.1029/2000GL012379.

Rebetez, M., 2004. Summer 2003 maximum and minimum daily temperatures over a 3300 m altitudinal range in the Alps. Climate Research 27, 45-50.

Redmond, K.T., 2002. The depiction of drought. Bulletin of the American Meteorological Society 83, 1143-1147.

Reichstein, M., Tenhunen, J.D., Roupsard, O., Ourcival, J.-M., Rambal, S., Miglietta, F., Peressotti, A., Valentini, R., 2002. Severe drought effects on ecosystem CO2 and H2O fluxes at three Mediterranean evergreen sites: Revision of current hypotheses? Global Change Biology 8, 999-1017.

Reinhold, B.B., Pierrehumbert, R.T., 1982. Dynamics of weather regimes: quasi-stationary waves and blocking. Journal of the Atmospheric Sciences 110, 1105–1145.

Rex, D.F., 1950. Blocking action in the middle troposphere and its effect on regional climate. Part I: An aerological study of blocking action. Tellus 2, 196-211.

Riemer, M., Jones, S.C., Davis, C.A., 2008. The impact of extratropical transition on the downstream flow: An idealized modelling study with a straight jet. Quarterly Journal of the Royal Meteorological Society 134, 69–91.

Rodó, X., Baert, E., Comín, F.A., 1997. Variations in seasonal rainfall in southern Europe during the present century: relationshpis with the North Atlantic Oscillation and the El Niño-Southern Oscillation. Climate Dynamics 13, 275-284.

Rodríguez-Puebla, C., Ayuso, S.M., Frias, M.D., Garcia-Casado, L.A., 2007. Effects of climate variation on winter cereal production in Spain. Climate Research 34, 223-232.

Rodriguez-Puebla, C., Encinas, A.H., Nieto, S, Garmendia J., 1998. Spatial and temporal patterns of annual precipitation variability over the Iberian Peninsula. International Journal of Climatology 18, 299-316.

Ropelewski, C.F., Halpert, M.S., 1987. Global and regional scale precipitation patterns associated with the El Nino/ Southern Oscillation. Monthly Weather Review 115, 1606-1626.

Rowntree, P.R., Bolton, J.A., 1983. Simulation of the atmospheric response to soil moisture anomalies over Europe. Quarterly Journal of the Royal Meteorological Society 109, 501-526.

Rubin, S., Ziv, B., Paldor, N., 2007. Tropical Plumes over eastern North Africa as a source of rain in the Middle East. Monthly Weather Review 35, 4135-4148.

Rudari, R., Entekhabi, D., Roth, G., 2005. Large-scale atmospheric patterns associated with mesoscale features leading to extreme precipitation events in northwestern Italy. Advances in Water Resources 28, 601-614.

Sampaio, A.J., 1990. A cultura do Trigo. Ministério da Agricultura, Pescas e Alimentação.

Sanchez-Lorenzo, A., Calbó, J., Martin-Vide, J., 2008. Spatial and temporal trends in sunshine duration over western Europe (1938-2004). Journal of Climate, 21, 6089-6098.

Sanchez-Lorenzo, A., Calbó, J., Brunetti, M., Deser, C., 2009. Dimming/brightening over the Iberian Peninsula: Trends in sunshine duration and cloud cover, and their relations with atmospheric circulation. Journal of Geophysical Research 114, D00D09, doi:10.1029/2008JD011394.

Schär, C., Vidale, P.L., Lüthi, D., Frei, C., Häberli, C., Liniger, M.A., Appenzeller C., 2004. The role of increasing temperature variability in European summer heat waves. Nature 427, 332–336.

Schneider, S.H., Semenov, S., Patwardhan, A., Burton, I., Magadza, C.H.D., Oppenheimer, M., Pittock, A.B., Rahman, A., Smith, J.B., Suarez, A., Yamin, F., 2007. Assessing key vulnerabilities and the risk from climate change. In: Parry, M.L., Canziani, O.F., Palutikof, J.P., van der Linden, P.J., Hanson, C.E. (Eds.), Climate Change 2007: Impacts, Adaptation and Vulnerability. Contribution of Working Group II to the Fourth Assessment Report of the Intergovernmental Panel on Climate Change. Cambridge University Press, Cambridge, UK, pp. 779-810.

Seneviratne, S.I., Lüthi, D., Litschi, M., Schär, C., 2006. Land-atmosphere coupling and climate change in Europe. Nature 443, 205-209, doi:10.1038/nature05095.

Seneviratne, S.I., Corti, T., Davin, E.L., Hirschi, M., Jaeger, E.B., Lehner, I., Orlowsky, B., Teuling, A.J., 2010. Investigating soil moisture-climate interactions in a changing climate: A review. Earth-Science Reviews 99, 3-4, 125-161.

Shukla, J., Mintz, Y., 1982. Influence of land-surface evapotranspiration on the Earth's climate. Science New Series 215, 1498-1501.

Smith, R.B., Barstad, I., 2004. A linear theory of orographic precipitation, Journal of the Atmospheric Sciences 61, 1377–1391.

Smith, T.M., Sapiano, M.R.P., Arkin, P.A., 2008. Historical reconstruction of monthly oceanic precipitation (1900-2006). Journal of Geophysical Research 113, D17115.

Smoyer-Tomic, K.E., Kuhn, R., Hudson, A., 2003. Heat-wave Hazards: An overview of heat-waves impacts on Canada. Natural hazards 28, 465–486, doi:10.1023/A:1022946528157.

Sordo, C., Frías, M.D., Herrera, S., Cofiño, A.S., Gutiérrez, J.M., 2008. Interval-based statistical validation of operational seasonal forecasts in Spain conditioned to El Niño–Southern Oscillation events. Journal of Geophysical Research 113, D17121, doi:10.1029/2007JD009536.

Sousa, P., Trigo, R.M., Aizpurua, P., Nieto, R., Gimeno, L., García-Herrera, R., 2011. Trends and extremes of drought indices throughout the 20th century in the Mediterranean, Natural Hazards and Earth System Sciences 11, 33-51.

Steadman, R.G., 1979. The assessment of sultriness. Part I: A temperature-humidity index based on human physiology and clothing science. Journal of Applied Meteorology 18, 861-873.

Stockdale, T.N., Anderson, D.l.T., Alves, J.O.S., Balmaseda, M.A., 1998. Global seasonal rainfall forecast using a coupled ocean-atmosphere model. Nature 392, 370-373.

Stöckli, R., Vidale, P.L., 2004. European plant phenology and climate as seen in a 20-year AVHRR land-surface parameter dataset. International Journal of Remote Sensing 25, 3303–3330.

Stohl, A., Hittenberger, M., Wotawa, G., 1998. Validation of the Lagrangian particle dispersion model FLEXPART against large scale tracer experiments. Atmospheric Environment 32, 4245-4264.

Stott, P.A., Stone, D.A., Allen, M.R., 2004. Human contribution to the European heatwave of 2003. Nature 432, 610–613.

Struglia, M.V., Mariotti, A., Filograsso, A., 2004. River discharge into the Mediterranean Sea: Climatology and aspects of the observed variability. Journal of Climate 17, 4740-4751 doi:10.1175/JCLI-3225.1.

Tebaldi, C., Hayhoe, K., Arblaster, J.M., Meehl G.A., 2006. Going to the extremes. Climatic Change 79, 185-211.

Thepenier, R.M., Cruette, D., 1981. Formation of cloud bands associated with the American subtropical jet stream and their interactions with midlatitude synoptic disturbances reaching Europe. Monthly Weather Review 109, 2209-2220.

Tippett, M.K., Barnston, A.G., 2008. Skill of multimodel ENSO probability forecasts. Monthly Weather Review 136, 3933-3946.

Tomasin, A., 2005. Forecasting the water level in Venice: physical background and perspectives. In: Fletcher, C.A., Spencer, T. (Eds.), Flooding and Environmental Challenges for Venice and its Lagoon: State of Knowledge, Cambridge University Press, Cambridge, UK, pp. 71-78.

Trigo, I.F., 2006. Climatology and interannual variability of storm tracks in the Euro-Atlantic sector: A comparison between ERA-40 and NCEP/NCAR reanalyses. Climate Dynamics 26, 127– 143.

Trigo, I.F., Davies, T.D., 2002. Meteorological conditions associated with sea surges in Venice: a 40 year climatology. International Journal of Climatology 22, 787–803, doi:10.1002/joc.719.

Trigo, R.M., García-Herrera, R., Díaz, J., Trigo, I.F., Valente, M.A., 2005. How exceptional was the early August 2003 heatwave in France? Geophysical Research Letters 32, L10701, doi:10.1029/2005GL022410.

Trigo, R.M., Osborn, T.J., Corte-Real, J.M., 2002. The North Atlantic Oscillation influence on Europe: climate impacts and associated physical mechanisms. Climate Research 20, 9–17.

Trigo, R.M., Pereira, J.M.C., Pereira, M.G., Mota, B., Calado, M.T., DaCamara, C.C., Santo, F.E. 2006. The exceptional fire season of summer 2003 in Portugal. International Journal of Climatology 26, 1741–1757.

Trigo, R.M., Pozo- Vázquez, D., Osborn, T.J., Castro-Diez, Y., Gámis-Fortis, S., Esteban-Parra, M.J., 2004. North Atlantic Oscillation influence on precipitation, river flow and water resources in the Iberian Peninsula. International Journal of Climatology 24, 925-944.

Trigo, R.M., Valente, M.A., Trigo, I.F., Miranda, P.M., Ramos, A.M., Paredes, D., García-Herrera, R., 2008. The Impact of North Atlantic Wind and Cyclone Trends on European Precipitation and Significant Wave Height in the Atlantic. Annals of the New York Academy of Sciences 1146, 212-234.

Trigo, R.M., Ramos, A.M., Nogueira, P.J., Santos, F.D., Garcia-Herrera, R., Gouveia, C., Santo, F.E., 2009. Evaluating the impact of extreme temperature based indices in the 2003 heatwave excessive mortality in Portugal. Environmental Science and Policy 12, 844-854.

Tsimplis, M., Marcos, M., Somot, S., 2008. 21st century Mediterranean sea level rise. Regional model prediction. Global and Planetary Change 63, 105-111.

Turato, B., Reale, O., Siccardi, F., 2004. Water vapor sources of the October 2000 Piedmont flood. Journal of Hydrometeorology 5**,** 693–712.

Türkeş, M., Erlat, E., 2005. Climatological responses of winter precipitation in Turkey to variability of the North Atlantic Oscillation during the period 1930-2001. Theoretical and Applied Climatology 81, 45-69.

Türkeş, M., Sümer, U.M., Demir, I., 2002. Re-evaluation of trends and changes in mean, maximum and minimum temperatures of Turkey for the period 1929–1999. International Journal of Climatology 22, 947–977, doi:10.1002/ joc.777.

van der Schrier, G., Briffa, K.R., Jones, P.D., Osborn, T.J., 2006. Summer moisture variability across Europe. Journal of Climate 19, 2818-2834.

van Oldenborg, G.J., Burgers, G., Klein T.A., 2000. On the El Niño teleconnection to spring precipitation in Europe. International Journal of Climatology 20, 565-574.

van Oldenborgh, G.J., Drijfhout, S., van Ulden, A., Haarsma, R., Sterl, A., Severijns, C., Hazeleger, W., Dijkstra, H., 2009. Western Europe is warming much faster than expected. Climate of the Past 5, 1-12, doi:10.5194/cp-5-1-2009.

van Oldenborgh, G.J., 2007. How unusual was autumn 2006 in Europe? Climate of the Past 3, 659-668.

Vautard, R., Yiou, P., 2009. Control of recent European surface climate change by atmospheric flow. Geophysical Research Letters 36, L22702, doi:10.1029/2009GL040480.

Vautard, R., Yiou, P., D'Andrea, F., de Noblet, N., Viovy, N., Cassou, C., Polcher, J., Ciais, P., Kageyama, M., Fan, Y., 2007. Summertime European heat and drought waves induced by wintertime Mediterranean rainfall deficit. Geophysical Research Letters 34, L07711, doi:10.1029/2006GL028001.

Vicente-Serrano, S.M., 2005. El Niño and La Niña influence on droughts at different timescales in the Iberian Peninsula. Water Resources Research 41, W12415, doi:10.1029/2004WR003908.

Vicente-Serrano, S.M., 2006a. Spatial and temporal analysis of droughts in the Iberian Peninsula (1910-2000). Hydrological Sciences Journal 51, 83-97.

Vicente-Serrano, S.M., 2006b. Differences in spatial patterns of drought on different time scales: an analysis of the Iberian Peninsula. Water Resources Management 20, 37-60.

Vicente-Serrano, S.M., 2007. Evaluating the impact of drought using remote sensing in a Mediterranean semi–arid region. Natural Hazards 40, 173-208.

Vicente-Serrano, S.M., Beguería, S., López-Moreno, J.I., 2010b. A Multi-scalar drought index sensitive to global warming: The Standardized Precipitation Evapotranspiration Index – SPEI. Journal of Climate 23, 1696–1718.

Vicente-Serrano, S.M., Beguería, S., López-Moreno, J.I., Angulo, M., El Kenawy, A., 2010a. A new global 0.5° gridded dataset (1901–2006) of a multiscalar drought index: comparison with current drought index datasets based on the Palmer Drought Severity Index. Journal of Hydrometeorology 11, 1033–1043, doi:10.1175/2010JHM1224.1.

Vicente-Serrano, S.M., González-Hidalgo, J.C., de Luis, M., Raventós, J., 2004. Spatial and temporal patterns of droughts in the Mediterranean area: the Valencia region (East-Spain). Climate Research 26, 5-15.

Vicente-Serrano, S.M., López-Moreno, J.I., Lorenzo-Lacruz, J., El Kenawy, A., Azorin-Molina, C., Morán-Tejeda, E., Pasho, E., Zabalza, J., Beguería, S., Angulo-Martínez, M., 2011. The NAO impacts on droughts in the Mediterranean region. In: Vicente-Serrano S.M., Trigo, R.M. (Eds.), Hydrological, socioeconomic and ecological impacts of the North Atlantic Oscillation in the Mediterranean region. Springer-Verlag, in press.

Vicente-Serrano, S.M., Cuadrat-Prats, J.M., Romo, A., 2006. Early prediction of crop productions using drought indices at different time scales and remote sensing data: application in the Ebro valley (NE Spain). International Journal of Remote Sensing 27, 511-518.

Vidale, P.L., Lüthi, D., Wegmann, R., Schär, C., 2007. European summer climate variability in a heterogeneous multi-model ensemble. Climatic Change 81, 209-232.

Vose, R.S., Schmoyer, R.L., Steurer, P.M., Peterson, T.C., Heim, R., 1992. The Global Historical Climatology Network: long-term monthly temperature, precipitation, sea level pressure, and station pressure data, ORNL/CDIAC-53, NDP-041 Carbon Dioxide Information Analysis Center, Oak Ridge National Laboratory, Oak Ridge, Tennessee.

Weisheimer, A., Doblas-Reyes, F.J., Jung, T., Palmer, T.N., 2011. On the predictability of the extreme summer 2003 over Europe. Geophysical Research Letters 38, L05704, doi:10.1029/2010GL046455.

Wentz, F.J., Ricciardulli, L., Hilburn, K., Mears, C., 2007. How much more rain will global warming bring? Science 317, 233-235.

Wilhite, D.A., 1993. Drought assessment, management and planning: Theory and case studies. Kluwer, Boston, p. 293.

Wilhite, D.A., 2000. Drought: A Global Assessment. Natural Hazards and Disasters Series. Routledge Publishers, London, p. 700.

Wilhite, D.A., Glantz, M.H., 1985. Understanding the drought phenomenon: the role of definitions. Water International 10, 111-120.

World Meteorological Organisation, 2006. Drought monitoring and early warning: concepts, progress and future challenges. WMO-No. 1006, ISBN 92-63-11006-9.

Xoplaki, E., González-Rouco, J.F., Gyalistras, D., Luterbacher, J., Rickli, R., Wanner, H., 2003a. Interannual summer air temperature variability over Greece and its connection to the large-scale atmospheric circulation and Mediterranean SSTs 1950-1999. Climate Dynamics 20, 537-554.

Xoplaki, E., González-Rouco, J.F., Luterbacher, J., Wanner, H., 2003b. Mediterranean summer air temperature variability and its connection to the large-scale atmospheric circulation and SSTs. Climate Dynamics 20, 723-739.

Xoplaki, E., González-Rouco, J.F., Luterbacher, J., Wanner, H., 2004. Wet season Mediterranean precipitation variability: influence of large scale dynamics and predictability. Climate Dynamics 23, 63-78.

Xoplaki, E., Luterbacher, J., Paeth, H., Dietrich, D., Steiner, N., Grosjean, M., Wanner, H., 2005. European spring and autumn temperature variability and change of extremes over the last half millennium. Geophysical Research Letters 32, L15713.

Yiou, P., Nogaj, M., 2004. Extreme climatic events and weather regimes over the North Atlantic: When and where? Geophysical Research Letters 31, L07202, doi:10.1029/2003GL019119.

Yiou, P., Goubanova, K., Li, Z.X., Nogaj, M., 2008. Weather regime dependence of extreme value statistics for summer temperature and precipitation. Nonlinear Processes in Geophysics 15, 365–378.

Yiou, P., Vautard, R., Naveau, P., Cassou, C., 2007. Inconsistency between atmospheric dynamics and temperatures during the exceptional 2006/2007 fall/winter and recent warming in Europe. Geophysical Research Letters 34**,** L21808, doi:10.1029/2007GL031981.

Yu, L., Jin, X., Weller, R.A., 2008. Multidecade Global Flux Datasets from the Objectively Analyzed Air-sea Fluxes (OAFlux) Project: Latent and Sensible Heat Fluxes, Ocean Evaporation, and Related Surface Meteorological Variables, Woods Hole Oceanographic Institution OAFlux Project Technical Report (OA-2008-01).

Zaitchik, B., Macalady, A.K., Bonneau, L.R., Smith, R.B., 2006. Europe's 2003 heat wave: A satellite view of impacts and land-atmosphere feedbacks. International Journal of Climatology 26, 743–769.

Zampieri, M., D'Andrea, F., Vautard, R., Ciais, P., de Noblet-Ducoudré, N., Yiou, P., 2009. Hot European summers and the role of soil moisture in the propagation of Mediterranean drought. Journal of Climate 22, 4747-4758.

Zanchettin, D., Rubino, A., Traverso, P., Tomasino, M., 2009. Teleconnections force interannual to decadal tidal variability in the Lagoon of Venice (northern Adriatic). Journal of Geophysical Research 114, D07106, doi:10.1029/2008JD011485.

Zangvil, A., Isakson, A., 1995. Structure of water vapor field associated with an early spring rainstorm over the eastern Mediterranean. Israel Journal of Earth Sciences 44, 159-168.

Ziv, B., 2001. A subtropical rainstorm associated with a tropical plume over Africa and the Middle-East. Theoretical and Applied Climatology 69, 91-102.

Zohdy, H.M, 1989. Lateral coupling between extratropical and tropical disturbances over Africa associated with Mediterranean. WMO PSMP Report Series No. 31, 37-75.

Zohdy, H.M, 1991. The impact of midlatitude geopotential anomalies on tropical weather systems. WMO PSMP Report Series No. 33, 121-133.

Zorita, E., Hughes, J.P., Lettemaier, D.P., von Storch, H., 1995. Stochastic characterization of regional circulation patterns for climate model diagnosis and estimation of local precipitation. Journal of Climate 8, 1023–1042.